

## AN ABSTRACT OF THE THESIS OF

Maria Adriana Martínez-Prado for the degree of Doctor of Philosophy in Civil Engineering presented on April 30, 2002. Title: Biodegradation of Methyl *tert*-Butyl Ether (MTBE) and its Breakdown Products by Propane and *iso*-Pentane Grown *Mycobacterium vaccae* and *Graphium sp.* : Cometabolism, Inhibition, Kinetics and Modeling.

Abstract approved: **Redacted for privacy**

Kenneth J. Williamson

*Mycobacterium vaccae* JOB5 and *Graphium sp.* were studied to evaluate their ability to cometabolize methyl *tert*-butyl ether (MTBE) and its metabolites after growth on two different alkanes, propane and *iso*-pentane. Both cultures were capable of cometabolizing MTBE and the metabolites, *tert*-butyl formate (TBF) and *tert*-butyl alcohol (TBA). MTBE, TBF, and TBA did not support growth of either microbe. Higher degradation rates were obtained in the bacterial system when the cultures were grown on *iso*-pentane. Nonlinear least squares regression and direct linear plot methods were used to estimate kinetic coefficients and provided comparable results.

The enzymes from *Mycobacterium vaccae* JOB5 and *Graphium* sp. that promote the cometabolism of MTBE and its metabolites exhibited similar kinetics and substrate inhibition. The presence of the substrate decreased the degradation rate of MTBE and TBA suggesting competitive inhibition and preference for the substrate. Blockage experiment with acetylene suggested the presence of an alkane monooxygenase for the metabolism of MTBE and TBA, and a hydrolytic enzyme for the degradation of TBF. The presence of a hydrolase enzyme was supported by the fact that TBF was degraded to TBA under either aerobic or anaerobic conditions and was not inhibited by the presence of acetylene, propane, or *iso*-pentane. Measured rates of abiotic hydrolysis of TBF were significantly less than biodegradation rates.

Acetylene acted as a reversible inhibitor for both cultures when tested in the presence of the growth media and as an inactivator when tested in the presence of a phosphate solution for the bacterial system.

Growth-batch reactor experiments were conducted to compare the degradation of *iso*-pentane and MTBE with the predicted degradation rates based upon kinetic constants determined from single and dual-compound experiments. Experimental data was modeled with Monod kinetics and STELLA<sup>®</sup> software. Reasonable predictions of reactor performance were achieved when Monod maximum utilization rates were increased compared to single and dual-compound experiments.

© Copyright by Maria Adriana Martínez Prado  
April 30, 2002  
All Rights Reserved

Biodegradation of Methyl *tert*-Butyl Ether (MTBE) and its Breakdown Products by  
Propane and *Iso*-pentane Grown *Mycobacterium vaccae* and *Graphium* sp. :  
Cometabolism, Inhibition, Kinetics and Modeling.

by

Maria Adriana Martínez-Prado

A THESIS

submitted to

Oregon State University

in partial fulfillment of  
the requirements for the  
degree of

Doctor of Philosophy

Presented April 30, 2002  
Commencement June, 2002

Doctor of Philosophy thesis of Maria Adriana Martínez-Prado presented on April  
30, 2002

APPROVED:

Redacted for privacy

---

Major Professor, representing Civil Engineering

Redacted for privacy

---

Head Department of Civil, Construction, and Environmental Engineering

Redacted for privacy

---

Dean of Graduate School

I understand that my thesis will become part of the permanent collection of Oregon State University libraries. My signature below authorizes release of my thesis to any reader upon request.

Redacted for privacy

---

Maria Adriana Martínez-Prado, Author

## ACKNOWLEDGMENT

The completion of my doctoral studies would not have been possible without the help and support of many people in my professional and personal life.

My doctoral studies were financially supported by the Country of Mexico through Consejo Nacional de Ciencia y Tecnología (CONACyT) and Instituto Tecnológico de Durango (ITD). The thesis project was sponsored by a grant from the Western Region Hazardous Substance Research Center (WRHSRC) funded by the US EPA.

I want to thank my advisor, Kenneth J. Williamson, for his guidance, encouragement, and unconditional support through all these years at OSU. I also thank my committee members, Lynda M. Ciuffetti, Mark Dolan, Lewis Semprini, and Ronald Guenther, for their time, energy and insight into my work. I would like to thank the Civil, Construction and Environmental Engineering Department, Faculty, and Staff for letting me be part of this great family. I thank Young Kim, Sarun Tejasen, Seungho Yu, and Kristin Skinner for their encouragement, valuable discussions and friendship.

I would also like to show my appreciation to my friends here in the United States and in Mexico for making my life more fruitful. A special thanks goes to

Carlos Cruz-Fierro for his valuable help in the development of the Visual Basic program and his friendship.

Lastly, I want to thank my family and my children, Addy, Joao, and Emmanuel, for believing in me. To my husband, Joaquin Pinto-Espinoza, an amazing human being, for his support, encouragement and love. He supported and helped me through the difficult times in my graduate studies. My recognition goes to him for his contribution in the programming needed in this thesis.

## CONTRIBUTION OF AUTHORS

Dr. Kenneth J. Williamson assisted in the conception and writing of each manuscript. Dr. Lynda M. Ciuffetti assisted in the conception and writing of manuscripts from Chapters 4 and 5. Dr. Ronald Guenther contributed to the development of mathematical independent solution for modeling presented in Appendix C. Dr. Mark Dolan contributed to the design of inhibition experiments presented in Chapter 3 and STELLA modeling presented in Chapter 2. Kristin Skinner contributed to the design of fungal experiments and to the writing of manuscript in Chapter 5. Dr. Michael Hyman at North Carolina State University developed the original idea of this project and provided helpful insight and advice.

This project was supported by a grant from the Western Region Hazardous Substance Research Center (WRHSRC) funded by the US EPA and by the Country of Mexico through Consejo Nacional de Ciencia y Tecnología (CONACyT) and Instituto Tecnológico de Durango (ITD).



## TABLE OF CONTENTS

	<u>Page</u>
Chapter 1    Introduction .....	1
1.1 Literature Review .....	2
1.1.1 Environmental impacts .....	2
1.1.2 Potential remedial mechanism .....	4
1.1.3 Biodegradation .....	6
1.1.4 MTBE degradation metabolites .....	7
1.1.5 MTBE metabolism as a primary substrate.....	9
1.1.6 MTBE aerobic cometabolism .....	10
1.1.7 MTBE anaerobic degradation .....	12
1.1.8 Scale-up and field studies .....	13
1.1.9 TBF hydrolysis .....	14
1.2 Physicochemical properties of compounds tested .....	15
1.3 Objectives .....	16
1.4 References .....	18
 Chapter 2    Biodegradation Kinetics of Methyl <i>tert</i> -Butyl Ether (MTBE) and its Breakdown Products by Propane and <i>Iso</i> -pentane Grown <i>Mycobacterium vaccae</i> JOB5 .....	 23
2.1 Abstract .....	24
2.2 Introduction .....	26
2.2.1 Degradation of MTBE.....	26
2.2.2 Kinetics and cometabolism.....	28
2.2.3 Objectives .....	29
2.3 Materials and Methods .....	30
2.3.1 Materials.....	30
2.3.2 <i>Mycobacterium vaccae</i> JOB5 growth .....	30
2.3.3 Analytical procedures .....	32
2.3.4 Abiotic TBF hydrolysis rate essay .....	33
2.3.5 Kinetic and inhibition essays .....	34
2.3.6 Control bottles .....	34

## TABLE OF CONTENTS (Continued)

	<u>Page</u>
2.3.7 Growth-batch reactor .....	35
2.3.8 Data analysis and modeling .....	36
2.4 Results.....	36
2.4.1 Cometabolism .....	37
2.4.2 TBF abiotic hydrolysis .....	39
2.4.3 Kinetic constants and inhibition .....	40
2.4.4 Growth batch reactor and STELLA modeling .....	51
2.5 Discussion .....	58
2.6 References .....	63
 Chapter 3     Degradation of Methyl <i>tert</i> -Butyl Ether (MTBE) and its Breakdown Products by Propane and <i>Iso</i> -pentane Grown <i>Mycobacterium vaccae</i> JOB5: Cometabolism and Inhibition .....	       68
3.1 Abstract .....	69
3.2 Introduction.....	70
3.2.1 MTBE metabolites.....	71
3.2.2 Acetylene as a monooxygenase inhibitor.....	71
3.3.3 Objectives .....	72
3.3 Materials and Methods .....	73
3.3.1 Chemicals .....	73
3.3.2 <i>Mycobacterium vaccae</i> JOB5 growth.....	73
3.3.3 Analytical procedures.....	75
3.3.4 Kinetic and inhibition essays .....	76
3.3.5 Transformation under anaerobic conditions .....	77
3.3.6 Blocking experiments with acetylene .....	77
3.3.7 Control bottles.....	79
3.4 Results.....	79

## TABLE OF CONTENTS (Continued)

	<u>Page</u>
3.5 Discussion .....	89
3.6 References .....	91
 Chapter 4 Kinetics of MTBE, TBF, and TBA Aerobic Cometabolism by an <i>n</i> -Alkane Grown Fungal Isolate, <i>Graphium sp.</i> ....	 93
4.1 Abstract .....	94
4.2 Introduction .....	95
4.3 Materials and Methods .....	98
4.3.1 Materials.....	98
4.3.2 <i>Graphium sp.</i> growth.....	98
4.3.3 Analytical procedures.....	101
4.3.4 Kinetic assays .....	103
4.3.5 Data analysis.....	104
4.4 Results.....	106
4.5 Discussion .....	118
4.6 References .....	123
 Chapter 5 MTBE Kinetics by <i>n</i> -Alkane Grown <i>Mycobacterium vaccae</i> and <i>Graphium sp.</i> ....	 126
5.1 Abstract .....	127
5.2 Introduction .....	128
5.3 Materials and methods .....	130
5.4 Results.....	134
5.5 Discussion .....	140
5.6 Acknowledgements.....	144

## TABLE OF CONTENTS (Continued)

	<u>Page</u>
5.7 References .....	145
Chapter 6    Conclusions and Engineering Significance	147
6.1 Degradation Kinetics of Methyl <i>tert</i> -Butyl Ether (MTBE) and its Breakdown Products by Propane and <i>Iso</i> - pentane Grown <i>Mycobacterium vaccae</i> JOB5.....	147
6.2 Degradation of Methyl <i>tert</i> -Butyl Ether (MTBE) and its Breakdown Products by Propane and <i>Iso</i> - pentane Grown <i>Mycobacterium vaccae</i> JOB5: Cometabolism and Inhibition .....	148
6.3 Kinetics of MTBE, TBF, and TBA Aerobic Cometabolism by an Alkane Grown Fungal Isolate, <i>Graphium sp.</i> .....	149
6.4 MTBE Kinetics by <i>n</i> -Alkane Grown <i>Mycobacterium</i> <i>vaccae</i> and <i>Graphium sp.</i> .....	150
6.5 Engineering significance .....	153
 Bibliography.....	 156
 Appendices.....	 165

## LIST OF FIGURES

<u>Figure</u>	<u>Page</u>
1.1 MTBE degradation pathway .....	8
1.2 Hydrolysis of <i>tert</i> - butyl formate (TBF) .....	14
2.1 Aerobic cometabolism of MTBE, TBF, and TBA by <i>iso</i> -pentane grown <i>Mycobacterium vaccae</i> JOB5 .....	38
2.2 Abiotic TBF hydrolysis .....	39
2.3 Initial degradation rate of <i>iso</i> -pentane .....	41
2.4 Biokinetic constants for <i>iso</i> -pentane by NLSR.....	42
2.5 $k_{max}$ and $K_s$ for TBF by direct linear plot .....	46
2.6 $k_{max}^{app}$ and $K_s^{app}$ for MTBE by direct linear plot.....	49
2.7 Inhibition type by direct linear plot .....	50
2.8 Modeling of <i>iso</i> -pentane metabolism and biomass production by <i>Mycobacterium vaccae</i> JOB5 in growth-batch reactors .....	54
2.9 Modeling of MTBE cometabolism by <i>Mycobacterium vaccae</i> JOB5 in growth-batch reactors .....	55
2.10 Modeling of TBA cometabolism by <i>Mycobacterium vaccae</i> JOB5 in growth-batch reactors .....	56
3.1 MTBE cometabolism by propane-grown <i>Mycobacterium</i> <i>vaccae</i> under aerobic conditions .....	80
3.2 Transformation of TBF under aerobic and anaerobic conditions by propane-grown <i>Mycobacterium vaccae</i> .....	81

## LIST OF FIGURES (Continued)

<u>Figure</u>	<u>Page</u>
3.3 Influence of acetylene on aerobic cometabolism of MTBE, TBF, and TBA by the <i>iso</i> -pentane-grown culture .....	84
3.4 Influence of acetylene on aerobic cometabolism of MTBE, TBF, and TBA by the propane-grown culture .....	84
3.5 Influence of media's trace composition on propane degradation.....	87
3.6 Influence of media's trace composition and acetylene on propane degradation .....	88
4.1 Fungal experimental design.....	104
4.2 Cometabolism of MTBE by propane-grown <i>Graphium sp.</i> liquid-culture .....	108
4.3 Filter-attached <i>Graphium sp.</i> growth on propane (triplicate).....	109
4.4 Initial degradation rate of single compound by filter-attached <i>Graphium sp.</i> grown on propane.....	104
4.5 NLSR method to determine $k_{max}$ and $K_s$ for propane .....	111
4.6 Lineweaver-Burk plot method to determine $k_{max}$ and $K_s$ for MTBE.....	112
4.7 Direct linear plot method to determine $k_{max}$ and $K_s$ for TBF.....	113
4.8 Estimation of kinetic constants, $k_{max}$ and $K_s$ , for propane by NLSR .....	115
4.9 Estimation of kinetic constants, $k_{max}$ and $K_s$ , for MTBE by NLSR .....	116

## LIST OF FIGURES (Continued)

<u>Figure</u>	<u>Page</u>
4.10    Estimation of kinetic constants, $k_{max}$ and $K_s$ , for TBF by NLSR .....	116
5.1     Acetylene influence on propane oxidation by <i>Graphium sp</i> .....	139

## LIST OF TABLES

<u>Table</u>	<u>Page</u>
1.1 Physical and chemical properties @ 25 °C.....	15
2.1 Kinetic constants with their 95% C.I. by NLSR .....	44
2.2 Kinetic constants, in the presence of the substrate with their 95% C.I. by NLSR .....	44
2.3 Kinetic constants by direct linear plot from single compound experiments .....	47
2.4 Kinetic constants by direct linear plot from dual compound experiments .....	47
2.5 Degradation rate in a matrix experiment (1:1) ratio for the propane-grown <i>Mycobacterium vaccae</i> culture .....	51
2.6 Parameters used in STELLA modeling for growth batch reactors.....	57
3.1 Degradation under anaerobic conditions (%) by <i>Mycobacterium vaccae</i> after 24 hours .....	82
3.2 Acetylene (AIRCO source) effect on <i>n</i> -alkane oxidation activity by <i>Mycobacterium vaccae</i> JOB5 .....	85
3.3 Acetylene (Calcium carbide source) effect on propane oxidation by <i>Mycobacterium vaccae</i> JOB5 in two different liquid composition .....	86
4.1 Kinetic coefficient values for filter-attached <i>Graphium</i> sp. grown on propane .....	114
5.1 Kinetic constants with their 95% C.I. by NLSR .....	137



## LIST OF TABLES (Continued)

<u>Table</u>	<u>Page</u>
5.2 Degradation (%) under anaerobic conditions with propane grown cultures after 24 hours exposure .....	137

## LIST OF APPENDICES

	Page
Appendix A Gas chromatography analysis .....	166
A.1 Propane and <i>iso</i> -pentane .....	166
A.1.1 Propane .....	167
A.1.2 <i>iso</i> -pentane .....	167
A.2 MTBE, TBF, and TBA .....	168
A.2.1 Liquid injection samples .....	168
A.2.2 Head space injection samples .....	169
Appendix B Culturing <i>Graphium sp.</i> .....	171
B.1 Stock cultures .....	171
B.2 Harvesting of conidia .....	172
B.3 Mineral salts growth medium .....	174
Appendix C Model development and STELLA modeling .....	176
C.1 Metabolism of propane and <i>iso</i> -pentane and cometabolism of MTBE, TBF, and TBA .....	171
C.1.1 Inhibition .....	179
C.1.2 Microbial growth .....	181
C.2 Bacterial system modeling .....	183
C.2.1 Low initial biomass concentration .....	183
C.2.2 Independent solution and Fortran code .....	187
C.2.3 High initial biomass concentration .....	197
C.3 Fungal system modeling .....	200

## LIST OF APPENDICES (Continued)

	<u>Page</u>
Appendix D Visual Basic program for direct linear plot.....	209
D.1 Instructions .....	209
D.2 Visual Basic program .....	211
D.3 Example .....	220
Appendix E Overall studies for <i>Graphium sp.</i> ....	226
E.1 Complete MTBE degradation under aerobic conditions ..	208
E.2 Acetylene influence on the degradation of propane, MTBE, and TBF .....	229
E.3 Degradation under anaerobic conditions .....	234
E.4 Degradation under anaerobic/aerobic conditions .....	235
E.5 Estimation of TBA degradation rate.....	236
E.6 Estimation of kinetic constants for propane-grown filter- attached <i>Graphium sp.</i> ....	239

## LIST OF APPENDIX FIGURES

<u>Figure</u>	<u>Page</u>
C.1     Diagram for STELLA simulation. Metabolism of <i>iso</i> -pentane and cometabolism of MTBE, TBF and TBA by <i>Mycobacterium vaccae</i> in growth batch reactor.....	184
C.2     Equations for model simulation in STELLA. Metabolism of <i>iso</i> -pentane and cometabolism of MTBE, TBF, and TBA by <i>iso</i> -pentane-grown <i>Mycobacterium vaccae</i> in growth batch reactor .....	185
C.3     Production of <i>Mycobacterium vaccae</i> in growth batch reactor ....	189
C.4     Fortran code.....	192
C.5     Growth batch reactor modeling with STELLA and Fortran code .....	196
C.6     Metabolism of <i>iso</i> -pentane by concentrated <i>iso</i> -pentane grown <i>M. vaccae</i> cells.....	197
C.7     Cometabolism of MTBE, TBF, and TBA by concentrated <i>iso</i> -pentane grown <i>M. vaccae</i> cells .....	199
C.8     Cometabolism of TBF, and TBA by concentrated <i>iso</i> -pentane grown <i>M. vaccae</i> cells .....	200
C.9     STELLA simulation diagram for the cometabolism of MTBE by propane-grown <i>Graphium sp.</i> (Filter-attached culture) .....	201
C.10    Equations for model simulation in STELLA. Cometabolism of MTBE by propane-grown <i>Graphium sp.</i> (Filter-attached culture) .....	202
C.11    STELLA simulation diagram for the cometabolism of TBF by Propane-grown <i>Graphium sp.</i> (Filter-attached culture).....	203

## LIST OF APPENDIX FIGURES (Continued)

<u>Figure</u>	<u>Page</u>
C.12	Equations for model simulation in STELLA. Cometabolism of TBF by propane-grown <i>Graphium</i> sp. (Filter-attached culture) 204
C.13	Cometabolism of MTBE by propane-grown <i>Graphium</i> sp. (filter-attached) .....206
C.14	Cometabolism of TBF by propane-grown <i>Graphium</i> sp. (filter-attached culture)..... 208
D.1	Direct linear plot method to determine $k_{max}$ and $K_s$ for TBF ..... 225
E.1	Degradation of MTBE in the absence and presence of propane .....227
E.2	<i>Graphium</i> sp. killed control bottle .....228
E.3	Inhibition of propane oxidation by acetylene .....229
E.4	Inhibition of propane oxidation by acetylene .....230
E.5	Inhibition of propane oxidation by acetylene ..... 230
E.6	Acetylene influence on MTBE degradation .....231
E.7	Acetylene influence on TBF degradation .....232
E.8	TBF influence on propane oxidation .....233
E.9	Degradation of propane, MTBE, TBF, and TBA under anaerobic conditions by <i>Graphium</i> sp.....234
E.10	Degradation of propane, MTBE, TBF, and TBA under anaerobic/aerobic conditions by <i>Graphium</i> sp. ....235

## LIST OF APPENDIX FIGURES (Continued)

<u>Figure</u>	<u>Page</u>
E.11    Degradation of propane, MTBE, TBF, and TBA in killed control bottle by <i>Graphium sp.</i> .....	236
E.12    TBA degradation from TBF bottles by <i>Graphium sp.</i> .....	238

## LIST OF APPENDIX TABLES

<u>Table</u>	<u>Page</u>
A.1 Retention time (min) of compounds analyzed by gas chromatography.....	170
C.1 Equations used in STELLA modeling for the degradation of substrate and cometabolism of MTBE, TBF, TBA .....	183
C.2 Parameters used in computation of biomass from <i>iso</i> -pentane metabolism in growth batch reactor.....	189
C.3 Parameters used in STELLA modeling for MTBE cometabolism by propane-grown <i>Graphium sp.</i> (filter-attached culture) .....	205
C.4 Parameters used in STELLA modeling for TBF cometabolism By propane-grown <i>Graphium sp.</i> (filter-attached culture).....	207
D.1 TBF experimental data (filter-attached <i>Graphium sp.</i> ) .....	220
D.2 Slope and intercept for TBF data .....	221
D.3 Results by pairs in the direct linear plot for TBF .....	222
D.4 Sorted values and best estimates of $k_{max}$ and $K_s$ for the cometabolism of TBF by <i>Graphium sp</i> .....	223
E.1 Propane and O <sub>2</sub> added to bottles M6 and M7 .....	228
E.2 TBA Kinetics experimental data by liquid sample analysis .....	237
E.3 TBA degradation rate from TBF experimental bottles .....	238
E.4 Propane experimental data .....	239
E.5 MTBE experimental data.....	240
E.6 TBF experimental data.....	240

## LIST OF APPENDIX TABLES (Continued)

<u>Table</u>	<u>Page</u>
E.7    Kinetic constants for propane metabolism with their 95% C.I. by NLSR .....	241
E.8    Kinetic constants for MTBE cometabolism with their 95% C.I. by NLSR .....	242
E.9    Kinetic constants for TBF cometabolism with their 95% C.I. by NLSR .....	242
E.10   Kinetic constants for propane metabolism by reciprocal plot .....	243
E.11   Kinetic constants for MTBE cometabolism by reciprocal plot .....	244
E.12   Kinetic constants for TBF cometabolism by reciprocal plot .....	244
E.13   Kinetic constants by direct linear plot .....	245



## DEDICATION

I want to dedicate this thesis to my parents José Luis Martínez-Ceceñas (†) and Juliana Prado de Martínez; to my brothers and sisters; to all my family and friends in México; to my husband Joaquin Pinto-Espinoza, and to my children Addy, Joao, and Emmanuel Pinto-Martínez for their support, encouragement and love in bad and good times through all my life.

# **Biodegradation of Methyl *tert*-Butyl Ether (MTBE) and its Breakdown Products by Propane and *iso*-Pentane Grown *Mycobacterium vaccae* and *Graphium* sp. : Cometabolism, Inhibition, Kinetics and Modeling**

## **CHAPTER 1. Introduction**

Since the early 1980s, methyl *tert*-butyl ether (MTBE) has been the most common octane booster and fuel oxygenate used in gasoline in the United States. Such gasoline additives have been required mainly because of the stringent phase-out requirements for lead. MTBE is colorless, flammable, and has a distinctive unpleasant odor. As an ether, MTBE contains up to 15% (v/v) oxygen that results in reduction of carbon monoxide emissions from internal combustion vehicles (Jacobs et al., 2000). MTBE can be synthesized easily and cheaply from a combination of isobutene and methanol or from methanol and *tert*-butyl alcohol (TBA).

MTBE was added to gasoline as an oxygenate, especially for localities that fail to meet ambient air quality standards. The Clean Air Act of 1990 mandated the use of so-called "reformulated gasoline;" by the late 1990s, widespread surface and groundwater MTBE contamination caused by gasoline spills and leakage became a crisis across the U.S. Currently, oxygenates are added to the majority of U.S. gasoline and 85% of all reformulated gasoline contains MTBE. Leaks from underground storage

tanks have resulted in MTBE being the second most common ground water pollutant in the U.S. (Squillace et al., 1996). A national strategy is presently being developed to attempt removal of MTBE already dispersed in the environment and phase out of MTBE is already planned by 2004 with ethanol as the suggested substitute.

MTBE is highly mobile and persistent. It is considered a possible human carcinogen (EPA, 1997) for which the Drinking Water Advisory has been set at 20 to 40  $\mu\text{g/L}$  (ppb). This Advisory was set to minimize human health risks and eliminate unpleasant tastes and odors in drinking water. A primary and secondary maximum contaminant level (MCL) for MTBE has been set by the State of California as 13 and 5  $\mu\text{g/L}$ , respectively.

## **1.1 Literature review**

### **1.1.1 Environmental impacts**

MTBE is considered to be chemically and biologically stable because of its tertiary carbon structure and ether linkage (Garnier et al., 1999). MTBE has high water solubility that ranges from 43 to 54 g/L (Squillace et

al., 1998; resulting in high groundwater concentrations when gasoline-containing MTBE contaminates aquifers. Reported values for the vapor pressure of MTBE (25 °C) ranges from 245 to 256 mm Hg (Zogorski et al., 1996). Due to its high water solubility and low vapor pressure, MTBE has a low dimensionless Henry's coefficient (0.022 @ 25 °C). MTBE is not strongly sorbed onto soils ( $K_{oc} = 1.05$ ), which results in a low retardation factor ( $R = 1.05$ ) and significant transport from the original source area. MTBE tends to remain in the water phase, is not easily air stripped, and moves rapidly with groundwater.

MTBE has been detected in different environmental compartments: lakes (Reuter et al. 1998); (Koenigsberg et al. 1999); storm water (Zogorski et al., 1997); groundwater (Squillace et al., 1996; Church et al., 1999; Landmeyer et al., 2001), and urban air (Grosjean et al., 1998). Production, transportation, use, and storage of the oxygenate compound and reformulated gasoline are the most common sources for the entrance of MTBE to these compartments. Common point sources of MTBE are gasoline spills and releases from fuel storage tanks. Non-point sources include precipitation, urban runoff, and dispersed sources of gasoline such as emissions from motorized watercraft. Most of the MTBE-related studies reported are concern environmental impact, especially the detection and remediation of MTBE in drinking water resources.

### **1.1.2 Potential remedial mechanisms**

MTBE has been subject of extensive research to find the best alternative for removal from contaminated sites. Both biotic and abiotic processes have been studied under aerobic or anaerobic conditions for in-situ or on-site bioremediation. Several strategies had been suggested to treat MTBE such as biostimulation and bioaugmentation (Salanitro et al., 2001); pump and treat; soil vapor extraction; air stripping and carbon adsorption; chemical oxidation (Leethem, 2001); natural attenuation (Soo and Wilson, 1999); aerobic degradation (Salanitro et al., 1994; Hanson et al., 1996); aerobic cometabolism (Hardison et al., 1997; Hyman et al., 1998; Garnier et al., 1999); anaerobic degradation (Finneran and Lovley, 2001; Yeh and Novak, 1994); and phytoremediation (Qizhi et al., 2001).

Degradation or transformation of a compound can occur by biotic and abiotic reactions. Complete breakdown or mineralization of the organic compound results in the production of carbon dioxide and water and may involve multiple steps and long time periods. The degradation pathway might be influenced by several factors including the media in which it is dispersed (air, water, or soil). For many compounds, biological transformation often provides the predominant decay pathways in soil and water, often leading to mineralization. However, most studies have

indicated that MTBE does not biodegrade rapidly in water and is often classified as recalcitrant.

MTBE degradation by microbes has been suggested to be site and microorganism specific. Few MTBE degraders (sole carbon and energy source) have been found and are not considered ubiquitous. Their growth rates are considered to be very slow (Deeb et al. 2001). Aerobic degradation of MTBE has been reported in mixed cultures derived from activated sludge (Salanitro et al., 1994; Park and Cowan, 1997), pure cultures on alkane oxidizing bacteria (Garnier et al., 1999; Hyman et al., 1998; Steffan et al., 1997), and a fungal strain, *Graphium* sp. (Hardison et al., 1997).

For example, Steffan et al., (1997) reported biodegradation of MTBE, ethyl tert-butyl ether (ETBE), and tert-amyl methyl ether (TAME) by several bacteria. Hanson et al., (1996, 1999) identified PM1 and YM1 as two isolated bacterial strains that can use MTBE as their only source of energy and carbon and are closely related to the *Sphingomonas* species. Anaerobic degradation of MTBE and TBA has also been reported (Finneran and Lovley, 2001) in which the addition of humic substances has been shown to stimulate the anaerobic degradation in aquifer sediments in which Fe (III) was available as an electron acceptor.

### 1.1.3 Biodegradation

MTBE degradation was suggested to be slow based on its chemical structure, physical and chemical properties, and early laboratory results. Many different microorganisms have been investigated under a variety of conditions related to their capability to degrade MTBE. Recent studies have shown that MTBE can be oxidized by direct metabolism as a sole source of carbon and energy or via cometabolism after growth on an easily degradable compound such as alkanes.

It has been reported that a number of bacteria and a fungal strain (*Graphium sp.*) can utilize alkanes as a primary substrate (Philips and Perry, 1974; Perry, 1980; Curry et al., 1996; Hardison et al., 1997). The alkanes are oxidized to the corresponding primary or secondary alcohols by mono-oxygenases through terminal or sub-terminal oxidation. Insertion of oxygen results in propane oxidation to 2-propanol with further oxidation to acetone (Perry, 1980). Propane also can be oxidized to 1-propanol undergoing terminal oxidation (Stephens and Dalton, 1986).

Propane-oxidizing bacteria utilize propane for energy and as a carbon source, using a propane mono-oxygenase enzyme (PMO) to start the oxidation of propane (Wacket et al., 1989). PMO is non-specific enough to oxidize some aliphatic hydrocarbons and short-chain alkenes (Tovanabootr, 1997; Curry et al., 1996; Hardison et al., 1997). Due to the

non-specificity, PMO has been suggested as responsible for the transformation of chlorinated hydrocarbons (CAH's) and some oxygenates such as MTBE, TAME, and ETBE. PMO in *Mycobacterium vaccae* JOB5 has been implicated in the degradation of trichloroethylene (TCE). Butane mono-oxygenase (BMO) also was suggested to be responsible for the butane oxidation and cometabolism of chloroform as well (Hamamura et al., 1997). A similar mono-oxygenase is suggested to be present in the filamentous fungus, *Graphium* sp..

#### **1.1.4 MTBE degradation metabolites**

MTBE breakdown products vary depending upon growth conditions and the microorganism species. *Tert*- butyl alcohol (TBA) is one of the most common intermediates reported, followed by *tert*-butyl formate (TBF), formaldehyde, 2-methyl 1-hydroxy 2-propanol (MHP), 2-hydroxyisobutyric acid (HIBA), 2-propanol and acetone. CO<sub>2</sub> has been directly produced from MTBE with no intermediates. Methane and carbon dioxide are the end products in the anaerobic degradation process for either MTBE or TBA. These metabolites were found reported in the studies reviewed in the following sections and same references apply. A general schematic of MTBE degradation is shown in Figure 1.1 based on these studies.



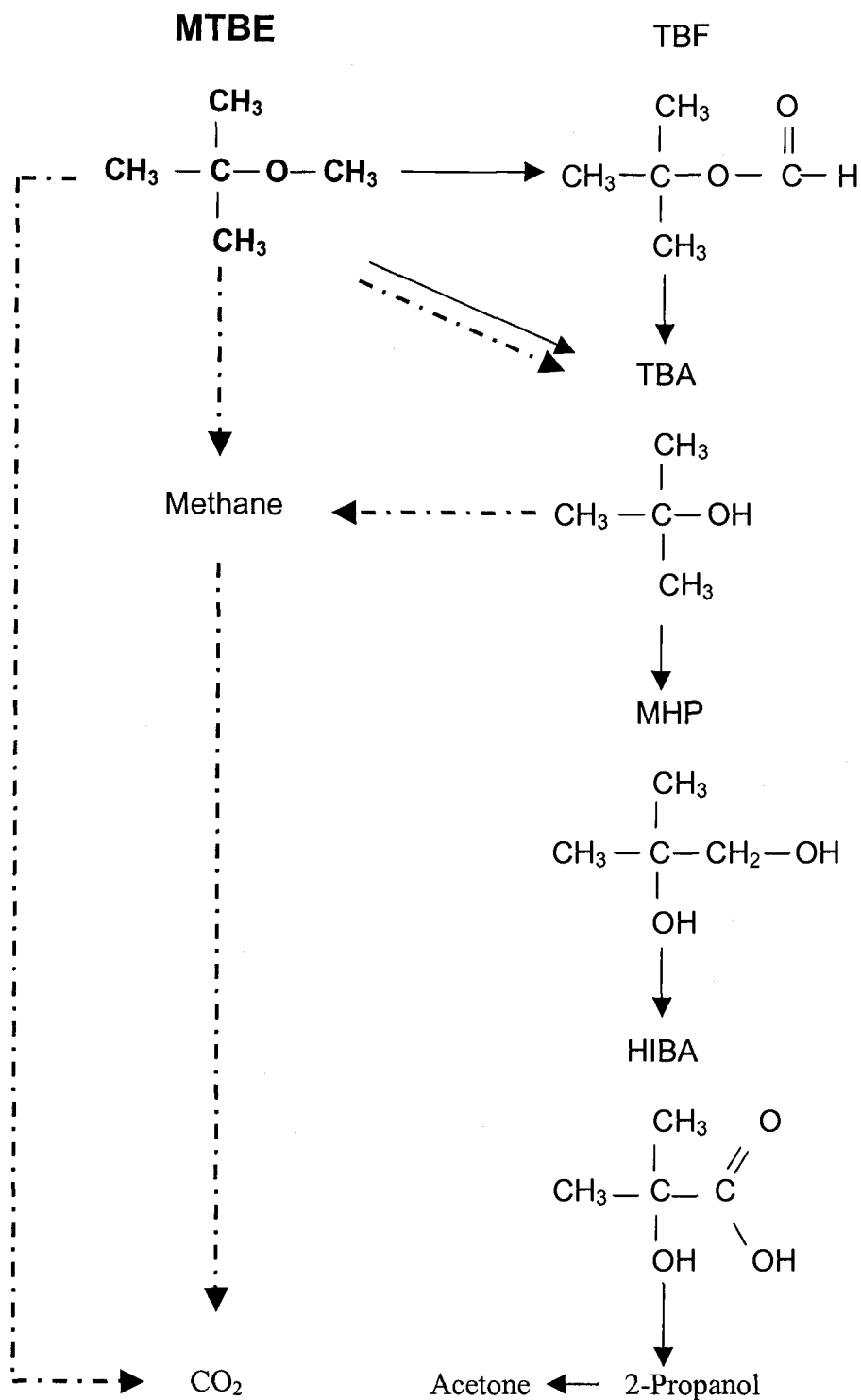


**Figure 1.1** MTBE degradation pathway. Metabolites observed from MTBE degradation under aerobic ( —————> ) and anaerobic ( - - - -> ) conditions. Summarized and adapted from all studies cited in literature review.

### 1.1.5 MTBE metabolism as a primary substrate

Several studies have reported the use of pure or mixed culture capable of direct MTBE degradation as the sole source of carbon and energy. Most of these microorganisms showed low biomass production, which may limit the degradation rates of MTBE.

Salanitro et al., (1994) and Salanitro and Wisniewski, (1996) reported BC-1 as a heterotrophic mixed culture that was able to grow on MTBE as a primary substrate. Growth rates (0.01 1/day) and yields (0.28 g cells/g MTBE) were very low. TBA was the only identified metabolite, which was further degraded at a slower rate when almost all MTBE was consumed. TBA was not utilized as a growth substrate. Park and Cowan (1997) reported a mixed culture for which MTBE and TBA supported growth as a primary source. Low growth rates and moderate cellular yields were obtained with a reduction in both by a decrease in temperature.

Mo et al., (1997) identified three pure cultures, *Methylobacterium mesophilicum* (ATC700107), *Rhodococcus* sp (ATC 700108, and *Arthrobacter ilicis* (ATC 700109), from the fruit of Ginkgo tree and from activated sludge that used MTBE as a primary substrate. The MTBE oxidation rates decreased when more easily degradable compounds such as TBA, TBF, isopropanol, acetone, and pyruvate were added. They concluded that MTBE is a poor growth substrate. Salanitro et al.,

(1997,1999) identified BC-4 (mixed culture), MC-100 (mixed culture), and SC-100 (*Rhodococcus* pure culture) that degrade MTBE to non-detectable levels.

A pure bacterial culture, PM1 (*Proteobacteria* member) (Hanson et al., 1999), was found to be capable of degrading MTBE as a sole carbon and energy source; the estimated yield was 0.18 mg cells/mg MTBE. TBA was not detected from MTBE metabolism, which suggests a high transformation rate. PM1 also utilized TBA as a primary growth substrate.

Mixed culture from biotrickling filters (Fortin et al., 1997; Fortin and Deshusses, 1998; Fortin and Deshusses, 1999) were found to mineralize MTBE with ultimate CO<sub>2</sub> production. Degradation of TBA occurred at about the same rate as MTBE. Low specific growth rates (0.025 1/day) and cellular yields (0.1 g dry weight/g MTBE) were also a characteristic of these MTBE- degraders as in other similar studies.

#### **1.1.6 MTBE aerobic cometabolism**

Aerobic cometabolism occurs in the presence of a growth-supporting substrate and results in the ability of microorganisms to transform non-growth supporting substrates such as MTBE. The production of oxygenases by alkane oxidizers suggests that cometabolism offers a biological strategy

for MTBE bioremediation from a contaminated site. Numerous laboratory and field studies had been conducted to demonstrate the applicability of cometabolism for MTBE. Studies on aerobic cometabolism have reported the ability of pure and mixed cultures to degrade MTBE to TBF, TBA or CO<sub>2</sub> after grown on alkanes or aromatic compounds.

Steffan et al., (1997) reported *Mycobacterium vaccae* JOB5, ENV420, ENV421 and ENV425, all propane-oxidizing bacteria, as able to cometabolize MTBE. TBA was produced from cometabolism. TBA degraded at a slow rate until all MTBE was removed. ENV425 mineralized MTBE. At least one enzyme involved in MTBE degradation is likely a soluble P-450, most likely a propane mono-oxygenase (PMO). Hardison et al., (1997) found that *Graphium* sp., a filamentous fungus, was able to cometabolize MTBE after grown on *n*-butane and propane. Based on the fact that acetylene and ethylene inhibited MTBE and alkane degradation, it was suggested that the same enzyme, a cytochrome P-450, oxidizes both. Oxidation rates of MTBE decreased in the presence of *n*-butane, suggesting competitive inhibition. TBF and TBA were the identified breakdown products. Hyman et al., (1998) and Hyman and O'Reilly, (1999) reported that *Xanthobacter*, *Alcaligenes eutrophus* and *Mycobacterium vaccae*, after growth on straight chain or branched alkanes, were able to degrade MTBE. Both TBF and TBA were the metabolites from MTBE oxidation. Similarly, *Pseudomonas aeruginosa* (Garnier et al., 1999),

isolated from a gasoline-contaminated soil consortium, degraded MTBE after growth on pentane. TBA was produced from MTBE oxidation and was further degraded. Competitive inhibition was observed between MTBE and pentane, suggesting a single enzymatic site for the two compounds. A mixed culture PEL-B201 (Koenigsberg et al., 1999) was found to cometabolize MTBE after growth on benzene. Benzene inhibited MTBE degradation, suggesting that this behavior is due to competitive inhibition. Microorganisms grown on benzene, o-xylene, camphor, and cyclohexanone achieved substantial MTBE degradation.

In summary, aerobic cometabolism has been shown to be effective for degradation of MTBE with a variety of different microorganisms.

#### **1.1.7 MTBE anaerobic degradation**

Only a few studies have reported the degradation of MTBE under anaerobic conditions. Yeh and Novak (1994) tested soils from three different geographical sites. MTBE was degraded in one soil with a low organic carbon content and under methanogenic conditions. MTBE degradability was influenced by the presence of easily degraded compounds. In another study in a contaminated aquifer, Hurt et al., (1999)

showed that MTBE was degraded under anaerobic conditions. TBA was detected only in the region of the aquifer where MTBE degradation occurred. A more recent study (Finneran and Lovley, 2001) reported the potential for the anaerobic degradation of both MTBE and TBA. The degradation was stimulated when humic substances were added to the aquifer sediments in which Fe (III) was available as an electron acceptor.

#### **1.1.8 Scale-up and field studies**

Supported by successful laboratory study results, several studies at field scale have been performed to evaluate the applicability of bioremediation to degrade MTBE. Fortin and Deshusses (1999) used biofilters that were inoculated with groundwater and aquifer material introducing MTBE in an air stream as the sole source of carbon and energy source. MTBE was degraded directly to CO<sub>2</sub> with no intermediate metabolites detected. In another study, a compost filter (Eweis et al., 1997) showed that pure and mixed cultures were able to oxidize MTBE also as a primary substrate. TBA, methanol, and toluene were also degraded by the culture. TBA did not accumulate in the system. Church et al., (1999) reported a study of aerobic MTBE degradation in packed columns with aquifer material. The degradation was influenced by the presence of BTEX

compounds (benzene, ethylene, toluene and xylene). TBA accumulated and no further degradation occurred.

Salanitro et. al., (1999) reported the degradation of about 2 to 8 mg/L of MTBE in an O<sub>2</sub>-amended aquifer zone at the Port Hueneme Naval Base Site in California over a period of 260 days. The oxygen was supplement to increase the concentration from 1 mg/L up to a maximum of 20 mg/L. Their results suggested the presence of natural occurring MTBE-degraders.

### 1.1.9 TBF hydrolysis

Hydrolysis is a potential degradation pathway for any organic compound containing sites susceptible to nucleophilic substitution in the presence of water (Mill, 1982). TBF has an ester group that can be hydrolyzed to TBA and formic acid as illustrated in Figure 1.2.

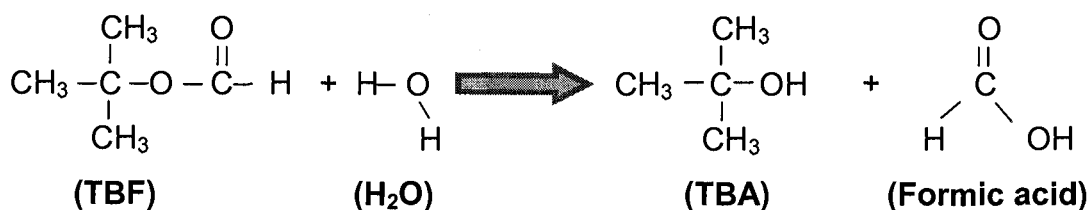


**Figure 1.2** Hydrolysis of *tert*- butyl formate (TBF)

## 1.2 Physicochemical properties of compounds tested

Table 1.1 summarizes the physical and chemical properties of substrates, propane and *iso*-pentane, and the co-substrates, MTBE, TBF, and TBA.

**Table 1.1** Physical and chemical properties @ 25 °C

Property	<i>Iso</i> -pentane	Propane	MTBE	TBF	TBA
Molecular Formula	C <sub>5</sub> H <sub>12</sub>	C <sub>3</sub> H <sub>8</sub>	C <sub>5</sub> H <sub>12</sub> O	C <sub>5</sub> H <sub>10</sub> O <sub>2</sub>	C <sub>4</sub> H <sub>10</sub> O
Molecular Weight (g/mol)	72.15	44.1	88.15	104.12	74.12
Solubility (g/m <sup>3</sup> )	47.8 – 49.6	62.4	43 – 54 (10 <sup>3</sup> )	17.4 x 10 <sup>3</sup>	Fully miscible
Vapor pressure (atm)	0.914	9.29	0.322	N.A.	0.041
Henry's Coefficient	56.5	28.9	0.022	0.024	0.0001
Boiling point (°C)	- 42.1	27.9	55.2	81- 83	82-83

**References:**

Mackay, D. and Shiu, W., 1982 (Propane and *iso*-pentane)

Garnier et al., 1999; Zogorski et al., 1996 (MTBE)

Church et al., 1999; MSDS Sigma Aldrich (TBF) MSDS Sigma Aldrich (TBA)



### 1.3 Objectives

In summary, it is suggested that an alkane monooxygenase in both microbial systems, *Mycobacterium vaccae* JOB5 and *Graphium sp.*, may be responsible for the degradation of non-supporting growth substrates such as MTBE. Previous studies at Oregon State University (OSU) indicated that both *Mycobacterium vaccae* JOB5 and *Graphium sp.* were able to degraded MTBE via cometabolism (Hyman et. al., 1998; Kwon, 1998; Hardison et. al., 1997) after utilizing alkanes as a primary substrate. *Graphium sp.* is a filamentous fungus eukaryote, and a soil born ascomycete. It has very different biological properties from those of *Mycobacterium vaccae* JOB5, a prokaryote and gram-positive bacterium. Both microorganisms seem to have similar behavior in regard to their alkane oxidation pathways and MTBE cometabolism.

Based upon this literature review, the following objectives were developed for this research:

- 1) To evaluate the potential of two different pure cultures, *Mycobacterium vaccae* JOB5 and *Graphium sp.*, to degrade MTBE and its metabolites under aerobic and

anaerobic conditions after grown on two different alkanes, *iso*-pentane and propane, as primary substrates.

- 2) To evaluate the influence of TBF abiotic hydrolysis in the biodegradation process.
- 3) To determine biokinetic constants for these two cultures from experimental data by established microbiological methods.
- 4) To elucidate the type of enzymes promoting the degradation of MTBE and its metabolites through evaluation of inhibition effects from acetylene.
- 5) To determine the ability of the biokinetic constant from Objective 3 to predict results from batch growth reactor experiments with the *Mycobacterium vaccae* culture using *iso*-pentane as the growth substrate and MTBE as a co-substrate.

## 1.4 References

- Church, C. D., P. G. Tratnyek, J. F. Pankow, J. E. Landmeyer, A. L. Baehr, M. A. Thomas and M. Schirmer. 1999. Effects of environmental conditions on MTBE degradation in model column aquifers. U. S. Geological Survey: 93 - 101.
- Curry, S., L. Ciuffetti and M. Hyman. 1996. Inhibition of growth of a *Graphium* sp. on gaseous *n*-alkanes by gaseous *n*-alkynes and *n*-alkenes. Appl. Environ. Microbiol. 62: 2198-2200.
- Deeb, R. A., H.-Y. Hu, J. R. Hanson, K. M. Scow and L. Alvarez-Cohen. 2001. Substrate interactions in BTEX and MTBE mixtures by an MTBE-degrading isolate. Environ. Sci. Technol. 35: 312-317.
- Eweis, J., D. P. Chang, E. Schroeder, K. Scow, R. Morton and R. Caballero. (1997). Meeting the challenge of MTBE biodegradation. 90th Annual Meeting and Exhibition of the Air and Waste Management Association, Toronto, Canada.
- Finneran, K. T. and D. R. Lovley. 2001. Anaerobic degradation of methyl *tert*-butyl ether (MTBE) and *tert*-butyl alcohol (TBA). Environ. Sci. Technol. 35: 1785-1790.
- Fortin, N., M. Deshusses, J. Eweis, R. S. Hanson, K. Scow, D. P. Chang and E. Schroeder. (1997). Biodegradation of MTBE: Kinetics, metabolism of degradation by-products and role of oxygen release compounds. 1997 ACS Pacific Pacific Conference on Chemistry and Spectroscopy.
- Fortin, N. Y. and M. Deshusses. 1999. Treatment of methyl *tert*-butyl ether vapors in biotrickling filters. 1. Reactor startup, steady-state performance, and culture characteristics. Environ. Sci. Technol. 33: 2980-2986.
- Garnier, P. M., R. Auria, C. Augur and S. Revah. 1999. Cometabolic biodegradation of methyl *t*-butyl ether by *Pseudomonas aeruginosa* grown on pentane. Appl. Microbiol. Biotechnol. 51: 498-503.
- Grosjean, E., D. Grosjean, R. Guanawardena and R. Rasmussen. 1998. Ambient concentrations of ethanol and methyl *tert*-butyl ether in Porto Alegre, Brazil, March 1996 to April 1997. Environ. Sci. Technol. 32: 736 - 742.

Hamamura, N., C. Page, T. Long, L. Semprini and D. Arp. 1997. Chloroform cometabolism by butane-grown CF8, *Pseudomonas butanorova* and *Mycobacterium vaccae* JOB5 and methane-grown *Methylosinus trichosporium* OB3b. *Appl. Environ. Microbiol.* 63: 3607-3613.

Hanson, J., K. M. Scow, M. Bruns and T. Brethour. (1996). Characterization of MTBE-degrading bacterial isolates and associated consortia. MTBE Workshop, Univ. of Calif., Davis.

Hanson, R. S., C. E. Ackerman and K. Scow. 1999. Biodegradation of methyl *tert*-butyl ether by a bacterial pure culture." *Appl. Environ. Microbiol.* 65: 4788 - 4792.

Hardison, L., S. Curry, L. Ciuffetti and M. Hyman. 1997. Metabolism of diethyl ether and cometabolism of methyl *tert*-butyl ether by a filamentous fungus, *Graphium* sp." *Appl. Environ. Microbiol.* 63: 3059-3067.

Hurt, K. L., J. T. Wilson, F. P. Beck and J. S. Cho. (1999). Anaerobic biodegradation of MTBE in a contaminated aquifer. Fifth International In Situ and On-Site Bioremediation Symposium, Monterrey, Ca., Battelle.

Hyman, M., P. Kwon, K. J. Williamson and K. O'Reilly. (1998). Cometabolism of MTBE by alkane-utilizing microorganisms. In G.B. Wickramanayake and R. Compounds. Batelle Press, Columbus, OH.

Hyman, M. and K. O'Reilly. (1999). Physiological and enzymatic features of MTBE-degrading bacteria. In *In Situ Bioremediation of Petroleum Hydrocarbon and Other Organic Compounds*, 5: 7-12. Batelle Press, Columbus. OH,.

Jacobs, J., J. Guertin and C. Herron. (2000). MTBE: effects on soil and groundwater resources, Lewis Publishers.

Koenigsberg, S., C. Sandefur, W. Mahaffey, M. Deshusses and N. Fortin. (1999). Peroxygen mediated bioremediation of MTBE. Fifth International In Situ and On-Site Bioremediation Symposium, Monterrey, Ca., Batelle Press, Columbus. OH,.

Kwon, P. O. 1998. A study of in-situ bioremediation of methyl *tert*-butyl ether (MTBE) through cometabolic processes by alkane-utilizing microorganisms. Project report. Oregon State University. Corvallis, OR.

Landmeyer, J. E., F. H. Chapelle, H. H. Herlong and P. M. Bradley. 2001. Methyl *tert*-butyl ether biodegradation by indigenous aquifer microorganisms under natural and artificial oxic conditions. *Environ. Sci. Technol.* 35: 1118 - 1126.

Leethem, J. T. 2001. In Situ Chemical oxidation of MTBE and BTEX in soil and groundwater: A case study. *AEHS, Contaminated Soil, Sediment and Groundwater, The magazine of Environmental Assessment & Remediation*: 54-58.

Mackay, D. and W. Ying 1981. Critical review of Henry's Law constants for chemicals of environmental interest. *J. Phys. Chem.* 10: 1175-1195.

Mill, T. 1982. Hydrolysis and oxidation processes in the environment. *Environ. Toxicol. Chem.* 1: 135-141.

Mo, K., O. Lora, A. E. Wanken and M. Javammardian. 1997. Biodegradation of methyl *t*-butyl ether by pure bacterial cultures. *Appl. Microbiol. Biotechnol.* 47: 69-72.

Park, K. and R. Cowan. (1997). Biodegradation of gasoline oxygenates. Fourth international in situ and on-site bioremediation symposium.

Perry, J. J. 1980. Propane utilization by microorganisms. *J. of Bacteriology* 26: 89 - 115.

Philips, W. E. and J. J. Perry. 1974. Metabolism of n-butane and 2-butanol by *Mycobacterium vaccae*. *J. of Bacteriology* 120: 987 - 989.

Qizhi, Z., L. C. Davis and L. E. Erickson. 2001. Transport of methyl *tert*-butyl ether through alfalfa plants. *Environ. Sci. Technol.* 35: 725 - 731.

Reuter, J. E., B. C. Allen, R. C. Richards, C. F. Pankow, C. R. Goldman, R. L. Scholl and J. S. Seyfried. 1998. Concentrations, sources, and fate of the gasoline oxygenate methyl *tert*-butyl ether (MTBE) in a multiple-use lake. *Environ. Sci. Technol.* 32: 3666 - 3672.

Salanitro, J., L. Diaz, M. Williams and H. Wisniewski. 1994. Isolation of a bacterial culture that degrades methyl *tert*-butyl ether. *Appl. Microbiol.* 60: 2593-2596.

Salanitro, J., G. Spinnler, P. Maner, H. Wisniewski and P. Johnson. (1999). Potential for MTBE bioremediation-*in situ* inoculation of specialized cultures. Conference on Petroleum Hydrocarbons and Organic Chemicals in Ground Water: Prevention, Detection and Remediation, Houston, TX.

Salanitro, J. and H. Wisniewski. (1996). Observations on the biodegradation and bioremediation potential of methyl *tert*-butyl ether. 17th Annual Meeting of the Society of Environmental Toxicology and Chemistry.

Salanitro, J. P., G. E. Spinnler, P. M. Maner and K. A. Lyons. 2001. Enhanced bioremediation of MTBE (Bioremedy) at retail gas stations. AEHS, Contaminated Soil, Sediment and Groundwater. The Magazine of Environmental Assessment & Remediation: 47-49.

Soo, C. J. and Wilson, J.T. (1999). Hydrocarbon and MTBE removal rates during natural attenuation application. Battelle Conference, In situ and On site Bioremediation. Batelle Press, Columbus. OH,.

Squillace, P., J. F. Pankow and J. Zogorski. (1998). Environmental behavior and fate of methyl *tert*-butyl ether (MTBE). The Southwest Focused Groundwater Conference, Anaheim, California, National Ground Water Association.

Squillace, P. J., J. S. Zogorski, W. G. Weber and V. Price. 1996. Preliminary assessment of the occurrence and possible sources of MTBE in groundwaters in the United States, 1993 -1994. Environ. Sci. Technol. 30: 721-30.

Steffan, J., K. McClay, S.Vainberg, C. Condee and D. Zhang. 1997. Biodegradation of the gasoline oxygenates methyl *tert*-butyl ether and *tert*-amyl methyl ether by propane-oxidizing bacteria. Appl. Environ. Microbiol. 63: 4216-4222.

Stephens, G. M. and H. Dalton. 1986. The role of terminal and subterminal oxidation pathways in propane metabolism by bacteria. J. of Gral. Microbiol. 132: 2453 - 2462.

Tovanabootr, A. 1997. Aerobic cometabolism of chlorinated aliphatic hydrocarbons by subsurface microbes grown on methane, propane, and butane from McClellan Air Force Base. M. S. Thesis. Oregon State University. Corvallis, OR.

EPA, 1997. Drinking Water Advisory: Consumer acceptability advice and health effects analysis on MTBE.

USGS, 2001. National survey of MTBE, other ether oxygenates and other VOCs in other community drinking-water resources. Report 01-399. Rapid City, South Dakota.

Wackett, L. P., G. A. Brusseau, S. R. Householder and R. S. Hanson. 1989. Survey of microbial oxygenase:trichloroethylene degradation by propane oxidizing bacteria. *Appl. Environ. Microbiol.* 55: 2960 - 2964.

Yeh, C. K. and J. T. Novak. 1994. Anaerobic biodegradation of gasoline oxygenates in soil. *Water Environ. Res.* 66: 744-752.

Zogorski, J., A. Morduchowist, A. Baehr, B. Bauman, D. Conrad, R. Drew, N. Korte, W. Lapham, J. Pankow and E. Washington. 1996. Fuel oxygenates and water quality: current understanding of sources, occurrence in natural waters, environmental behavior, fate, and significance. Washington, D.C., Interagency Oxygenated Fuel Assessment, Office of Science and Technology Policy, Executive Office of the President.

Zogorski, J., A. Morduchowist, A. Baehr, B. Bauman, D. Conrad, R. Drew, N. Korte, W. Lapham, J. Pankow and E. Washington. 1997. Fuel oxygenates and water quality. Washington, D.C. Interagency Oxygenated Fuel Assessment, Office of Science and Technology Policy, Executive Office of the President.

## Chapter 2

**“Degradation Kinetics of Methyl *tert*-Butyl Ether (MTBE) and its Breakdown Products by Propane and *Iso*-pentane Grown *Mycobacterium vaccae* JOB5”**

**Adriana Martínez-Prado, Kenneth J. Williamson  
and Lynda Ciuffetti**

**To Be Submitted to:**

**Water Research  
International Association on Water Quality, London, U.K.**



## 2.1 Abstract

*Mycobacterium vaccae* JOB5, a bacterial strain, was able to aerobically cometabolize MTBE when grown on propane and *iso*-pentane as a primary substrate. Similar patterns were observed with both alkanes. Two breakdown products of MTBE cometabolism were identified: *tert*-butyl formate (TBF) and *tert*-butyl alcohol (TBA); the latter was further transformed to carbon dioxide. No growth was observed when MTBE, TBF, or TBA was used as the sole source of carbon and energy. Biokinetic coefficients ( $K_s$  and  $k_{max}$ ) were estimated for the metabolism of *iso*-pentane and propane; and the cometabolism of MTBE, TBF, and TBA, by non-linear least squares and direct linear plot methods. The influence of propane and *iso*-pentane on the cometabolism of MTBE, TBF, and TBA was tested at a single concentration. The concentration of the alkanes corresponded to the substrates- $K_s$  value. The ranking of the maximum degradation rates were TBF > propane > MTBE > TBA for the propane-grown system; and *iso*-pentane > TBF > MTBE > TBA for the *iso*-pentane-grown system. When comparing the oxidation rate of the two alkanes tested it was found that the culture oxidized *iso*-pentane at a much higher rate ( $k_{max}$ ) than propane, about 4-fold. However the affinity constant was much higher (lower  $K_s$  value) for propane than for *iso*-pentane, about one order of magnitude. The *iso*-pentane grown system offered a higher maximum degradation rate for

the cometabolism of MTBE, about 3-fold, as compared to the propane system. Because of that, this system was further tested in growth batch reactors. The growth batch reactor experiments were conducted to compare the degradation of *iso*-pentane and MTBE with the predicted degradation rates based upon kinetic constants determined from single and dual-compound experiments. Growth batch reactor showed a faster degradation rate. Experimental data was modeled with Monod kinetics and STELLA<sup>®</sup> software.

## 2.2 Introduction

### 2.2.1. Degradation of MTBE

Methyl *tert*-butyl ether (MTBE) is a common U.S. gasoline additive since the late 1970s (Salanitro et al., 1998; Jacobs et al., 2000). Ethers (such as MTBE), and alcohols (such as *tert*-butyl alcohol, TBA) are both examples of fuel oxygenates used to replace lead. Oxygenates are used to raise octane ratings, reduce harmful emissions (e.g. carbon monoxide and ozone), and increase combustion efficiency of gasoline to meet the mobile source requirements of the Clean Air Act of 1990. MTBE had been the additive of choice because of its low cost, ease of production, and favorable transfer and blending characteristics.

The U.S. EPA previously supported MTBE use to meet air quality standards. However, the EPA has recently recommended curtailment of MTBE use because of its nation-wide contamination of groundwater that will result in millions of dollars of water treatment, cleanup, and replacement water costs (Jacobs et al., 2000; Wilson et al., 2001). The U.S. Geological Survey (USGS) has shown MTBE to be the second most common groundwater contaminant in the U.S. (Squillace et al., 1996;

Zogorski et al., 1996). Laboratory studies have found that MTBE causes tumors in rats and mice (Burleigh-Flayer et al., 1992; Chun et al., 1992), but human effects are unknown. The EPA has classified MTBE as a possible carcinogen (EPA, 1997).

Early laboratory studies on MTBE reported its resistance to biological attack in aerobic and anaerobic environments (Sulfito and Mormille, 1993). More recent studies have reported that fungal and bacterial cultures were able to degrade MTBE via cometabolism (Hardison et al., 1997; Steffan et al., 1997; Garnier et al., 1999) or as a primary substrate (Salanitro et al., 1994; Hanson et al., 1996; Mo et al., 1997; Hanson et al., 1999). Propane-oxidizing microorganisms had been found capable of cometabolizing MTBE aerobically. The same enzymatic activity also has been observed for microbes grown on individual major aliphatic components of gasoline such as *iso*-pentane (Hyman et al., 1998; Kwon 1998; Hyman and O'Reilly 1999), suggesting that substrates present within gasoline itself can support MTBE degradation.

MTBE breakdown products are affected by both aerobic or anaerobic conditions and the dominant culture. *Tert*-butyl alcohol (TBA) is the most common intermediate reported from MTBE oxidation (Hardison et al., 1997; Church et al., 1999; Hyman and O'Reilly 1999). *Tert*-butyl formate (TBF) also has been identified as a metabolite (Hardison et al.,

1997; Hyman et al., 1998; Hyman and O'Reilly 1999), followed by formaldehyde, 2-methyl 1-hydroxy 2-propanol (MHP), 2-hydroxyisobutyric acid (HIBA), 2-propanol and acetone (Steffan et al,1997). CO<sub>2</sub> has been directly produced from MTBE with no intermediates (Fortin et al., 1997; Fortin and Deshusses, 1998; Fortin and Deshusses, 1999). Methane and carbon dioxide are the end products in the anaerobic degradation process for either MTBE or TBA (Yeh and Novak 1994; Finneran and Lovley, 2001).

### **2.2.2. Kinetics and cometabolism**

Numerous laboratory and field studies had been conducted to demonstrate the applicability of cometabolism to bioremediate a variety of compounds (McCarty et al., 1998; Deeb et al., 2000; Stocking et al., 2000; Salanitro et al., 2001). Aerobic cometabolism occurs after a microbial community (mixed or pure) develops on a growth-supporting substrate, and results in the ability of microorganisms to transform non-growth supporting substrates such as MTBE, TBF, or TBA. The production of oxygenases by alkane oxidizers suggests that cometabolism offers a biological strategy for MTBE bioremediation from a contaminated site.

Kinetics of cometabolism had been studied extensively for compounds such as chlorinated aliphatic hydrocarbons (CAHs). Several

methods have been reported to estimate kinetic parameters and inhibition type such as: Lineweaver-Burk plot (Kenner and Arp, 1993; Chang and Alvarez-Cohen, 1996); non-linear least squares regression (NLSR) (Haston and McCarty, 1999) and direct linear plot (Cornish-Bowden, 1999). Recently, a combination of NLSR and direct linear plots have been proposed by Kim, 2000; and Kim et al., 2002 resulting in an accurate method for the determination of kinetic coefficients and inhibition type as well.

### **2.2.3. Objectives**

The objective of this study was to determine the kinetics of the MTBE degradation by a pure bacterial culture, *Mycobacterium vaccae* JOB5, grown on two different alkanes, *iso*-pentane and propane. The impact of TBF abiotic hydrolysis was studied due to the susceptibility of TBF to hydrolyze in water. Kinetic constants ( $k_{max}$  and  $K_s$ ) for propane, *iso*-pentane MTBE, TBF, and TBA were estimated and compared for different biomass, initial substrate and co-substrate concentrations, and mixtures of substrate and co-substrates. Predicted kinetic coefficients were used to model growth batch reactor experimental data with STELLA<sup>®</sup> software.

## 2.3 Materials and methods

### 2.3.1 Materials

*Mycobacterium vaccae* (*M. vaccae*) JOB5 (ATCC 29678) was obtained from the American Type Culture Collection (Rockville, Md.). MTBE (99.8 %), propane (98 %), acetylene (99.6 %), *iso*-pentane (99.5 %), *tert*-butyl formate (TBF) (99 %), *tert*-buty alcohol (TBA) (99 %), and dimethyl sulfoxide (DMSO) were obtained from Aldrich Chemical Company Co., Inc. (Milwaukee, Wis.). All gases were of the highest purity available and all other chemicals were at least of reagent grade.

### 2.3.2 *Mycobacterium vaccae* JOB5 growth

*Mycobacterium vaccae* was grown in the *Xantobacter* Py2 medium (Hamamura et al., 1997) with the modification that iron was added as 1 ml/L of Fe-EDTA solution and 1ml/L of micronutrient solution. Cultures were grown in a 700-ml glass bottles (Wheaton Scientific, Millville, N.J.) sealed with screw caps fitted with butyl rubber septa with identical liquid

and headspace volume. Propane and iso-pentane were selected as growth substrates. A volume of 60-ml propane was added by using a syringe fitted with 0.25 mm pore size sterile filters. Iso-pentane (350  $\mu$ l) was added using the "water trap" method because of its high volatility and flammability; it is added to experimental bottles trapped between two separate volumes of water with a liquid-tight syringe (Hamilton Company). Bottles were adjusted to 1-atm pressure and shaken at 200 rpm at 30 °C. Cells were harvested when growth had produced an optical density ( $OD_{600}$ ) of about 0.85.

In order to obtain a reproducible culture, 800  $\mu$ l of harvested cells were added to a 2-ml autoclaved cryogenic vial receiving 70  $\mu$ l of DMSO and stored in an -80°C freezer to ensure consistent inoculums for the experiments (Kim, 2000; Hamamura et al., 1997). When inoculums were needed, the frozen cells were thawed, washed, and rinsed three times with fresh media to remove DMSO and possible toxicity. Cell growth of *M. vaccae* was monitored by removing 1 ml of the culture and measuring optical density ( $OD_{600}$ ). Bacterial biomass was determined as total suspended solids (TSS) by filtering a known volume through a 0.1-mm membrane filter (Micro separation Inc., Westboro, MA) and drying at 60°C for 24 hours.



### **2.3.3 Analytical procedures**

The degradation of alkanes was monitored with a gas chromatograph (Model HP6890) fitted with a flame ionization detector (GC-FID) and a 30-m x 0.45-mm I.D., 2.55- $\mu$ m DB-MTBE column (Agilent Technology, Willmington, DE) at an oven temperature of 65 °C and gas flow rates for helium, hydrogen and air of 15, 35, and 250 ml/min, respectively. In all experiments, 100- $\mu$ l headspace samples were taken and analyzed directly without further preparation.

MTBE, TBF, and TBA were monitored with a gas chromatograph (Model HP5890A) fitted with a flame ionization detector (GC-FID) and a 3' x 1/8 " I.D. stainless steel column packed with Porapak Q (80/100 mesh) (Alltech Associates, Inc., Deerfield, IL) with an oven temperature of 135°C and a detector temperature of 220°C. Helium was used as the carrier gas with a 40 ml/min flow rate. In all experiments, liquid samples (2  $\mu$ l) were taken and analyzed directly without further preparation. Appropriate external standard curves were developed for all cases. Carbon dioxide accumulation and oxygen consumption were monitored with a gas chromatograph (Model HP5890). A Carboxen 1000 column (15 ft x 1/8 in; Supelco, Bellefonte, PA.) was used at a temperature of 30 °C for a 7 min run using Argon as the carrier gas at 15 ml/min. Sample lock gas-tight and

liquid-tight syringes (Fisher Scientific) were used for all gas chromatography analysis.

All experiments were conducted in 27.8 -ml glass vials (Supelco, Bellefonte, PA) crimped with aluminum seals fitted with butyl stoppers. The mixture reaction had a total volume of 5-ml of autoclaved Py2 media.

#### **2.3.4 Abiotic TBF hydrolysis rate assay**

Experimental bottles were prepared under sterile conditions to minimize microbial contamination. A wide range of TBF concentrations from 1.5 to 135 mg/L in Py2 media was tested in duplicate. TBF was added from a saturated solution prepared in a 10 mM phosphate solution (pH = 7) to avoid significant hydrolysis of TBF. Bottles were continuously shaken at 200 rpm at  $20 \pm 0.5$  °C. Liquid samples (2  $\mu$ l) were removed from experimental bottles and directly analyzed by GC-FID to follow TBF transformation and TBA production with time.

### **2.3.5 Kinetic and inhibition assays**

Cells were harvested from cultures by centrifugation (6000 x g for 15 min), concentrated, and washed three times with the same fresh Py2 media. The mixture reaction consisted of the same Py2 media and concentrated cells. Propane and *iso*-pentane were added by removing known volumes from double flasks or water-trap bottles, respectively. MTBE, TBF, or TBA was added as needed from either stock or saturated aqueous solution. Bottles were placed in a rotatory shaker (200 rpm) at 20°C. Initial concentration of compounds in the experimental bottles was measured before cells were added to initiate the reaction. Liquid and headspace samples were taken for MTBE, TBF, and TBA, and propane and *iso*-pentane, respectively.

### **2.3.6 Control bottles**

In all experiments, an abiotic control and a killed cell control were included. The abiotic control was identical to an experimental treatment, except cells were not added. The killed control was identical to an experimental treatment, but cells were poisoned with a solution of 10% HgCl<sub>2</sub>.

### 2.3.7 Growth-batch reactor

Growth batch reactor experiments were designed as previously described with the following exceptions. Cultures were started from frozen cells to promote growth. After 10 hours, the experimental bottles were opened in a sterile laminar flow hood and were gently hand-shaken to remove all *iso*-pentane. A liquid sample, 1 ml, was withdrawn to determine the initial concentration of biomass by measurements of OD<sub>600</sub> and protein content (Gornall et al., 1949). Next, all bottles were recapped and *iso*-pentane and MTBE were added. Bottles were placed in a rotatory shaker at 200 rpm. After reaching equilibrium, liquid and headspace samples were analyzed by GC analysis to determine the initial concentrations of both MTBE and *iso*-pentane. Consumption of *iso*-pentane, MTBE, and oxygen and production of TBF and TBA were followed with time. All samples were analyzed for OD<sub>600</sub>, pH, and concentrations of protein, O<sub>2</sub>, *iso*-pentane, MTBE, TBF, and TBA. Oxygen was added as required to maintain aerobic conditions.

### 2.3.8 Data analysis and modeling

Kinetic constants  $k_{max}$  and  $K_s$  were determined by two different methods, non-linear least squares regression (NLSR) and direct linear plot by fitting the initial degradation rate measured at different substrate concentrations to the Michaelis–Menten/Monod equation, following the method proposed by Kim, 2000 and Kim et al., 2002 as already introduced.

*Mycobacterim vaccae* biomass production and *iso*-pentane, MTBE and TBA degradation in a batch growth reactor were modeled with the kinetic coefficients determined from single- and dual-compound experiments fit to the actual experimental data using STELLA ® software (High Performance System, Inc. Hanover, NH).

## 2.4 Results

When cultured on propane and *iso*-pentane, *M. vaccae* JOB5 degraded propane and *iso*-pentane at a rate of 75 and 66  $\mu\text{mol/h}$  with a doubling time of cells of 7.8 and 8.6 hours, respectively. The cell yields for the bacterial cultures were  $0.80 \pm 0.01$  and  $0.61 \pm 0.02$  mg TSS/mg substrate consumed for propane and *iso*-pentane, respectively. TBF and TBA were

two intermediates identified from MTBE oxidation. Mineralization was suggested based on CO<sub>2</sub> accumulation determined in TBA experimental bottles.

Experiments conducted to determine if the culture could grow on MTBE and its breakdown products showed no growth when MTBE, TBF, or TBA were used as the sole source of carbon and energy. It was concluded that the degradation of MTBE and breakdown products occurred primarily via cometabolism.

#### **2.4.1 Cometabolism**

MTBE, TBF, and TBA cometabolism for one *iso*-pentane-grown culture are shown in Figure 2.1. The same molar masses of each compound were initially added singly to the experimental bottles and measured as a function of time. The *iso*-pentane grown cells were harvested, concentrated, and added to give an initial concentration of 490 mg TSS/L in each bottle. Degradation occurred in all bottles with the relative degradation rates of TBF > MTBE > TBA. For this particular case, the initial degradation rates were calculated from initial slopes of the degradation plots as 0.95, 0.29, and 0.14  $\mu\text{mol/h}$ , respectively.

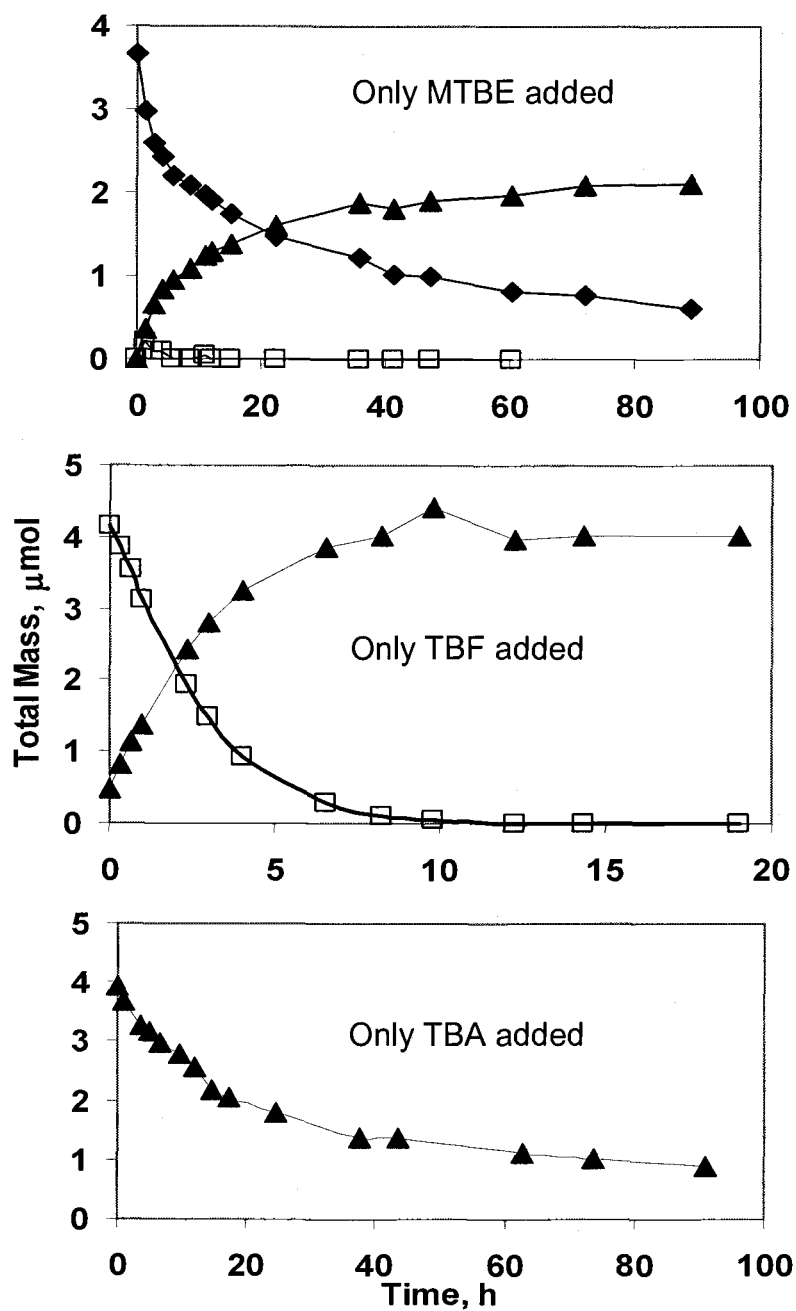


**Figure 2.1** Aerobic cometabolism of MTBE, TBF, and TBA by *iso*-pentane grown *Mycobacterium vaccae* JOB5. Same molar mass (4  $\mu\text{mol}$ ) of compounds, in separate experiments, were incubated with 490 mg TSS/L. Transformation of compounds were followed with time by gas chromatography (2  $\mu\text{l}$  liquid samples). MTBE (♦), TBF (□) and TBA (▲).

### 2.4.2 TBF abiotic hydrolysis

TBF has an ester group that can be hydrolyzed to TBA and formic acid through nucleophilic substitution (Mill, 1982 ;Church et al., 1999). In the hydrolysis experiments, the disappearance of TBF corresponded to > 95% TBA formed. Duplicate bottles for ten different concentrations (range of 1.5 to 135 mg/L) were run. All results followed first order kinetics. The TBF hydrolysis rate ( $K_h$ ) was determined to be  $0.061 \pm 0.005 \text{ day}^{-1}$ , which corresponded to a half-life of  $11.43 \pm 0.82 \text{ d}$ . An example for a single concentration is shown in Figure 2.2.

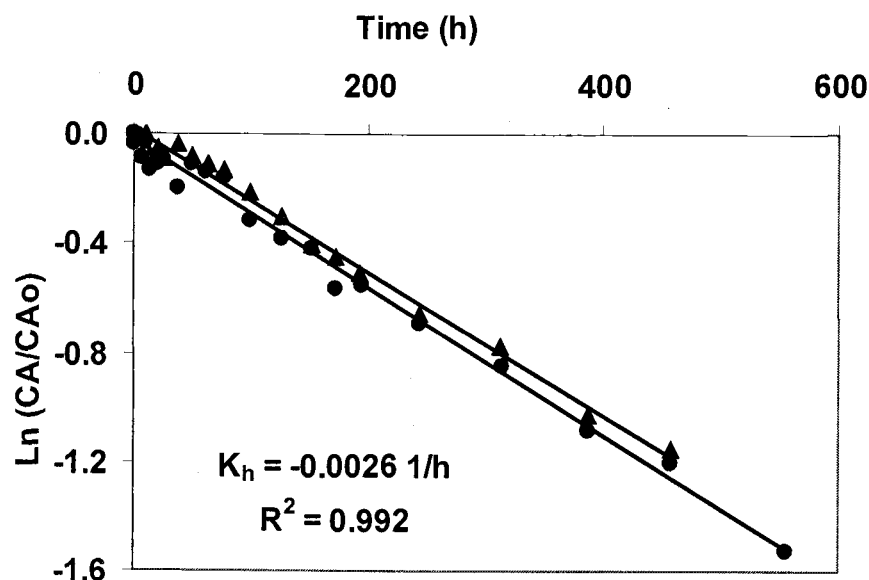


**Figure 2.2.** Abiotic TBF hydrolysis. Duplicate bottle at an initial liquid concentration of 12 mg/L in Py2 media. At indicated times, 2  $\mu\text{l}$  liquid samples were removed from experimental bottle and immediately analyzed by gas chromatography, Rep 1 (●) and Rep 2 (▲)



### 2.4.3 Kinetic constants and inhibition

The Monod kinetic constants,  $k_{max}$  and  $K_s$ , were determined for the two growth substrates, MTBE, TBF, and TBA. In addition, the inhibition effects were measured for MTBE, TBF, and TBA when either propane or *iso*-pentane was present (for a single concentration). Initial degradation rates were measured for different concentrations of biomass and compounds of interest. Only duplicates for MTBE, TBF, and TBA were determined because liquid injection samples on the poropak Q column had a minimum of 15 minutes per sample elution time for all 3 compounds. For single and dual compound batch kinetics,  $k_{max}$  and  $K_s$  were determined by fitting the data to Equation. 2.1 where  $\frac{dM}{dt}$  is the degradation rate in  $\mu\text{mol/h}$ ;  $k_{max}$ , the maximum degradation rate in  $\mu\text{mol/mgTSS-h}$ ;  $K_s$ , the half-saturation coefficient in  $\mu\text{M}$ ;  $M$ , the total mass of compound added in  $\mu\text{mol}$ ;  $V_L$ , volume of liquid phase in L;  $V_G$ , volume of headspace in L; and  $H_{cc}$  = dimensionless Henry's coefficient (Mackay and Ying 1981; Church et al., 1999; Garnier et al., 1999).

$$\frac{dM}{dt} = \left[ \frac{-k_{max} \left( \frac{M}{V_L + V_G * H_{cc}} \right)}{K_s + \left( \frac{M}{V_L + V_G * H_{cc}} \right)} \right] (X * V_L) \quad (2.1)$$

The two unknowns ( $k_{\max}$  and  $K_s$ ) were determined by fitting the experimental data using non-linear least squares regression (NLSR) with the statistical software SPLUS.

An example of experimental data for the metabolism of *iso*-pentane by *iso*-pentane-grown bacterial culture is shown in Figure 2.3 for a triplicate set of bottles of a single concentration. The results of 8 plots such as Figure 2.3 were best fit to Equation 2.1 using NLSR as shown in Figure 2.4.

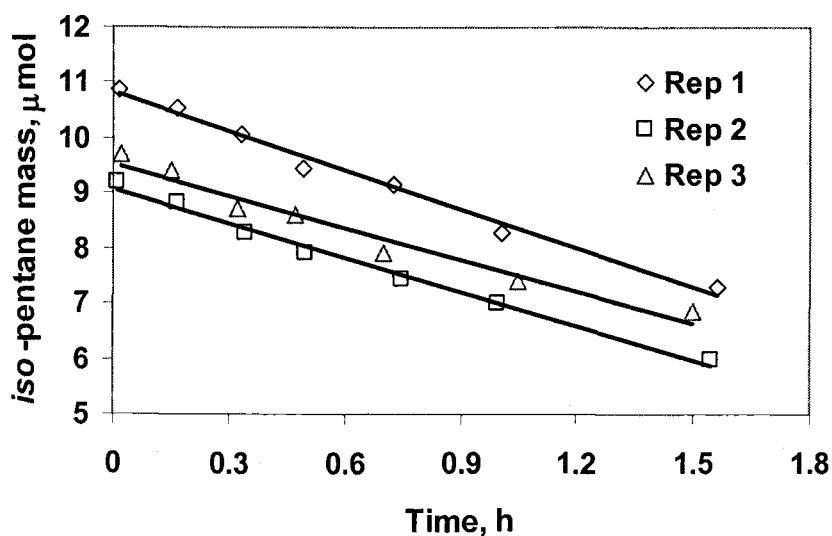


**Figure 2.3** Initial degradation rate of *iso*-pentane. Metabolism of *iso*-pentane by *iso*-pentane-grown *Mycobacterium vaccae* JOB5. Cell biomass added (7.5 mg TSS) to triplicate bottles.

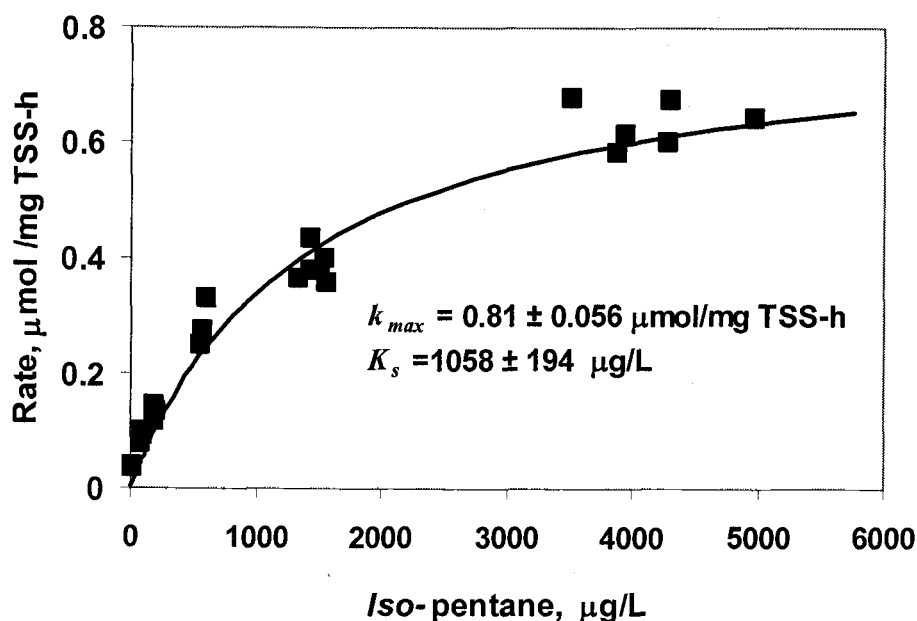


**Figure. 2.4** Biokinetic constants for *iso*-pentane by NLSR. Initial degradation rate for various initial concentrations of *iso*-pentane (■) and increasing biomass (mg TSS/L). Solid line represents the best fit to Equation 2.1 by NLSR and SPLUS statistical software.

The substrates, propane and *iso*-pentane appeared to competitively inhibit the co-substrates MTBE and TBA in that degradation rates of MTBE and TBA decreased when substrates were present. Equation 2.1 was modified to account for competitive inhibition resulting in Equation 2.2 where  $I_L$  is the concentration of the inhibitor ( $\mu\text{mol/L}$ ) and  $K_{ic}$  is the inhibition (competitive) constant ( $\mu\text{mol/L}$ ). With competitive inhibition,  $k_{\max}$  equals  $k_{\max}^{app}$  (apparent, inhibitor present) while  $K_s^{app}$  (apparent) increases with increasing inhibitor concentration ( $I_L$ ).

$$\frac{dM}{dt} = \left[ \frac{-k_{\max} \left( \frac{M}{V_L + V_G * H_{cc}} \right)}{K_s \left( 1 + \frac{I_L}{K_{ic}} \right) + \left( \frac{M}{V_L + V_G * H_{cc}} \right)} \right] (X * V_L) \quad (2.2)$$

The concentration of the inhibitor,  $I_L$ , can also be expressed in terms of total mass by  $I_L = \left( \frac{M_i}{V_L + V_G H_{cci}} \right)$ , where  $M_i$  is the total mass of the inhibitor ( $\mu\text{mol}$ ) and  $H_{cci}$  is the Henry's coefficient of the inhibitor.

The estimated kinetic constants and their confidence intervals (C.I.) for the metabolism of both substrates, and the cometabolism of MTBE, TBF and TBA obtained from single compound experimental data fit by Equation 2.1 are summarized in Table 2.1. *Iso*-pentane-grown culture yielded a higher degradation rates ( $k_{\max}$ ) for *iso*-pentane and MTBE as compare to the propane-grown culture as observed from tabulated values.

The competitive inhibition effects are shown from the results of cometabolism of MTBE, TBF, and TBA in the presence of the substrates in Table 2.2. The substrate or inhibitor concentrations of propane or *iso*-pentane are listed in the table. Experimental data was fitted to Equation 2.1 by NLSR. Reported values of  $k_{\max}^{app}$  and  $K_s^{app}$  include the inhibition effects, since no particular case of inhibition was considered.

**Table 2.1** Kinetic constants with their 95% C.I. by NLSR

Compound Name	$k_{max}$ ( $\mu\text{mol}/\text{mg TSS-h}$ )	$K_s$ ( $\text{mg/L}$ )
Propane-grown system		
Propane	$0.173 \pm 0.011$	$0.194 \pm 0.035$
MTBE	$0.062 \pm 0.002$	$14 \pm 2$
TBF	$0.73 \pm 0.034$	$28 \pm 4$
TBA	$0.049 \pm 0.004$	$34 \pm 10$
Iso-pentane-grown system		
Iso-pentane	$0.81 \pm 0.056$	$1.06 \pm 0.19$
MTBE	$0.20 \pm 0.011$	$12 \pm 3$
TBF	$0.372 \pm 0.024$	$8.7 \pm 2.6$
TBA	$0.028 \pm 0.0015$	$11 \pm 2.3$

**Table 2.2** Kinetic constants , in the presence of the substrate, with their 95% C.I. by NLSR

Compound Name	Propane concentration ( $\mu\text{g/L}$ )	$k_{max}^{app}$ ( $\mu\text{mol}/\text{mg TSS-h}$ )	$K_s^{app}$ ( $\text{mg/L}$ )
Propane-grown system			
MTBE	250	$0.045 \pm 0.007$	$47 \pm 21$
TBF	250	$0.81 \pm 0.07$	$47 \pm 9$
TBA	250	$0.0425 \pm 0.005$	$89 \pm 29$
Compound Name	Iso-pentane concentration ( $\mu\text{g/L}$ )	$k_{max}^{app}$ ( $\mu\text{mol}/\text{mg TSS-h}$ )	$K_s^{app}$ ( $\text{mg/L}$ )
Iso-pentane-grown system			
MTBE	250	$0.187 \pm 0.006$	$16 \pm 2.6$
	700	$0.198 \pm 0.011$	$18 \pm 3$
TBF	250	$0.534 \pm 0.04$	$14.3 \pm 3.9$
TBA	125	$0.0682 \pm 0.0034$	$12 \pm 2$

Kinetic constants were also estimated with the direct linear plot method introduced by Cornish-Bowden (1995) and applied to cometabolic analysis by Kim et al., (2002). This is an alternative way of plotting the Michaelis-Menten equation represented by Equation 2.3, where  $v$  is the initial degradation rate, and  $S_L$  is the aqueous substrate concentration (mg/L).

$$k_{\max} = v + \frac{v}{S_L} K_s \quad (2.3)$$

If  $k_{\max}$  is plotted against  $K_s$ , a straight line is obtained with a y-intercept of  $v$  and an x-intercept of  $-S_L$ . Values of  $v$  are plotted on the y-axis (0,y) and the corresponding negative value of  $S_L$  (x,0) are plotted on the x-axis. Each pair then is joined and extrapolated; the intersection coordinates define a unique pair of  $k_{\max}$  and  $K_s$  values that satisfy both observations. The medians of each set are the best estimates of the kinetic constants. An example of the best estimates obtained for TBF degradation by the propane-grown culture is illustrated in Figure 2.5.

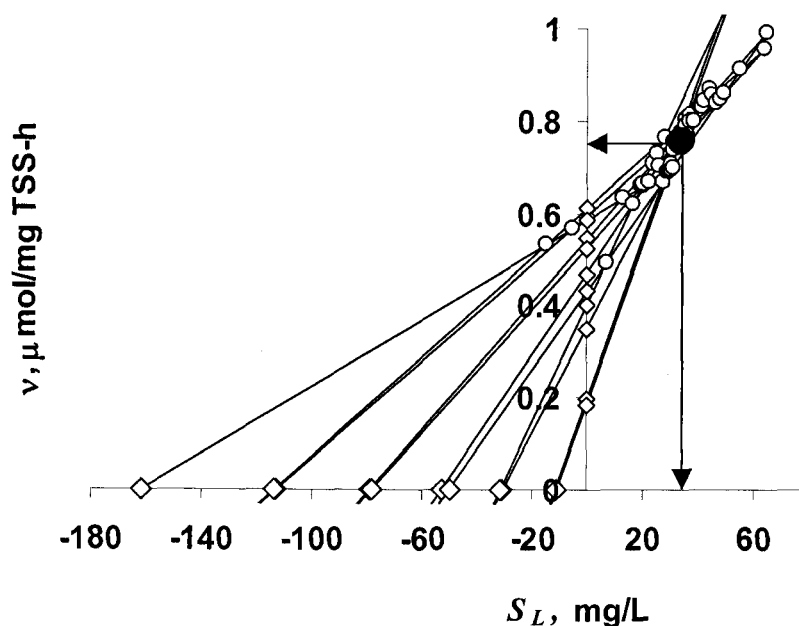


**Figure 2.5**  $k_{max}$  and  $K_s$  for TBF by direct linear plot. Experimental data is plotted by pairs, (y,0) versus (0,x), joined and extrapolated. The small open symbols (○) at the intersection of two lines represents a unique pair of  $k_{max}$  and  $K_s$  that satisfies those two sets of observations. The large solid circle (●) represents the median values as the best estimates for  $k_{max}$  and  $K_s$ .

Tables 2.3 and 2.4 summarize the values for the kinetic constants estimated with this method from degradation experiments with single and dual compounds, respectively.

**Table 2.3** Kinetic constants by direct linear plot from single compound experiments

Compound Name	$k_{max}$ ( $\mu\text{mol}/\text{mg TSS-h}$ )	$K_s$ ( $\text{mg/L}$ )
Propane	0.182	0.31
MTBE	0.062	14
TBF	0.76	34
TBA	0.044	27
iso-pentane	0.58	0.51
MTBE	0.192	13
TBF	0.356	11.4
TBA	0.0255	7.1

**Table 2.4** Kinetic constants by direct linear plot from dual compound experiments

Compound Name	Propane concentration ( $\mu\text{g/L}$ )	$k_{max}^{app}$ ( $\mu\text{mol}/\text{mg TSS-h}$ )	$K_s^{app}$ ( $\text{mg/L}$ )
Propane-grown system			
MTBE	250	0.034	45
TBF	250	0.69	38
TBA	250	0.040	127
Compound Name	iso-pentane concentration ( $\mu\text{g/L}$ )	$k_{max}^{app}$ ( $\mu\text{mol}/\text{mg TSS-h}$ )	$K_s^{app}$ ( $\text{mg/L}$ )
iso-pentane-grown system			
MTBE	250	0.19	19
	700	0.21	20
TBF	250	0.486	13.6
TBA	125	0.061	7



The direct linear plot method was used to verify competitive inhibition of *iso*-pentane on MTBE (Kim, et al., 2002). Experimental data at 0, 250, and 700  $\mu\text{g iso/L}$  (concentration of inhibitor) was analyzed with this method, as shown in Figure 2.6, to obtain the best estimates ( $k_{max}$  and  $K_s$ ). A direct linear plot of only the best estimates (median), for the kinetic constants for MTBE, was constructed at those three different *iso*-pentane concentrations as shown in Figure 2.7. The plot shows a shift of the best estimates (apparent values of  $k_{max}$  and  $K_s$ ) to the right, verifying competitive inhibition between *iso*-pentane and MTBE.

The kinetic parameters  $K_s$  and  $K_{ic}$  can be also determined by plotting the best estimates obtained for  $K_s^{app}$  versus the inhibitor concentration,  $I_L$ , by the linearized equation for competitive inhibition as shown in Equation 2.4 (Kim et al., 2002).

$$K_s^{app} = K_s + \frac{K_s}{K_{ic}} I_L \quad (2.4)$$

The slope of Equation 2.4 provides a linear correlation of  $\frac{K_s}{K_{ic}}$  and the intercept equal to  $K_s$ . The values of  $K_{ic}$  and  $K_s$  obtained from our results were 164 and 22  $\mu\text{mol/L}$ , respectively. The  $R^2$  for the linear correlation was 0.80. Improved estimates of the  $K_{ic}$  value could be obtained by using higher inhibitor-concentrations.

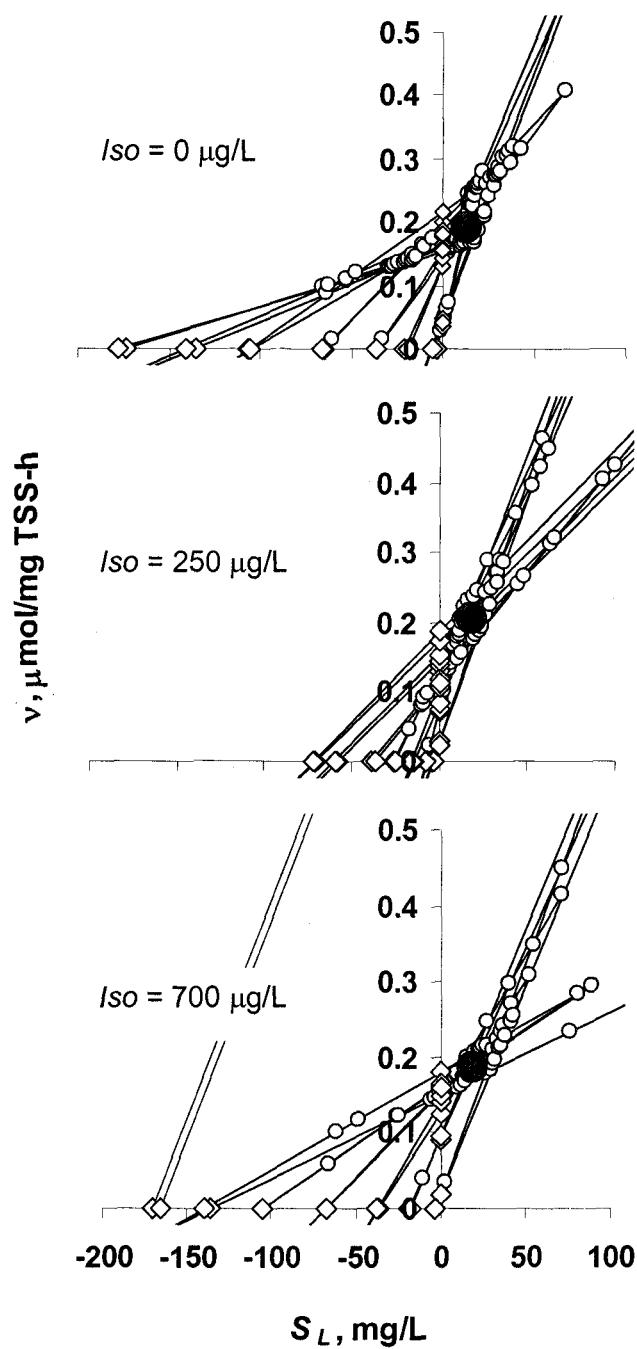


**Figure 2.6**  $k_{\text{max}}^{\text{app}}$  and  $K_s^{\text{app}}$  for MTBE by direct linear plot. Experimental data analyzed at three different  $iso$ -pentane concentrations, as indicated in figure. The large solid circle (●) represents the median values as the best estimates.

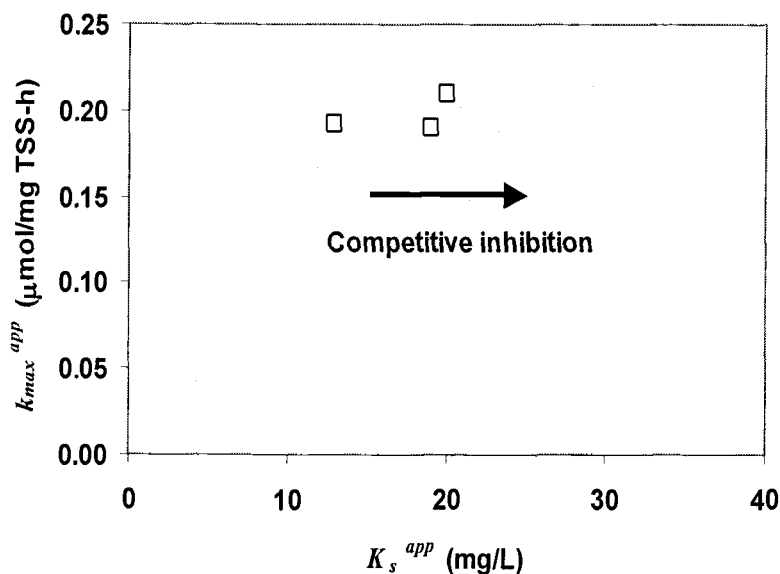


**Figure 2.7** Inhibition type by direct linear plot. Best estimates (median) of MTBE at increasing concentration of *iso*-pentane (inhibitor). Competitive inhibition is denoted by a shifting to the right.

The effect of MTBE, TBF, and TBA on the degradation of the substrates, propane, and *iso*-pentane were determined by testing a single concentration of the substrate at increasing concentrations of MTBE, TBF and TBA. In all the cases, the degradation of both substrates was lower when MTBE, TBF, or TBA was present as compared to the experimental bottles with substrate only.

Interactions among MTBE, TBF, and TBA in a 1:1 ratio were qualitatively tested with the propane-grown culture. These results showed that oxidation rates for both MTBE and TBA notably decreased when both

were present. The presence of TBF further decreased MTBE and TBA oxidation rates. However, MTBE and TBA did not significantly influence TBF degradation (see Table 2.5).

**Table 2.5** Degradation rate in a matrix experiment (1:1) ratio for the propane-grown *Mycobacterium vaccae* culture

Case	Degradation Rate ( $\mu\text{mol/h}$ )		
	M	F	A
M	1.4	---	---
F	---	2.05	---
A	---	---	0.90
M + A	0.67	N.D.	0.125
M + F	0.25	1.70	N.O.*
F + A	---	2.11	N.O.*
M + F + A	N.O.	2.12	N.O.*

M = MTBE

F = TBF

A = TBA

N.D. Not detected

N.O. Not observed

\* TBA accumulation rate = TBF degradation rate

Biomass concentration = 1320 mg TSS/L

#### 2.4.4 Growth batch reactor and STELLA modeling

Similar to the rate of substrate utilization or MTBE transformation, Monod kinetics were also used to express the rate of microbial growth as a function of growth and cell decay by Equation 2.5. where,  $Y$  = biomass yield, mg TSS/ $\mu\text{mol}$  substrate consumed and  $b$  = cell decay rate,  $\text{day}^{-1}$ . No toxic effects from degradation of co-substrates and a typical cell decay rate

were assumed. Table C.1 in Appendix C lists the equations used in STELLA modeling .

$$\frac{dX}{dt} = Y \frac{k_{\max} X \left( \frac{M}{V_L + V_G H_{cc}} \right)}{K_s + \left( \frac{M}{V_L + V_G H_{cc}} \right)} - (b)X \quad (2.5)$$

For the growth batch reactor experiments, oxidation of the substrate and cometabolism of MTBE and its breakdown products (triplicate bottles) were followed for 100 h. For the first 30 h, MTBE oxidation was not significant because the initial biomass was low (21 mg TSS/L) and the presence of *iso*-pentane competitively inhibited MTBE oxidation. After 50 hours, the MTBE degradation rate reached its maximum and all MTBE was consumed by hour 56. TBF and TBA were detected in all samples with the corresponding accumulation of TBA., MTBE, TBF and TBA were completely consumed within 74 h. The consumption rate for MTBE, TBF, and TBA was faster than those observed in the kinetic experiments.

Biomass production was measured in all samples as a function of protein and converted to mg TSS/L since kinetic constants were expressed in terms of mg TSS units. Protein content was determined as 0.43 mg protein per mg TSS.

Equations 2.1, 2.2, and 2.5 were used to model the experimental data with STELLA as shown in Figures 2.8, 2.9 and 2.10. Numerical integration in time was performed in STELLA® using a fourth-order Runge Kutta method. The STELLA calculations were verified by comparison to output from a separately developed solution of Equations 2.1, 2.2, and 2.5 (Equations C.8, C.10, and C.11 in Section C.2.2 in Appendix C). A linear relationship of biomass produced as a function of *iso*-pentane consumed was obtained; computed data from this relationship was compared to the experimental data with an excellent agreement. A Fortran program was written for this purpose (see Appendix C) and identical results to the solution provided by STELLA were obtained.

Table 2.6 summarizes the parameters used to model the growth batch reactor for results in Figures 2.8, 2.9 and 2.10. It can be observed that the degradation rates in the growth batch reactors were higher than the ones observed in kinetic experiments, especially for TBA. A reason why this faster rate occurred could be that the substrate, *iso*-pentane, was not limited in the system with the consecutive production of the reductant required to degrade the co-substrates. When resting cell experiments were performed biomass was harvested, concentrated, and maintained in the absence of the substrate until used in the experiment; additionally, degradation rates were estimated over a short period of time, whereas the growth batch reactors were followed for a longer period of time.

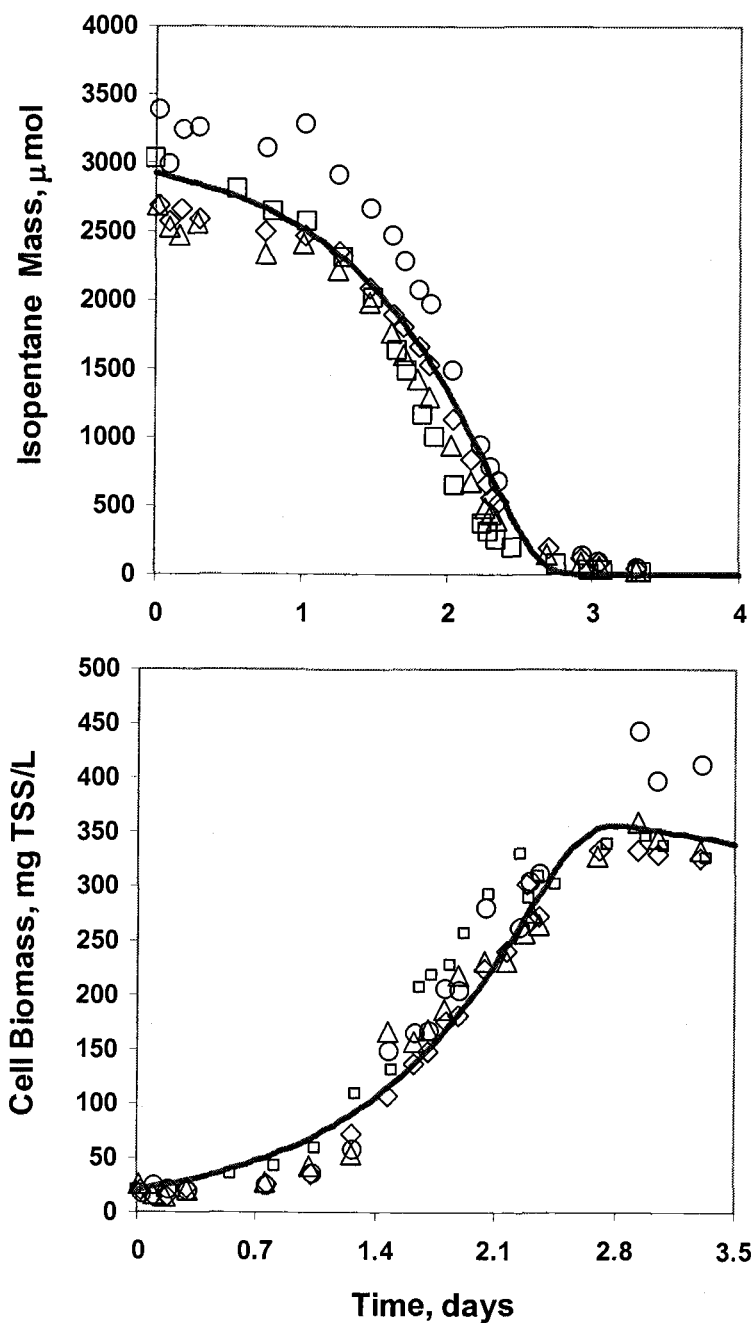


**Figure 2.8** Modeling of *iso*-pentane metabolism and biomass production by *Mycobacterium vaccae* in growth-batch reactors. Experimental data of triplicate bottles in the presence ( $\circ \diamond \triangle$ ) and absence of MTBE ( $\square$ ). Best fit to experimental data (solid line) by Equation 2.2 and 2.5 with STELLA

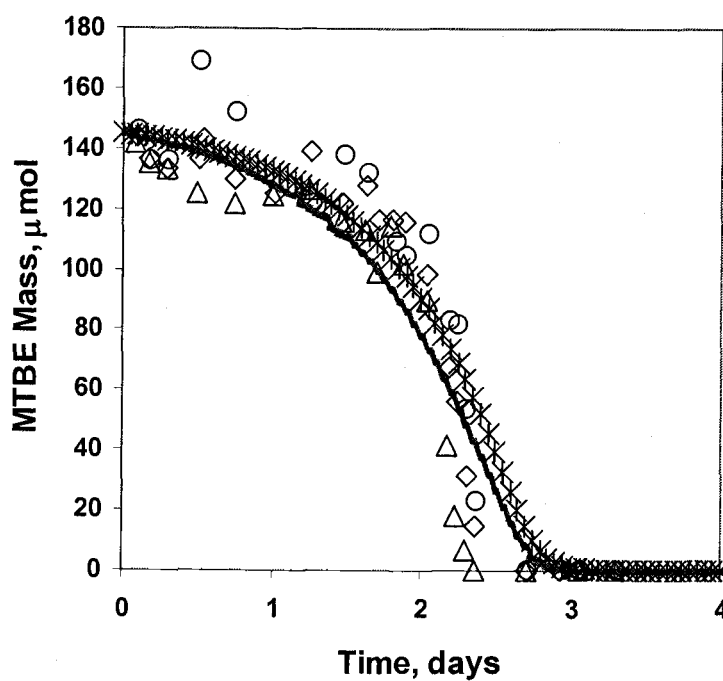


**Figure 2.9** Modeling of MTBE cometabolism by *Mycobacterium vaccae* in growth-batch reactors. Experimental data of triplicate bottles in the presence of *iso*-pentane (○◇△).  $K_{ic}$  value obtained from direct linear plot (---) and when assumed to be equal to  $K_s$  *iso*-pentane (\*) (see Table 2.6) by Equation 2.2 with STELLA software.



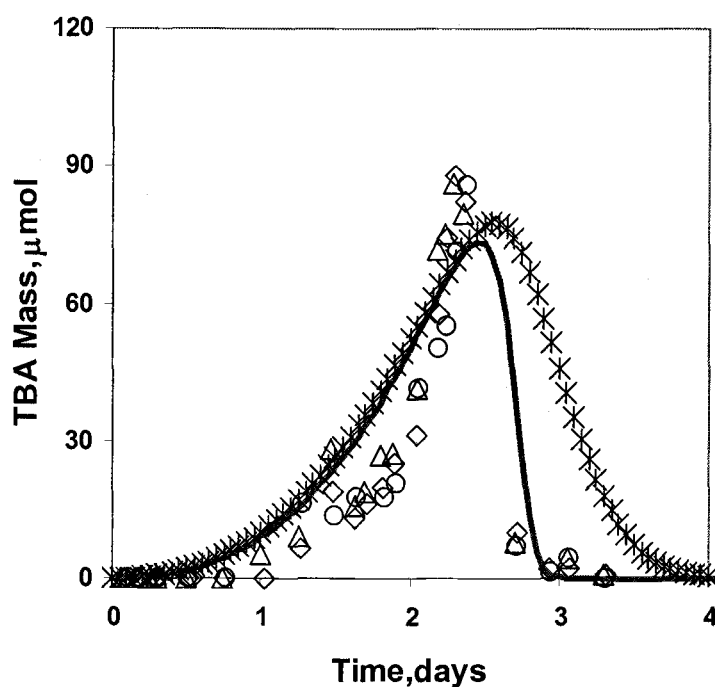


**Figure 2.10** Modeling of TBA cometabolism by *Mycobacterium vaccae* in growth-batch reactors. Experimental data of triplicate bottles in the presence of *iso*-pentane ( $\circ\diamond\triangle$ ). When  $K_{ic}$  value for TBA assumed equal to  $K_s$  *iso*-pentane ( $*$ ) and when TBA parameters adjusted (---) (see Table 2.6) by Equation 2.2 with STELLA software.

**Table 2.6** Parameters used in STELLA modeling for growth batch reactors

Parameter	Kinetic Experiments	Selected for Modeling	UNITS
Yield	0.044	0.044	mg TSS/ $\mu$ mol iso
$k_{max-iso}$	20	30	$\mu$ mol iso/mgTSS-d
$K_{s-iso}$	14.67	14.67	$\mu$ mol iso/L
MTBE Case 1 (---)			
$k_{max-MTBE}$	4.8	4.8	$\mu$ mol MTBE/mgTSS-d
$K_{s-MTBE}$	164 <sup>a</sup>	164	$\mu$ mol MTBE/L
$K_{ic(ISO-MTBE)}$	22 <sup>*</sup>	22	$\mu$ mol iso/L
MTBE Case 2 (*)			
$k_{max-MTBE}$	4.8	4.8	$\mu$ mol MTBE/mgTSS-d
$K_{s-MTBE}$	164 <sup>a</sup>	164 <sup>a</sup>	$\mu$ mol MTBE/L
$K_{ic(ISO-MTBE)}$	22 <sup>a</sup>	14.67 <sup>b</sup>	$\mu$ mol iso/L
$k_{max-TBF}$	10.1	10.1	$\mu$ mol TBF/mgTSS-d
$K_{s-TBF}$	140	140	$\mu$ mol TBF/L
TBA Case 1 (*)			
$k_{max-TBA}$	1.64	1.64	$\mu$ mol TBA/mgTSS-d
$K_{s-TBA}$	94	94	$\mu$ mol TBA/L
$K_{ic(ISO-TBA)}$	7(assumed) <sup>c</sup>	7	$\mu$ mol iso/L
TBA Case 2 (---)			
$k_{max-TBA}$	1.64	20	$\mu$ mol TBA/mgTSS-d
$K_{s-TBA}$	94	94	$\mu$ mol TBA/L
$K_{ic(ISO-TBA)}$	7(assumed) <sup>c</sup>	1.0	$\mu$ mol iso/L
$V_{LIQ} = V_{GAS} = 0.35$ L Cell conc. = 21 mg TSS/L Cell decay (b) = 0.075 1/day (typical value) <sup>a</sup> Obtained from direct linear plot analysis <sup>b</sup> $k_{max-MTBE} = K_{s-iso}$ <sup>c</sup> Concentration at which the kinetic experiments were performed			

## 2.5 Discussion

TBF and TBA were both identified as metabolites from MTBE aerobic degradation by *Mycobacterium vaccae* JOB5. No growth was observed when MTBE, TBF, or TBA was used as the sole source of carbon and energy. The ranking of the maximum degradation rates were TBF > propane > MTBE > TBA for the propane-grown system, and *iso*-pentane > TBF > MTBE > TBA for the *iso*-pentane-grown system.

Competitive inhibition was suggested in both systems when the substrates (propane and *iso*-pentane), MTBE or TBA were present at the same time. In the kinetic studies, it was clearly observed that the degradation of MTBE and TBA were inhibited by the presence of propane and *iso*-pentane. The same effect was observed when measuring the degradation of the substrates in the presence of MTBE and TBA.

TBF was found to have a hydrolysis rate constant of  $0.061 \pm 0.005$  ( $\text{day}^{-1}$ ) and a half-life  $11.43 \pm 0.82$  days at pH 7.5. Even though TBF undergoes abiotic hydrolysis, the rate is slow enough to probably not influence biotic degradation rates. The high rate of biotic degradation means that TBF will not significantly accumulate as the case for TBA. This could be one of the reasons that most studies report the appearance of TBA as the most common and stable MTBE-breakdown product.

$K_s$  and  $k_{max}$  constants were determined from kinetic data by two different methods: NLSR and direct linear plot. Both methods gave comparable values. Because  $K_s$  and  $k_{max}$  are highly correlated as shown by Equations 2.1 and 2.2, the use of non-linear methods is suggested.

When comparing the oxidation rate of the two alkanes tested by the bacterial culture, it was found that the culture oxidized *iso*-pentane at a much higher rate ( $k_{max}$ ) than propane, about 4-fold. However, the affinity constant was much higher (lower  $K_s$  value) for propane than for *iso*-pentane, about one order of magnitude. The *iso*-pentane grown system offered a higher maximum degradation rate for the cometabolism of MTBE, about 3-fold, as compared to the propane system. TBF maximal degradation rate was the fastest in both systems; however, it was twice as large for the propane-grown system than for the *iso*-pentane.

Competitive inhibition was suggested among the substrates and MTBE and TBA. A direct linear plot further suggested competitive inhibition of *iso*-pentane on MTBE by testing three different *iso*-pentane concentrations. It was identified as a shift to the right in a plot prepared with the best estimates found for each inhibitor concentration tested. A combination of both methods, NLSR and direct linear plot, was successful to determine kinetic constants and inhibition type for chlorinated solvents (Kim et al., 2002).

Maximal degradation rate for *iso*-pentane and MTBE, were higher as compared to the propane system. Because of this, growth batch reactor studies were further performed. Kinetic coefficients determined from single or dual-compound experiments were used to model growth batch reactor experimental data. In general, the growth batch reactor showed a faster degradation rate. The best fit was obtained when the  $k_{max}$  for *iso*-pentane was 1.5 times higher than the estimated from experiments. Competitive inhibition coefficient ( $K_{ic}$ ) for MTBE obtained from direct linear plot analysis was used to model the experimental data.

TBA kinetic experiments were the most challenging because of the slow degradation rates and very high biomass concentrations needed to determine initial rates. As such, estimates of the  $K_{ic}$  values from experimental data could not be obtained. The  $K_{ic}$  value of TBA was first assumed to be the concentration of the substrate at which the kinetic study was performed. Modeled TBA accumulation was almost identical to the experimental data. TBA tends to accumulate in the system and can be considered as a limiting step of the mineralization of MTBE.

Many cometabolism studies reported in the literature assumed competitive inhibition among the substrate and co-substrate to occur, based on the hypothesis that both must bind to the same enzyme and compete for the active site (Kim, 2000). Another common assumption is that the  $K_{ic}$  of the co-substrate is equal to the independently measured  $K_s$  of

the substrate, however it has not been validated in all cases (Kim, 2000). For this study, an approximate fit was obtained when assuming  $K_{ic}$  of MTBE equal to  $K_s$  *iso*-pentane. However, when  $K_{ic}$  of TBA was set equal to  $K_s$  of *iso*-pentane, the experimental data were not fit well by the model predictions. A much lower value of  $K_{ic}$  was needed to provide the best fit. This illustrates the need of performing kinetic experiments to determine inhibition type and accurate  $K_{ic}$  values.

Our conclusions are that *Mycobacterium vaccae* can be considered as an option for the degradation of the fuel additive, MTBE. Both propane and *iso*-pentane grown *Mycobacterium vaccae* JOB5 were found able to aerobically cometabolize MTBE and its breakdown products. Degradation of MTBE, TBF, and TBA in growth batch reactors was taken to completion using *iso*-pentane as a growth supporting substrate. These results provide evidence that TBA does accumulate, but also 100 % degradation was achieved after former compounds (MTBE and TBF) were degraded. *iso*-pentane is a major component of gasoline, thus MTBE degradation can be achieved and no addition of substrate is required. Significant MTBE reduction can be expected from cometabolic MTBE degradation at point sources of gasoline spills if oxygen is present.

Aerobic cometabolism by microorganisms has been successfully applied in the bioremediation of a variety of chlorinated aliphatic

hydrocarbons (McCarty et al., 1998; Tovanabootr, 1997; Hamamura et al., 1997; Semprini et al., 1998; Rungkamol, 2001)

Our results suggest that similar approaches can be applied to the bioremediation of MTBE from gasoline-spills contamination. The systematic methods used in this study provided accurate kinetic values that were shown to successfully model growth experiments for cometabolism of *iso*-pentane and cometabolism of MTBE.

More detailed kinetic studies are suggested to evaluate the interaction of substrates, MTBE, TBF, and TBA in the presence of gasoline during the cometabolism process and to clearly identify inhibition relationships. Such information would lead to a better understanding of this complex system and to better models of possible remediation of contaminated groundwaters.

## 2.6 References

- Burleigh-Flayer, H. D., J. S. Chun and W. J. Kintigh. (1992). Methyl *tertiary*-butyl ether vapor inhalation oncogenicity study in CD1 mice. Export, PA, Bushy Run Research Center.
- Chang, H. L. and L. Alvarez-Cohen. 1996. Biodegradation of individual and multiple chlorinated aliphatic hydrocarbons by methane-oxidizing cultures. *Appl. Environ. Microbiol.* 62: 3371-3377.
- Chun, J. S., H. D. Burleigh-Flayer and W. J. Kintigh. (1992). Methyl *tertiary*-butyl ether: vapor inhalation oncogenicity study in Fischer 344 rats. Export, PA, Bushy Run Research Center.
- Church, C. D., J. F. Panko and a. P. Trantnyek. 1999. Hydrolysis of *tert*-butyl formate: Kinetics, products and implications for the environmental impact of methyl *tert*-butyl ether. *Environ. Toxicol. Chem.* 18: 2789-2796.
- Church, C. D., P. G. Trantnyek, J. F. Pankow, J. E. Landmeyer, A. L. Baehr, M. A. Thomas and M. Schirmer. (1999). Effects of environmental conditions on MTBE degradation in model column aquifers. U. S. Geological Survey : 93 - 101.
- Cornish-Bowden, A. (1995). *Fundamentals of enzyme kinetics*. London, Portland Press. Ltd.
- Deeb, R. A., K. M. Scow and L. Alvarez-Cohen. 2000. Aerobic MTBE biodegradation: An examination of past studies, current challenges and future research directions." *Biodegradation* 11: 171 - 186.
- EPA, (1997). *Drinking Water Advisory: Consumer acceptability advice and health effects analysis on MTBE*.
- Finneran, K. T. and D. R. Lovley. 2001. "Anaerobic degradation of methyl *tert*-butyl ether (MTBE) and *tert*-butyl alcohol (TBA)." *Environ. Sci. Technol.* 35: 1785-1790.
- Fortin, N., M. Deshusses, J. Eweis, R. S. Hanson, K. Scow, D. P. Chang and E. Schroeder. (1997). Biodegradation of MTBE: Kinetics, metabolism of degradation by-products and role of oxygen release compounds. 1997 ACS Pacific Pacific Conference on Chemistry and Spectroscopy.



- Fortin, N. Y. and M. A. Deshusses. 1999. Treatment of methyl *tert*-butyl ether vapors in biotrickling filters. 1: Reactor startup, steady-state performance, and culture characteristics." Environ. Sci. Technol. 33: 2980-2986.
- Fortin, N. Y. and M. A. Deshusses. 1999. Treatment of methyl *tert*-butyl ether vapors in biotrickling filters. 2: Analysis of the rate limiting step and behavior under transient conditions. Environ. Sci. Technol. 33: 2987-2991.
- Garnier, P. M., R. Auria, C. Augur and S. Revah. 1999. Cometabolic biodegradation of methyl *t*-butyl ether by *Pseudomonas aeruginosa* grown on pentane. Appl. Microbiol. Biotechnol. 51: 498-503.
- Gornall, G., C. J. Bardawill and M. David. 1949. Determination of serum proteins by means of the biuret reaction. J. Biol. Chem. 177: 751-766.
- Hamamura, N., C. Page, T. Long, L. Semprini and D. Arp. 1997. Chloroform cometabolism by butane-grown CF8, *Pseudomonas butanorova* and *Mycobacterium vaccae* JOB5 and methane-grown *Methylosinus trichosporium* OB3b. Appl. Environ. Microb. 63: 3607-3613.
- Hanson, J., K. M. Scow, M. Bruns and T. Brethour (1996). Characterization of MTBE-degrading bacterial isolates and associated consortia. MTBE Workshop, Univ. Calif., Davis.
- Hanson, R. S., C. E. Ackerman and K. Scow. 1999. Biodegradation of methyl *tert*-butyl ether by a bacterial pure culture. Appl. Environ. Microbiol. 65: 4788 - 4792.
- Hardison, L., S. Curry, L. Ciuffetti and M. Hyman. 1997. Metabolism of diethyl ether and cometabolism of methyl *tert*-butyl ether by a filamentous fungus, *Graphium* sp. Appl. Environ. Microbiol. 63: 3059-3067.
- Haston, Z. C. and P. L. McCarty. 1999. Chlorinated ethene half-velocity coefficients ( $K_s$ ) for reductive dehalogenation. Environ. Sci. Technol. 33: 223-226.
- Hyman, M., P. Kwon, K. J. Williamson and K. O'Reilly. (1998). Cometabolism of MTBE by alkane-utilizing microorganisms. In G.B. Wickramanayake and R. Compounds, Batelle Press, Columbus, OH.

Hyman, M. and K. O'Reilly. (1999). Physiological and enzymatic features of MTBE-degrading bacteria. In situ bioremediation of petroleum hydrocarbon and other organic compounds, Batelle Press, Columbus. OH.

Jacobs, J., J. Guertin and C. Herron. (2000). MTBE: Effects on soil and groundwater resources, Lewis Publishers.

Kenner, W. K. and D. J. Arp. 1993. Kinetic studies of ammonia monooxygenase inhibition in *Nitrosomonas europaea* by hydrocarbons and halogenated hydrocarbons in an optimized whole-cell assay. Appl. Environ. Microbiol. 59: 2501-2510.

Kim, Y. 2000. Aerobic cometabolism of chlorinated aliphatic hydrocarbons by a butane-grown mixed culture: transformation abilities, kinetics and inhibition. Ph.D.. Thesis. Oregon State University: Corvallis, OR.

Kim, Y., D. J. Arp and L. Semprini. 2002. A combined method for determining inhibition type, kinetic parameters, and inhibition coefficients for aerobic cometabolism of 1,1,1-Trichloroethane by a butane-grown mixed culture. Biotechnology and Bioengineering 77: 564-576.

Kwon, P. O. 1998. A study of in-situ bioremediation of methyl *tert*-butyl ether (MTBE) through cometabolic processes by alkane-utilizing microorganisms Project report. Oregon State University: Corvallis, OR.

Mackay, D. and W. Ying. 1981. "Critical review of Henry's Law constants for chemicals of environmental interest. J. Phys. Chem. 10: 1175-1195.

McCarty, P., M. Goltz, G. Hopkins, M. Dolan, J. Allan, B. Kawakami and T. Carrothers. 1998. Full scale evaluation of in-situ cometabolic degradation of Trichloroethylene in groundwater through toluene injection. Environ. Sci. Technol. 32: 88-100.

Mill, T. 1982. Hydrolysis and oxidation processes in the environment. Environ. Toxicol. Chem. 1: 135-141.

Missen, R. W., C. A. Mims and B. A. Saville. (1999). Chemical reaction engineering and kinetics. Toronto, Canada, John Wiley & Sons, Inc.

Mo, K., O. Lora, A. E. Wanken and M. Javammardian. 1997. Biodegradation of methyl *t*-butyl ether by pure bacterial cultures. Appl. Microbiol. Biotechnol 47: 69-72.

Rungkamol, D. 2001. Aerobic cometabolism of 1,1,1-Trichloroethane and other chlorinated aliphatic hydrocarbons by indigenous and bioaugmented butane-utilizers in Moffett field microcosms. M.S. Thesis. Oregon State University: Corvallis, OR.

Salanitro, J., C. Chou, H. Wisniewski and T. Vipond. (1998). Perspectives on MTBE degradation and the potential for in-situ aquifer bioremediation. Southern Regional Conference on the Nat. G.W. Association.

Salanitro, J., L. Diaz, M. Williams and H. Wisniewski. 1994. Isolation of a bacterial culture that degrades methyl *tert*-butyl ether. Appl. Microbiol. 60: 2593-2596.

Salanitro, J. P., G. E. Spinnler, P. M. Maner and K. A. Lyons. 2001. Enhanced bioremediation of MTBE (Bioremedy) at retail gas stations. AEHS, Contaminated Soil, Sediment and Groundwater, The magazine of Environmental Assessment & Remediation: 47-49.

Semprini, L., R. L. Ely and M. M. Lang. 1998. Modeling of cometabolism for the in-situ biodegradation of Trichloroethylene and other chlorinated aliphatic hydrocarbons. Bioremediation 1: 89-134.

Squillace, P. J., J. S. Zogorski, W. G. Weber and V. Price. 1996. Preliminary assessment of the occurrence and possible sources of MTBE in groundwaters in the United States, 1993 -1994. Environ. Sci. Technol. 30: 721-730.

Steffan, J., K. McClay, S. Vainberg, C. Condee and D. Zhang. 1997. Biodegradation of the gasoline oxygenates methyl *tert*-butyl ether and *tert*-amyl methyl ether by propane-oxidizing bacteria. Appl. Environ. Microbiol. 63: 4216-4222.

Stocking, A. J., R. A. Deeb, A. E. Flores, W. Stringfellow, J. Talley, R. Brownell and M. C. Kavanaugh. 2000. Bioremediation of MTBE : A review from a practical perspective. Biodegradation 11: 187-201.

Sulfit, J. M. and M. R. Mormille. 1993. Anaerobic biodegradation of known and potential gasoline oxygenates in the terrestrial sub-surface. Environ. Sci. Technol. 27: 976-978.

Tovanabootr, A. 1997. Aerobic cometabolism of chlorinated aliphatic hydrocarbons by subsurface microbes grown on methane, propane, and butane from McClellan Air Force Base. M.S. Thesis. Oregon State University: Corvallis, OR.

Wilson, B. H., H. Shen, D. Pope and S. Schmelling. (2001). Cost of MTBE remediation. The Sixth International In Situ and On-Site Bioremediation Symposium, San Diego, California, Battelle Press.

Yeh, C. K. and J. T. Novak. 1994. Anaerobic biodegradation of gasoline oxygenates in soil. *Water Environ. Res.* 66: 744-752.

Zogorski, J., A. Morduchowist, A. Baehr, B. Bauman, D. Conrad, R. Drew, N. Korte, W. Lapham, J. Pankow and E. Washington. 1996. Fuel Oxygenates and Water Quality: Current Understanding of Sources, Occurrence in Natural Waters, Environmental Behavior, Fate, and Significance. Washington, D.C., Interagency oxygenated fuel assessment, office of science and technology policy, executive office of the President.

## Chapter 3

**“Degradation of Methyl *tert*-Butyl Ether (MTBE) and its Breakdown Products by Propane and *Iso*-pentane Grown *Mycobacterium vaccae* JOB5: Cometabolism and Inhibition”**

**Adriana Martínez-Prado, Kenneth J. Williamson  
and Lynda M. Ciuffetti**

**To Be Submitted to:**

**Water Research  
International Association on Water Quality, London, U.K.**

### 3.1 Abstract

A pure bacterial strain, *Mycobacterium vaccae* JOB5, was studied for its potential to aerobically cometabolize MTBE when grown on propane or *iso*-pentane as a primary substrate. Similarities were observed between the two alkane-grown bacterial systems. *Tert*-butyl formate (TBF) and *tert*-butyl alcohol (TBA) were the two intermediates identified from MTBE aerobic cometabolism. TBA was mineralized. Anaerobic and inhibition studies were performed on both alkanes, MTBE, and its breakdown products. Propane, *iso*-pentane, MTBE, and TBA were not oxidized under anaerobic conditions and were inhibited by acetylene. On the other hand, TBF was further transformed to TBA under anaerobic conditions, but at a slower rate than under aerobic conditions, and acetylene did not affect its degradation. Competitive inhibition was observed between MTBE, TBA, and the substrates. These results suggest that at least two different enzymes are present in the degradation pathway: a monooxygenase, responsible for the oxidation of propane, *iso*-pentane, MTBE, and TBA, and a hydrolytic enzyme for the transformation of TBF. Acetylene inhibition was reversible and the reversibility was found to be influenced by the trace composition of the liquid media.

### 3.2 Introduction

Methyl *tert*-butyl ether (MTBE), a fuel additive that has been used in gasoline since the early 1980s has been classified by the USGS (United States Geological Survey) as the second most common groundwater contaminant in the United States (Squillace et al., 1996). Fuel oxygenates, such as MTBE or TBA, were used as a lead substitute to enhance octane levels and to improve combustion to minimize carbon monoxide and ozone emissions (Jacobs et al., 2000). MTBE has been classified as a possible carcinogen and, although health risks of MTBE in humans are still unknown, a Drinking Water Advisory of 40 µg/L has been set based on taste and odor thresholds (EPA, 1997).

The phase out of MTBE is being presently debated in many states. Protection of water resources from MTBE contamination is the priority of many agencies. The cleanup cost associated with MTBE contamination is estimated to be in the range of 100s of millions of dollars. The average cost of MTBE remediation was reported to be a function of drinking water impact (Wilson et al., 2001). In general, the cleanup cost was about twice the cost for sites with drinking water impacts, as compared to sites with no drinking water impacts. Overall, cleanup costs for underground storage tanks (USTs) were found to be lower than the cleanup costs for drinking water wells contaminated with MTBE.

### 3.2.1 MTBE metabolites

MTBE metabolites, from either aerobic or anaerobic degradation, have been reported to be culture-dependent (Deeb et al., 2000). *Tert*-butyl alcohol (TBA) and *tert*-butyl formate (TBF) are examples of MTBE-oxidation intermediates (Hardison et al., 1997; Hyman et al., 1998; Garnier et al., 1999; Hyman and O'Reilly, 1999) with the former as the most common. Formaldehyde, 2-methyl 1-hydroxy 2-propanol (MHP), and 2-hydroxyisobutiric acid (HIBA) have been also reported (Steffan et al, 1997). Carbon dioxide can be directly produced from MTBE with no intermediates, especially when MTBE is used as a growth substrate. For anaerobic degradation, methane and carbon dioxide have been reported as the two end products for either MTBE or TBA (Yeh and Novak, 1994; Finneran and Lovley, 2001).

### 3.2.2 Acetylene as a monooxygenase inhibitor

Acetylene has been found to be either an inhibitor or an inactivator of several monooxygenases (MO). It has been reported to be an inactivator of particulate methane (pMMO) and soluble methane (sMMO) monooxygenases for *Methylococcus capsulatus* (Prior and Dalton, 1985);



butane monooxygenase (BMO) from butane-grown *Mycobacterium vaccae*, *Pseudomonas butanovora* and CF8 (Hamamura et al., 1997), and ammonia monooxygenase (AMO) from *Nitrosomonas europea* (Kenner and Arp, 1993). In the case of *Graphium* sp., acetylene has been reported as growth inhibitor (Curry et al., 1996) and as an inhibitor of the degradation of primary substrates and co-substrates, propane and butane, and MTBE, respectively (Hardison et al., 1997).

### 3.2.3 Objectives

This paper addresses the cometabolism and inhibition processes by a pure bacterial culture, *Mycobacterium vaccae* JOB5 for MTBE and its metabolites. Studies included the metabolism of propane and iso-pentane, and cometabolism of MTBE, TBF, and TBA under aerobic conditions in the absence and presence of acetylene, a known monooxygenase-activity inhibitor. Transformation processes under anaerobic conditions were also evaluated. The reversibility of inhibition with acetylene was tested to determine the influence of acetylene source and liquid media composition.

### 3.3 Materials and methods

#### 3.3.1 Chemicals

*Mycobacterium vaccae* JOB5 (ATCC 29678) was obtained from the American Type Culture Collection (Rockville, Md.). MTBE (99.8 %), propane (98 %), acetylene (99.6 %), *iso*-pentane (99.5 %), *tert*-butyl Formate (TBF) (99 %), *tert*-butyl Alcohol (TBA) (99 %), and dimethyl sulfoxide (DMSO) were obtained from Aldrich Chemical Company Co., Inc. (Milwaukee, Wis.). All gases were of the highest purity available, and all other chemicals were reagent grade or better.

#### 3.3.2 *Mycobacterium vaccae* JOB5 growth

*Mycobacterium vaccae* was grown in the *Xantobacter* Py2 medium (Hamamura et al., 1997) with the modification that iron was added as 1 ml/L of Fe-EDTA solution and 1ml/L of the micronutrient solution. Cultures were grown in a 700-ml glass bottles (Wheaton Scientific, Millville, N.J.) sealed with screw caps fitted with butyl rubber septa with identical liquid and headspace volume. Propane and *iso*-pentane were the two alkanes

selected as growth substrates. A volume of 60 ml propane was added by using a syringe fitted with 0.25 mm pore size sterile filters. A volume of 350  $\mu$ l of *iso*-pentane was added using the "water trap" method because of its high volatility and flammability. In the water trap method, *iso*-pentane is added to experimental bottles trapped between two separate volumes of water with a liquid-tight syringe (Hamilton Company). Bottle headspaces were adjusted to a pressure close to 1 atm and shaken at 200 rpm at 30°C. Cells were harvested at an optical density (OD<sub>600</sub>) of about 0.85 at 600 nm.

In order to obtain a reproducible culture, 800  $\mu$ l of harvested cells were added to a 2-ml autoclaved cryogenic vial receiving 70  $\mu$ l of DMSO and stored in an -80°C freezer to ensure consistent inoculums for the experiments (Kim, 2000; Hamamura et al., 1997). When inoculums were needed, the frozen cells were thawed, washed, and rinsed three times with fresh media to remove DMSO and possible toxicity. Cell growth of *M. vaccae* was monitored by removing 1 ml of the culture and measuring optical density (OD<sub>600</sub>) using an HP8453 UV-Visible spectrophotometer. Bacterial biomass was determined as total suspended solids (TSS). TSS was measured by filtering a known volume through a 0.1-mm membrane filter (Micro separation Inc., Westboro, MA) and drying at 60 °C for 24 h.

### 3.3.3 Analytical procedures

Alkanes and acetylene concentrations were monitored with a gas chromatograph (Model HP6890) fitted with a flame ionization detector (GC-FID). A 30 m x 0.45 mm I.D., 2.55  $\mu$ m DB-MTBE column was used (Agilent Technology, Willmington, DE) at an oven temperature of 65 °C; gas flow rates for helium, hydrogen and air were 15, 35, and 250 ml/min, respectively. In all experiments, 100  $\mu$ l headspace samples were taken and analyzed directly without further preparation.

MTBE, TBF, and TBA were monitored with a gas chromatograph (Model HP5890A) fitted with a flame ionization detector (GC-FID). A 3' x 1/8" I.D. stainless steel column packed with Porapak Q (80/100 mesh) (Alltech Associates, Inc., Deerfield, IL) was used at an oven temperature of 135°C and a detector temperature of 220°C. Helium was used as the carrier gas with a 40 ml/min flow rate. In all experiments, liquid samples (2  $\mu$ l) were taken and analyzed directly without further preparation. Appropriate external standard curves were developed for all cases. MTBE and TBF were monitored, only for qualitative experiments using the DB-MTBE column listed first. Carbon dioxide accumulation and oxygen consumption were monitored with a gas chromatograph (Model HP5890) fitted with a thermal conductivity detector (GC-TCD). A Carboxen 1000

column (15' x 1/8"; Supelco, Bellefonte, PA.) was used at a temperature of 30°C for a 7 min run using Argon as the carrier gas at 15 ml/min.

All experiments were conducted in 27.8-ml glass vials (Supelco, Bellefonte, PA) crimped with aluminum seals fitted with butyl stoppers. The mixture reaction had a total volume of 5-ml of autoclaved Py2 media, unless stated differently.

#### **3.3.4 Kinetic and inhibition essays**

Cells were harvested from cultures by centrifugation (6000 x g for 15 min), concentrated, and washed three times with the same fresh Py2 media. Propane and *iso*-pentane were added by removing known volumes from double flasks or water-trap bottles, respectively. MTBE, TBF, or TBA was added as needed from either stock or saturated aqueous solution. Bottles were placed in a rotatory shaker (200 rpm) at 20°C. Initial concentrations of compounds in the experimental bottles were measured before cells were added to initiate the reaction. Liquid and headspace samples were taken for MTBE, TBF, and TBA, and for propane and *iso*-pentane, respectively. Abiotic and killed controls were also included in all experiments.

### **3.3.5 Transformation under anaerobic conditions**

*iso*-pentane, propane, MTBE, TBF, and TBA, were tested for transformation under anaerobic conditions. To create these conditions, bottles containing Py2 medium were purged with nitrogen treated in a tube furnace at 600°C for 45 minutes. Headspace measurements were performed by GC-TCD to ensure anaerobic conditions were established. Compounds were added to the bottles as previously described and shaken at 200 rpm at 20°C. Initial concentrations for each compound were determined before cells were added. After harvesting, the cells also were purged of oxygen, following the same protocol described above, and added to experimental bottles to initiate the reaction. Abiotic and killed controls were also included.

### **3.3.6 Blocking experiments with acetylene**

Experiments were performed to follow the degradation of growth substrates (propane and *iso*-pentane), MTBE, TBF, and TBA in the presence of acetylene. Acetylene (AIRCO source) was added in different amounts, 0.5%, 1.1%, and 2.2% (v/v), for testing inhibition on both alkanes

in Py2 media. Degradation of the substrate was followed for a fixed period of time by analyzing headspace samples. After that time, bottles were purged 15 min with N<sub>2</sub> to strip all acetylene, the cap was removed under sterile conditions to allow oxygen equilibration with the atmosphere, and then the bottles were recapped. The substrate was added again and the degradation of the substrate was followed again to observe if cells had recovered alkane oxidation activity.

Similar studies were performed to test acetylene (calcium carbide source) effect on propane degradation in Py2 media and 10 mM phosphate buffer solution. Acetylene concentrations tested were 0, 0.11, 2.2 and 4.5% (v/v). Acetylene was made in the laboratory from the reaction of calcium carbide and water. Small amounts (few grams) of calcium carbide are added to a 200-ml double flask filled with water. A sleeve stopper is inserted in the side neck and the double flask is placed in a ventilated hood and sit still. Reaction starts immediately producing acetylene gas. Acetylene gas is trapped between two volumes of water as a result of water displacement to the upper section of the double flask.

The inhibition effect on MTBE, TBF and TBA at a single concentration of acetylene (0.5% (v/v) (AIRCO source) was also tested. Control bottles with cells in the presence of the substrate only and no addition of acetylene was also included in the experimental set up as well as a killed control.

### 3.3.7 Control bottles

In all experiments, an abiotic control and a killed cell control were included. The abiotic control was identical to an experimental treatment, except no cells were added. The killed control was identical to an experimental treatment, but cells were poisoned with a 10% solution of  $\text{HgCl}_2$ .

## 3.4 Results

*Mycobacterium vaccae* JOB5 was found able to aerobically cometabolize MTBE after grown on propane and *iso*-pentane as a carbon and energy source. TBF and TBA were the two intermediates or breakdown products identified from MTBE oxidation. Carbon dioxide accumulation was observed from TBA oxidation. No growth was observed when MTBE, TBF, or TBA was used as the sole source of carbon and energy. It was concluded that degradation of MTBE and breakdown products occurred via cometabolism. Figure 3.1 shows an example of the cometabolism of MTBE, TBF, and TBA by propane-grown culture. Culture was harvested after growth on propane; concentrated cells (3.125 mg TSS) were incubated with 4  $\mu\text{mol}$  of MTBE under aerobic conditions and degradation



was followed with time. TBF was formed from MTBE oxidation and further degraded to TBA; an increase in  $\text{CO}_2$  (qualitatively) was observed from TBA oxidation. No MTBE oxidation was observed in the killed control.

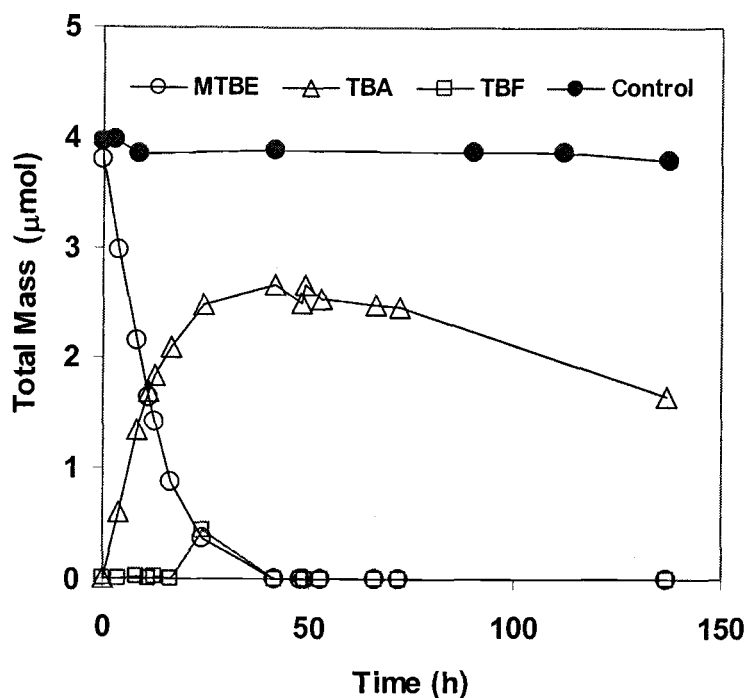


**Figure 3.1** MTBE cometabolism by propane grown *Mycobacterium vaccae* under aerobic conditions.

For experiments under anaerobic conditions, no significant degradation of propane, *iso*-pentane, MTBE and TBA occurred. TBF was the only compound degraded, but at a slower rate as compared to the rate under aerobic conditions which caused TBA to build up in the system. It

was estimated that the oxidation rate of TBF was about 1.4 times faster under aerobic conditions than under anaerobic conditions; Figure 3.2 shows an example for the propane-grown system.

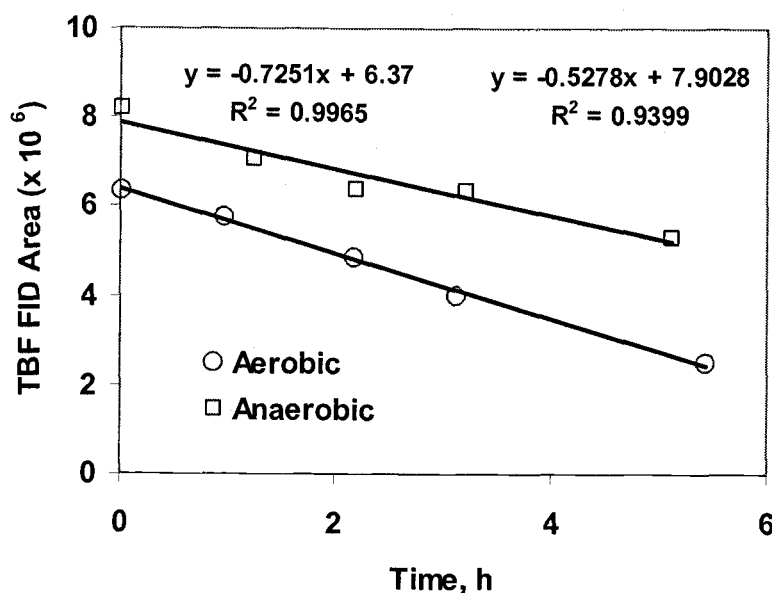


**Figure 3.2.** Transformation of TBF under aerobic and anaerobic conditions by propane-grown *Mycobacterium vaccae*.

Concentrated cells of the propane-grown culture (7 mg TSS) were exposed to propane (4  $\mu\text{mol}$ ), MTBE (2  $\mu\text{mol}$ ), TBF (3  $\mu\text{mol}$ ), and TBA (3  $\mu\text{mol}$ ) under anaerobic conditions. In a similar experiment with *iso*-pentane grown culture, concentrated cells (7.5 mg TSS/L) were incubated with *iso*-pentane (3  $\mu\text{mol}$ ), MTBE (2  $\mu\text{mol}$ ), TBF (3  $\mu\text{mol}$ ) and TBA (3  $\mu\text{mol}$ ) under

anaerobic conditions and degradation of all compounds was monitored for the same period of time, 24 hours.

For independent bottles, for each alkane system, and after 3 h under anaerobic conditions oxygen was added and degradation of both substrates, MTBE, and TBA took place immediately with a faster rate for TBF until complete consumption. Bottles kept under anaerobic conditions for 24 hours showed little propane, *iso*-pentane, and MTBE degradation (<10%) whereas TBF was transformed (95 -100 %) with a corresponding build up of TBA (> 80%). A killed control was also included with no significant change for the substrates or MTBE. A small decrease in TBF and a small increase in TBA occurred, probably due to TBF abiotic hydrolysis. Results of these experiments are summarized in Table 3.1.

**Table 3.1** Degradation under anaerobic conditions (%)  
by *Mycobacterium vaccae* after 24 hours

Compound	Propane grown culture	<i>iso</i> -pentane grown culture
Propane	7	-----
<i>iso</i> -pentane	-----	8
MTBE	9	9
TBF	97	100
TBA	0*	0*

\* TBA accumulated in the system as a result of TBF transformation

The data in Figure 3.1 and Table 3.1 suggest that the alkane monooxygenase responsible for the degradation of the substrate is the same enzyme that cometabolizes MTBE and TBA. Acetylene has been shown to be useful to identify monooxygenase reactions; for example, acetylene was reported to inhibit the alkane monooxygenase in bacterial and fungal cultures (Hamamura et al., 1997; 1997; Steffan et al.; 1997 Hardison et al., 1997).

The influence of acetylene on the cometabolism of MTBE, TBF and TBA by our culture was evaluated. The same initial mass of each compound was tested in independent bottles. The final biomass concentration for the experiments performed was 1500 and 625 mg TSS/L for *iso*-pentane and propane-grown culture, respectively. A killed control bottle was also included in the experimental set up; no significant degradation took place

Figures 3.3 and 3.4 show the results for both bacterial systems. MTBE and TBA degradation were totally inhibited by the presence of acetylene suggesting that a monooxygenase enzyme is responsible for the cometabolism of those two compounds, maybe the same enzyme as the for the growth substrates. In the case of TBF degradation, however, no effect was observed. Degradation trace lines overlapped in both cases.

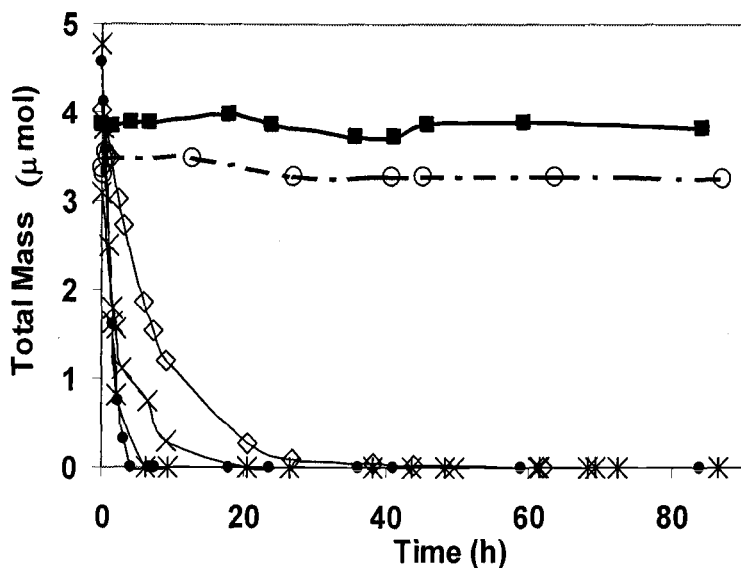


**Figure 3.3.** Influence of acetylene on aerobic cometabolism of MTBE, TBF, and TBA. by the *iso*-pentane-grown culture. MTBE(x); TBF(\*); TBA(◇). MTBE+C<sub>2</sub>H<sub>2</sub>(○), TBF+C<sub>2</sub>H<sub>2</sub>(●), TBA+C<sub>2</sub>H<sub>2</sub>(■)

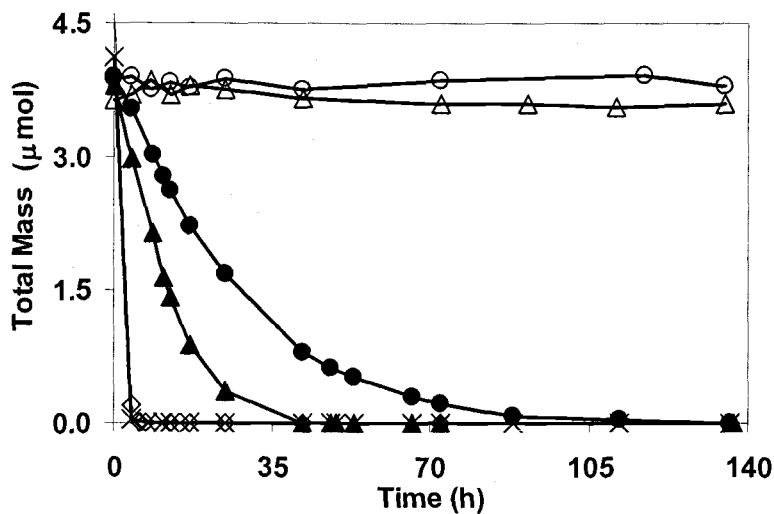


**Figure 3.4** Influence of acetylene on aerobic cometabolism of MTBE, TBF, and TBA by the propane-grown culture. MTBE(▲), TBF (\*), and TBA(●). MTBE+C<sub>2</sub>H<sub>2</sub>(△), TBF+C<sub>2</sub>H<sub>2</sub>(◇), TBA+C<sub>2</sub>H<sub>2</sub>(○)

Experiments to follow the degradation of the growth substrates in the absence and presence of acetylene were performed in two different scenarios. In the first case, concentrated cells of propane and *iso*-pentane grown cultures (1350 mg TSS/L) were exposed to 4  $\mu$ M substrate at 0, 200, 400, and 800  $\mu$ M solutions (0, 0.5, 1.1, and 2.2 % (v/v) respectively) acetylene (AIRCO source) in Py2 media. Degradation of both substrates, propane and *iso*-pentane, were followed with time by headspace GC analysis. Results of these experiments are summarized in Table 3.2. Data suggested acetylene acted as a reversible inhibitor. Once acetylene was removed cell recovered and the substrates were oxidized at about the same rate at both acetylene concentrations tested.

**Table 3.2** Acetylene (AIRCO source) effect on alkane oxidation activity by *Mycobacterium vaccae* JOB5. Cells (1350 mgTSS/L) were incubated with Py2 media and 100  $\mu$ l of alkane. Degradation followed for 3 hours in the presence and absence of C<sub>2</sub>H<sub>2</sub> (purged)

Acetylene % (v/v) [ $\mu$ M]	Acetylene present		After C <sub>2</sub> H <sub>2</sub> purged and readdition of substrate	
	propane	<i>iso</i> -pentane	propane	<i>iso</i> -pentane
0.5 [200]	Partially inhibited	Partially inhibited	N.T.	N.T.
1.1 [400]	Complete inhibition	Complete inhibition	56% of activity recovered	60 % of activity recovered
2.2 [800]	Complete inhibition	Complete inhibition	50% of activity recovered	57 % of activity recovered

N.T. Not tested

In the second case, liquid solutions of 10 mM phosphate buffer and Py2 media were used with acetylene from two different sources: 99.6 % AIRCO and laboratory made acetylene from calcium carbide (Hyman and Arp, 1987). Acetylene concentrations were 40, 800 and 1600  $\mu\text{M}$  (0.11, 2.2, and 4.4 % (v/v), respectively). The same amounts of concentrated cells (1350 mg TSS/L) were incubated with 100  $\mu\text{l}$  propane (4  $\mu\text{mol}$ ) in the absence and presence of acetylene at the concentrations listed previously. Degradation of the substrate was followed with time; after 2 h, the acetylene treated bottles were purged as described in materials and methods. The same amount of substrate was added and degradation of the substrate followed again. Results of these experiments are summarized in Table 3.3.

**Table 3.3** Acetylene (calcium carbide source) effect on propane oxidation by *Mycobacterium vaccae* JOB5 in two different liquid composition

Acetylene		Degradation (%) in Py2 media		Degradation (%) in 10 mM phosphate	
% (v/v)	[ $\mu\text{M}$ ]	A(+)	A(-) at 14 h	A(+)	A(-) at 14 h
0.11	40	0	94	0	18
2.2	800	0	100	0	8
4.4	1600	0	100	0	5

A(+) in the presence of acetylene

A(-) After acetylene purged and new addition of propane

All propane degraded at 9 h (Py2 media) and 19 h (phosphate), no acetylene added.

Same biomass (1350 mgTSS/L) and propane addition (100  $\mu\text{l}$ ) in all cases

A significant difference in the degradation of propane in the Py2 media and phosphate buffer solution was found when cells were not exposed to acetylene (Figure 3.5). The influence of acetylene on propane oxidation activity in the two different media composition is shown in Figure 3.6. It is hypothesized that the trace composition of the Py2 media results in a more rapid degradation and propane oxidation recovery. The Py2 media is complex and includes nutrients and trace elements such as Fe, Cu, Zn, Co, Mn, Ni, Mg, Na, and Ca (see Appendix B for exact composition).

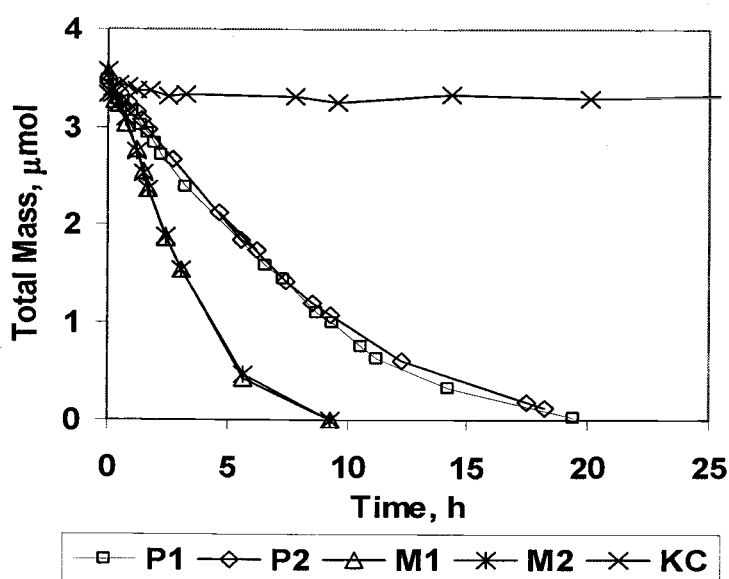


**Figure 3.5** Influence of media's trace composition on propane degradation. Propane-grown harvested *M. vaccae* JOB5 (1350 mg TSS/L) in two different liquid media: P (Phosphate solution), and M (Py2 media) were incubated with 100  $\mu$ l propane. Faster degradation on Py2 media and no degradation at all on killed control (KC).



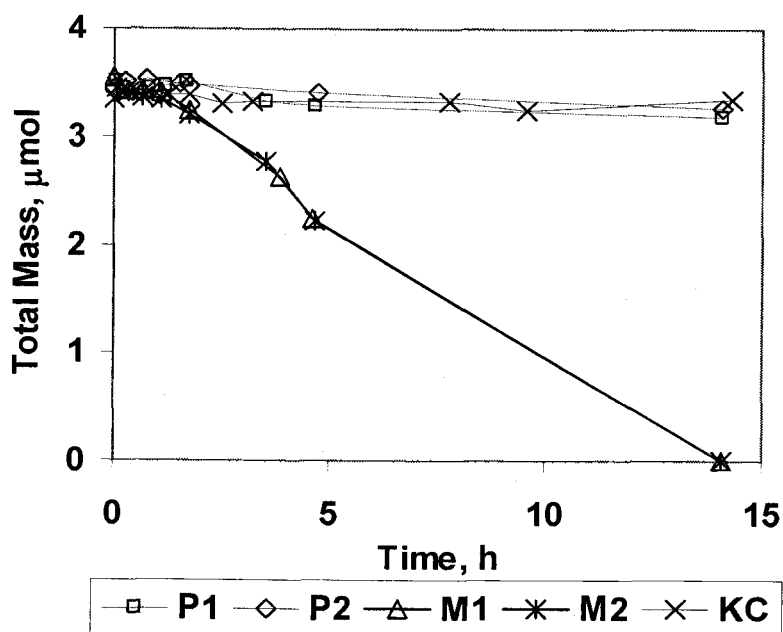


**Figure 3.6** Influence of media's trace composition and acetylene on propane degradation. After 2 hours exposure to 2.2 % (v/v) acetylene, bottles were purged and propane ( $100 \mu\text{l}$ ) added again. No degradation took place in P (Phosphate solution), or killed control (KC), and all propane consumed in M (Py2 media) bottles.

### 3.5 Discussion

Propane, *iso*-pentane, MTBE, and TBA were not degraded under anaerobic conditions and were inhibited by acetylene under aerobic conditions. In contrast, TBF was not inhibited by the presence of propane, *iso*-pentane, or acetylene. Similar results were observed for anaerobic degradation; with both substrates, TBF was the only compound degraded. TBF degradation rate was slower under anaerobic conditions. The estimated degradation rate for TBF under aerobic conditions was about 1.4 times faster than under anaerobic conditions.

The effect of acetylene in *M. vaccae* JOB5 with both substrates tested in this study was reversible when Py2 media used. Once acetylene was removed from the system, cells were able to re-establish oxidation activity confirming that acetylene acts as a reversible inhibitor. However, opposite results were obtained when a phosphate buffer was used instead of Py2 media. Hyman and Arp (1987) reported the effects of acetylene on inhibition experiments based on its source, mainly because of the presence of contaminants. Our results with the buffer system are comparable to those reported by Hamamura et al. (1997) with similar acetylene concentration for a butane grown culture. This suggests that a nutrient or trace element in the Py2 media protects the enzyme from losing its degradation capacity. One hypothesis is the presence of iron. More detailed

studies need to be performed to determine the reasons of this significant difference.

Our conclusions are that a similar metabolic patterns in the transformation of MTBE was observed, independently of which alkane was used as a carbon source, either propane or *iso*-pentane. The same influence of acetylene was observed in the degradation of the growth-supporting substrate, and in the cometabolism of MTBE, TBF, and TBA. At least two different enzymes appear to be involved in the degradation process; one for the oxidation of propane, *iso*-pentane, MTBE, and TBA; and a second one responsible for the transformation of TBF, most likely a hydrolase. More studies are needed to determine the number of enzymes involved in this process.

To the best of our knowledge, the results derived from this study provide the first evidence that TBF can be biologically degraded under anaerobic conditions.

### 3.6 References

- Curry, S., L. Ciuffetti and M. Hyman. 1996. Inhibition of growth of a *Graphium* sp. on gaseous *n*-alkanes by gaseous *n*-alkynes and *n*-alkenes. *Appl. Environ. Microbiol.* 62: 2198-2200.
- Deeb, R. A., K. M. Scow and L. Alvarez-Cohen. 2000. Aerobic MTBE biodegradation: An examination of past studies, current challenges and future research directions." *Biodegradation* 11: 171 - 186.
- EPA, (1997). Drinking Water Advisory: Consumer acceptability advice and health effects analysis on MTBE.
- Finneran, K. T. and D. R. Lovley. 2001. "Anaerobic degradation of methyl *tert*-butyl ether (MTBE) and *tert*-butyl alcohol (TBA)." *Environ. Sci. Technol.* 35: 1785-1790.
- Garnier, P. M., R. Auria, C. Augur and S. Revah. 1999. Cometabolic biodegradation of methyl *t*-butyl ether by *Pseudomonas aeruginosa* grown on pentane. *Appl. Microbiol. Biotechnol.* 51: 498-503.
- Hamamura, N., C. Page, T. Long, L. Semprini and D. Arp. 1997. Chloroform cometabolism by butane-grown CF8, *Pseudomonas butanorova* and *Mycobacterium vaccae* JOB5 and methane-grown *Methylosinus trichosporium* OB3b. *Appl. Environ. Microb.* 63: 3607-3613.
- Hardison, L., S. Curry, L. Ciuffetti and M. Hyman. 1997. Metabolism of diethyl ether and cometabolism of methyl *tert*-butyl ether by a filamentous fungus, *Graphium* sp. *Appl. Environ. Microbiol.* 63: 3059-3067.
- Hyman, M., P. Kwon, K. J. Williamson and K. O'Rilley. (1998). Cometabolism of MTBE by alkane-utilizing microorganisms. In G.B. Wickramanayake and R. Compounds, Batelle Press, Columbus, OH.
- Hyman, M. and K. O'Reilly. (1999). Physiological and enzymatic features of MTBE-degrading bacteria. In situ bioremediation of petroleum hydrocarbon and other organic compounds, Batelle Press, Columbus. OH.
- Hyman, M. R. and D. J. Arp. 1987. quantification and removal of some contaminating gases from aceylene to sutdy gas-utilizing enzymes and microorganisms. *Appl. Environ. Microbiol.* 53: 298-303.

Jacobs, J., J. Guertin and C. Herron. (2000). MTBE: Effects on soil and groundwater resources, Lewis Publishers.

Kenner, W. K. and D. J. Arp. 1993. Kinetic studies of ammonia monooxygenase inhibition in *Nitrosomonas europaea* by hydrocarbons and halogenated hydrocarbons in an optimized whole-cell assay. Appl. Environ. Microbiol. 59: 2501-2510.

Kim, Y. 2000. Aerobic cometabolism of chlorinated aliphatic hydrocarbons by a butane-grown mixed culture: transformation abilities, kinetics and inhibition. Ph.D.. Thesis. Oregon State University: Corvallis, OR.

Prior, S. D. and H. Dalton. 1985. Acetylene as a suicide substrate and active site probe for methane monooxygenase from *Methylococcus capsulatus* (Bath). FEMS Microbiol Lett. 29: 105-109.

Squillace, P. J., J. S. Zogorski, W. G. Weber and V. Price. 1996. Preliminary assessment of the occurrence and possible sources of MTBE in groundwaters in the United States, 1993 -1994. Environ. Sci. Technol. 30: 721-30.

Steffan, J., K. McClay, S. Vainberg, C. Condee and D. Zhang. 1997. Biodegradation of the gasoline oxygenates methyl *tert*-butyl ether and *tert*-amyl methyl ether by propane-oxidizing bacteria. Appl. Environ. Microbiol. 63: 4216-4222.

Wilson, B. H., H. Shen, D. Pope and S. Schmelling. (2001). Cost of MTBE remediation. The Sixth International In Situ and On-Site Bioremediation Symposium, San Diego, California, Battelle Press.

Yeh, C. K. and J. T. Novak. 1994. Anaerobic biodegradation of gasoline oxygenates in soil. Water Environ. Res. 66: 744-752.

## Chapter 4

**“Kinetics of MTBE, TBF, and TBA Aerobic Cometabolism by  
an Alkane Grown Fungal Isolate, *Graphium sp.*”**

**Adriana Martínez-Prado, Kristin Skinner, Lynda M. Ciuffetti and.  
Kenneth J. Williamson**

**To Be Submitted To:**

**Applied and Environmental Microbiology  
American Society for Microbiology**

## 4.1 Abstract

A fungal isolate, *Graphium sp.*, was tested for its potential to grow on two alkanes, propane and *iso*-pentane. Liquid-suspension and filter-attached culture approaches were performed. For *Graphium sp.* grown in liquid-suspension, the yields (mg dry mass/mg substrate consumed) were 0.56 for 7 days growth in propane with  $1 \times 10^6$  initial conidia inocula, and 0.35 for 45 days growth in *iso*-pentane with  $5 \times 10^6$  initial conidia inocula. Filter-attached cultures grown on propane yielded  $0.33 \pm 0.04$  mg dry mass/mg propane for 5 days growth with  $2.5 \times 10^6$  initial conidia inocula. This approach was not studied for *iso*-pentane because of slow growth rates and low mycelial yields in liquid suspension cultures. MTBE was aerobically cometabolized by both approaches on propane, but yielded lower MTBE oxidation rates with liquid-suspensions. The two identified breakdown products of MTBE degradation were *tert*-butyl formate (TBF) and *tert*-butyl alcohol (TBA). *Graphium sp.* did not grow on MTBE, TBA, and TBF as the sole sources of carbon and energy.

Kinetic constants ( $k_{max}$  and  $K_s$ ) for propane, MTBE, and TBF were estimated from kinetic experiments, for the propane-grown filter-attached culture. Estimation methods included, non-linear least squares regression (NLSR), direct linear plot and reciprocal plot methods. A degradation rate

for TBA was estimated from the degradation of TBF in resting cells experiments.

## 4.2 Introduction

Methyl *tert*-butyl ether (MTBE) has been commonly added as an U.S. fuel oxygenate during the last 20 years (Salanitro et al., 1998). MTBE was used to create oxygenated or reformulated gasoline (RFG) to meet the mobile source requirements of the Clean Air Act of 1990. MTBE commonly was chosen because of its low cost, ease of production, and favorable transfer and blending characteristics. However, states are presently phasing out the use of MTBE because of its extensive contamination of surface and groundwater throughout the U.S. (Jacobs et al., 2000). MTBE is a serious groundwater pollutant because of its mobility, persistence, and toxicity, and it is now the second most common groundwater pollutant in the U.S. (Squillace et al., 1996). MTBE is classified as a possible human carcinogen (EPA, 1997). The Drinking Water Advisory has been set at 20 - 40  $\mu\text{g/L}$  (ppb), mainly to minimize human health risks and eliminate unpleasant tastes and odors. The health risk of MTBE exposure to humans is still largely unknown. MTBE has a high water solubility (43 to 54 g/L) that results in high groundwater concentrations when gasoline-containing MTBE



contaminates aquifers. It has a low Henry's coefficient ( $H = 0.022$  @  $25\text{ }^{\circ}\text{C}$ ) and a low biodegradation rate in both water and soil. MTBE is not strongly sorbed onto soils ( $K_{oc} = 1.05$ ), which results in a low retardation factor ( $R=1.05$ ) and significant transport from the original source area.

MTBE is considered to be chemically and biologically stable because of its tertiary carbon structure and ether linkage (White et al., 1996; Garnier et al., 1999). However, some alkane oxidizing microorganisms have been reported to cometabolically oxidize MTBE (Hardison et al., 1997; Steffan et al., 1997). Cometabolism is defined as the transformation of a non-growth supporting substrate, in the presence of a growth-supporting substrate, in this case MTBE and propane, respectively. Such enzymatic activity has been also observed for microbes grown on aliphatic components of gasoline such as *iso*-pentane (Hyman et al., 1998; Hyman and O'Reilly, 1999). This suggests that substrates present within gasoline itself can support the growth of MTBE oxidizing organisms.

MTBE metabolites or intermediates may vary under either aerobic or anaerobic conditions. *Tert*-butyl alcohol (TBA) has been reported as the most stable MTBE breakdown product (Hardison et al., 1997; Steffan et al., 1997; Garnier et al., 1999). Few studies had reported *tert*-butyl formate (TBF) as an intermediate of aerobic MTBE oxidation (Hardison et al., 1997; Hyman et al., 1998). Others have shown that carbon dioxide is directly produced from MTBE oxidation (Bradley et al., 1999). Anaerobic

degradation of MTBE and TBA results in the production of methane and carbon dioxide (Yeh and Novak, 1994; Finneran and Lovley, 2001).

Previous studies at OSU have shown that *Mycobacterium vaccae* JOB5 and *Graphium sp.* aerobically cometabolize MTBE (Hardison et al., 1997; Hyman et al., 1998; Hyman and O'Reilly, 1999). Hardison et al. (1997) reported aerobic cometabolism of MTBE by propane and *n*-butane grown *Graphium sp.*; however, in these studies kinetic constants ( $k_{max}$  and  $K_s$ ) were not reported from kinetic experimental data at different biomass and for a wide concentration range.

*Graphium sp.*, a soil-borne ascomycete, is one of the few eukaryotes known to utilize gaseous alkanes as a growth substrate (Zajic et al., 1969; Davies et al., 1974; Curry et al., 1996; Hardison et al., 1997). This microorganism was first isolated when natural gas was used as carbon and energy source from sewage and after selection in an enrichment culture (Zajic et al., 1969). Studies with fungi indicated that the alkane oxidization pathway includes alcohol, aldehyde and fatty acids metabolites (Zajic et al., 1969). It is suggested that the initial step in the oxidation of alkanes by *Graphium sp.* is catalyzed by a cytochrome P-450 monooxygenase, which was supported with the fact that the presence of acetylene and ethylene prevented its growth (Curry et al., 1996; Hardison et al., 1997).

This paper addresses the estimation and comparison of the biokinetic constants  $k_{max}$  (maximal degradation rate,  $\mu\text{mol/mg dry mass-h}$ )

and  $K_s$  (half-saturation constant,  $\mu\text{mol/L}$ ) from kinetic experiments obtained by three different methods: non-linear least squares regression, direct linear plot, and Lineweaver Burk reciprocal plot.

### 4.3 Materials and methods

#### 4.3.1 Materials

*Graphium* sp. (ATCC 58400) was obtained from the American Type Culture Collection (Rockville, M. D.). Methyl *tert*-butyl ether (99.8 %), propane (98 %), *iso*-pentane (99.5 %), *tert*-butyl formate (99 %), and *tert*-butyl alcohol (99 %), were obtained from Aldrich Chemical Company Co., Inc. (Milwaukee, WI.). All other chemicals used were reagent grade or better.

#### 4.3.2 *Graphium* sp. growth

Procedure to grow the fungal cultures were adapted from Hardison et. al., (1997). Sterile conditions were practiced throughout the whole

process. Stock cultures were maintained at 25 °C under constant illumination on potato dextrose agar (PDA) plates. Conidia were harvested from 6 to 10 day mycelia grown on PDA plates and were used to inoculate either liquid or filters.

For liquid culture, 700-ml glass bottles (Wheaton Scientific, Millville, N.J.) were used to grow the liquid suspension cultures in 100 ml mineral salts medium (MSM) (Curry et al., 1996). Bottles were sealed with screw caps fitted with butyl rubber septa (Wheaton Scientific) and inoculated with the conidia suspension ( $1 \times 10^6$ ). Either propane or *iso*-pentane was added as a growth-supporting substrate. Propane gas was transferred from the original cylinder to a double flask container trapped with water. A volume of 60 ml was withdrawn from the double-flask and added to the experimental bottle as an overpressure by using a syringe fitted with 0.25 mm pore size sterile filters. Because *iso*-pentane is a liquid alkane, highly flammable, and highly volatile, it was added (300  $\mu$ l) using the "water trap" method with a liquid-tight syringe. This method allowed isolating or trapping *iso*-pentane between two separate volumes of water in the syringe. Liquid suspension cultures were incubated for 7 days at  $25 \pm 0.5$  °C at 125 rpm on a rotatory shaker. Pressure was equilibrated to 1 atm by adding pure oxygen to maintain aerobic conditions along the incubation period.

For the cultures grown on glass filters, the same procedures were followed as for the conidia and adapted from Hardison et. al., (1997). Sterile

glass petri dishes with glass microfiber filters (Whatman GF/A) were used. Wicks of thick blotting paper (Sigma # P7176) were cut to fit into the bottom of the petri dish and a 7 cm x 4 cm glass filter was placed on top. Wick and filter were wetted with 8 ml of autoclaved MSM. The GF/A filter was inoculated with about  $2.5 \times 10^6$  conidia by pipetting, wetting as much of the filter as possible with the conidial suspension. The inoculated petri dishes were placed into a tight-sealing container with two septum inserted into the lid. The 7.8 L container was closed and the edges wrapped with parafilm to prevent leaks. Propane was injected at 15% (v/v). 1.5 L of headspace was removed and replaced with 1.2 L of 98% propane and 500 ml pure of oxygen using a 60-ml autoclaved plastic syringe fitted with 0.25 mm pore size sterile filters. The container was incubated at  $25 \pm 1$  °C in constant illumination for 5 days. A pressure of 1 atm was maintained by adding pure oxygen during the experiment.

Mycelial yields of *Graphium* sp. were determined from dry weight measurements (Hardison et al., 1997). Liquid cultures were vacuum filtered through previously dried and weighed miracloth (Calbiochem, La Jolla, Ca.). Mycelia and miracloth were dried at 65 °C for 24 hours and reweighed. For the attached-cultures, filters with mycelia growth were dried at 65 °C for 24 hours at the end of the experiments and reweighed. Biomass (mg dry mass) was obtained from the weight difference.

### 4.3.3 Analytical procedures

The degradation of alkanes and the cometabolism of MTBE and its metabolites were monitored with a gas chromatograph (Model HP6890) fitted with a flame ionization detector (GC-FID). A 30 m x 0.45 mm I.D., 2.55  $\mu$ m DB-MTBE column was used (Agilent Technology, Wilmington, DE) at an oven temperature of 65 °C; gas flow rates for helium, hydrogen and air were 15, 35, and 250 ml/min, respectively. In all experiments, headspace samples were taken and analyzed directly without further preparation. Appropriate external standard curves were developed for each chemical. Reported dimensionless Henry's Law coefficients (Mackay and Ying, 1981; Church et al., 1999; Garnier et al., 1999) were used to estimate concentrations in the liquid phase at equilibrium

For the liquid-cultures, MTBE, TBF, and TBA were monitored with a gas chromatograph (Model HP5890A) fitted with a flame ionization detector (GC-FID). A 3' x 1/8 " I.D. stainless steel column packed with Porapak Q (80/100 mesh) (Alltech Associates, Inc., Deerfield, IL) was used at an oven temperature of 135 °C and a detector temperature of 220 °C. Helium was used as the carrier gas with a 40 ml/min flow rate. In all experiments, liquid samples (2  $\mu$ l) were taken and analyzed directly without further preparation. Appropriate external standard curves were developed for all cases.

Oxygen consumption and carbon dioxide production were monitored from headspace measurements with a gas chromatograph (Model HP5890) fitted with a thermal conductivity detector (GC-TCD). A 15' x 1/8". Carboxen 1000 column from Supelco (Bellefonte, PA.) was used at a temperature of 30 °C for a 7 min run using Argon as the carrier gas at 15 ml/min. Sample lock gas-tight and liquid-tight syringes (Fisher Scientific) were used for all gas chromatography analysis.

Liquid volume contained in the filters was estimated by adding 2 ml of water to several filters, allowing it to absorb, and collecting the remaining water with an automated pipette to determine the remaining volume. The estimated volume was  $1.3 \pm 0.15$  ml.

Liquid was collected from filters at the end of the experiments as follows. GFA filters were carefully removed from serum vials; as the filters were removed, any liquid that accumulated on the sides of the vials was absorbed onto the filters by wiping the sides of the vial. The filters were then folded once lengthwise, with the fungal culture on the interior of the fold. The filter was wrapped around a 10-ml glass test tube and covered with a small strip of plastic wrap. The test-tube was placed in a 50-ml disposable centrifuge tube that was trimmed (to 45-ml line) to fit in a Beckman J-20 rotor. The disposable centrifuge tubes were balanced by filling the glass test tube with water. The rotor was placed in a Beckman centrifuge, and centrifuged at 6000 X g for 5 minutes. During centrifugation,

the liquid contained in the filters was drawn into the disposable centrifuge tube. This liquid was collected and placed into a 1.5-ml eppendorf tube.

#### **4.3.4 Kinetic assays**

*Graphium* sp. experiments were adapted from Hardison et. al., (1997). Liquid suspension cultures (Figure 4.1A) were harvested by gentle vacuum filtration and washed three times with 100 ml MSM. Mycelia then were resuspended in 50 ml of fresh MSM in a sterile 700-ml bottle. Bottles were sealed with screw caps fitted with butyl rubber septa. MTBE was added to the bottles and shaken in a rotary table at 125 rpm.

Filter-attached cultures growing in glass petri plates were removed from the container after five days of growth. Fungal cultures growing on the glass filters then were carefully transferred to 164-ml sterile serum vial bottles. Multiple filters were used to increase the biomass in each treatment. After the fungus was added to the bottle, the gas phase was calculated to be 157 to 163 ml and the liquid phase was between 1.3 to 6.5 ml, depending on the treatment. Serum vial bottles were sealed with a Teflon stopper and an aluminum crimp seal (Figure 4.1B). Chemicals were added as needed. Filter-attached cultures were not shaken during the experiment. The experimental designs are illustrated in Figure 4.1.



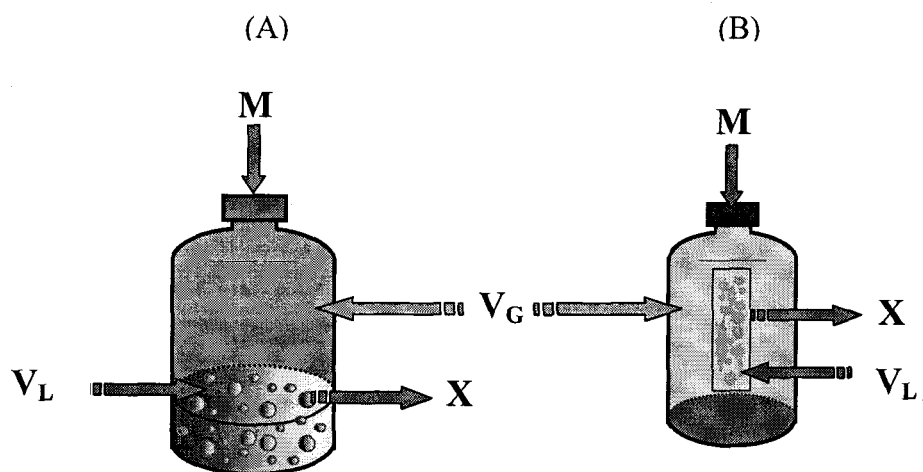


**Figure 4.1** Fungal experimental design. (A) Liquid – suspension culture (B) Filter-attached culture.  $V_L$  = Liquid phase (L),  $V_G$  = Gas phase (L),  $X$  = biomass (mg dry mass/L),  $M$  = total mass of compound to test ( $\mu\text{mol}$ ).

#### 4.3.5 Data analysis

The metabolism of propane and cometabolism of MTBE, TBF, and TBA were obtained from initial degradation rate to determine the maximal degradation rate,  $k_{max}$  ( $\mu\text{mol}/\text{mg dry mass-h}$ ), and the half-saturation coefficient,  $K_s$  ( $\mu\text{mol}/\text{L}$ ). The degradation rates of propane, MTBE, TBF, and TBA were described by Michaelis-Menten/Monod kinetics, described by Equation 4.1.

$$\frac{dM}{dt} = - \frac{k_{\max} \left( \frac{M}{V_L + H_{cc} * V_G} \right)}{K_s + \left( \frac{M}{V_L + H_{cc} * V_G} \right)} * V_L X \quad (4.1)$$

The kinetic constants were determined by three different methods as follows:

1) Non-linear least square regression (NLSR) analysis by fitting the differential form of Equation 4.1. The initial degradation rate ( $dM/dt$ ), was measured experimentally at different substrate concentration, and the two unknowns ( $k_{\max}$  and  $K_s$ ) determined by fitting the data with the statistical software SPLUS (Mathsoft Inc., Cambridge, MA). The initial entry values of the kinetic constants,  $k_{\max}$  and  $K_s$ , for the NLSR analysis, were obtained visually from initial rate versus concentration plots.

2) Lineweaver-Burk reciprocal plot. Equation 4.2, where  $v$  is the substrate degradation rate and  $S_L$  is the aqueous substrate concentration, is used to estimate  $K_s / k_{\max}$  as the slope and  $1 / k_{\max}$  as the y-intercept of a plot of  $1/v$  versus  $1/S_L$ .

$$\left( \frac{1}{v} \right) = \frac{1}{k_{\max}} + \frac{K_s}{k_{\max}} \frac{1}{S_L} \quad (4.2)$$

3) Direct linear plot. A plot was prepared with the initial degradation rate,  $v$ , (0,y) versus the corresponding negative value of the substrate concentration,  $S_L$  (x,0). Each pair of values are joined with a straight line and extrapolated to allow it to cross with any other line. Equation 4.3 describes the relationship of the kinetic constants where the intersection coordinates define a unique pair of  $k_{max}$  and  $K_s$  that satisfies both observations.

$$k_{max} = v + \frac{v}{S_L} K_s \quad (4.3)$$

The medians of each set provide the best estimates of the kinetic constants. The median, unlike the averages, is very robust thus less sensitive to outliers or extreme values that inevitably occur in the direct linear plot (Cornish-Bowden, 1995; Kim, 2000; Kim et al., 2002).

## 4.4 Results

*Grahium* sp. was tested for its potential to grow on *iso*-pentane as a growth substrate. *Iso*-pentane supported growth of *Graphium* sp., but at very slow rate and with low mycelial yields. For *Graphium* sp. grown in liquid suspension, the yields for propane and *iso*-pentane (mg dry mass/mg

substrate consumed) were 0.56 for 7 days growth with  $1 \times 10^6$  initial conidia inocula and 0.35 for 45 days growth with  $5 \times 10^6$  initial conidia inocula. Filter-attached cultures grown on propane yielded  $0.33 \pm 0.04$  mg dry mass/mg propane for 5 days with  $2.5 \times 10^6$  initial conidia inocula. This approach was not studied for *iso*-pentane because of slow growth rate and low mycelia yields at even a five-fold inoculum increase in liquid-suspension cultures.

Liquid-suspension of propane-grown *Graphium* *sp.* cultures yielded low MTBE oxidation rates. The maximum initial rate for a 10  $\mu$ mole addition was 6.7 nmole MTBE / h / mg dry mass (see Figure 4.2). When *Graphium* *sp.* was grown in a liquid-suspension culture, the biomass was manipulated during harvesting (filtering, rinsing and resuspending), which appeared to adversely affect the cometabolism rates. To avoid cell damage from manipulation, *Graphium* *sp.* kinetic experiments were completed with propane-grown filter-attached cultures.

*Tert*-butyl formate (TBF) and *tert*-butyl alcohol (TBA) were the two identified breakdown products from MTBE cometabolism. TBA was further degraded to CO<sub>2</sub>. No growth was observed when MTBE, TBF, or TBA was used as the sole source of carbon and energy.

*Graphium* *sp.* degraded propane at a rate of  $0.33 \pm 0.005$  mmol propane/hour as shown in Figure 4.3. Propane consumption occurred with no apparent lag phase.

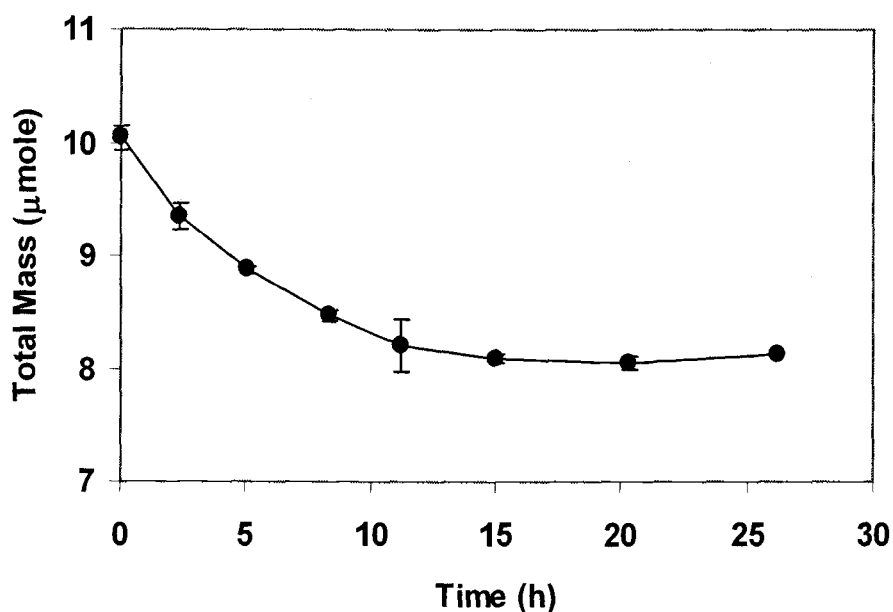


**Figure 4.2** Cometabolism of MTBE by propane-grown *Graphium* sp. liquid-culture. *Graphium* mycelia were grown on propane as described in materials and methods. The harvested mycelia (45 mg dry mass) were resuspended in 50 ml MSM in 700-ml bottle (triplicate) sealed with screw cap and butyl rubber septa. 10  $\mu$ mol MTBE were added from aqueous saturated solution to initiate the reaction. MTBE degradation (●) was followed with time and determined by immediately analyzing 2  $\mu$ l liquid-phase samples by GC-FID.

Kinetic experiments were design to measure the metabolism of propane and cometabolism of MTBE, TBF, and TBA. All experiments were designed to measure the initial degradation rate of the compound being tested in all bottles. Compounds were tested over a wide concentration range with increasing biomass (number of filters/bottle). Biomass was limited to 5 filters to avoid physical interaction of the filters. The

degradation rate for the substrate and cometabolism of MTBE and its metabolites were TBF > propane > MTBE > TBA. Data from single bottles for the three different compounds; propane, MTBE and TBF are shown in Figure 4.4.

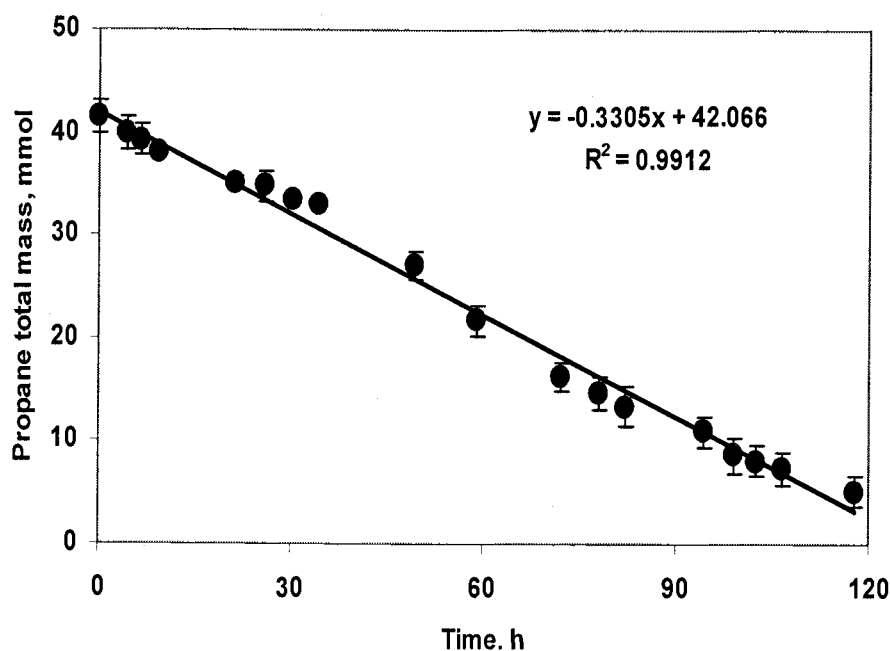


**Figure 4.3.** Filter-attached *Graphium* sp. growth on propane as a substrate (triplicate). Petri dishes containing inoculated filters ( $2.5 \times 10^6$  conidia) were placed into the 7.8 L container and propane was added as described in material and methods. Propane degradation (●) was measured as a function of time by directly analyzing 50  $\mu$ l of headspace samples by gas chromatography

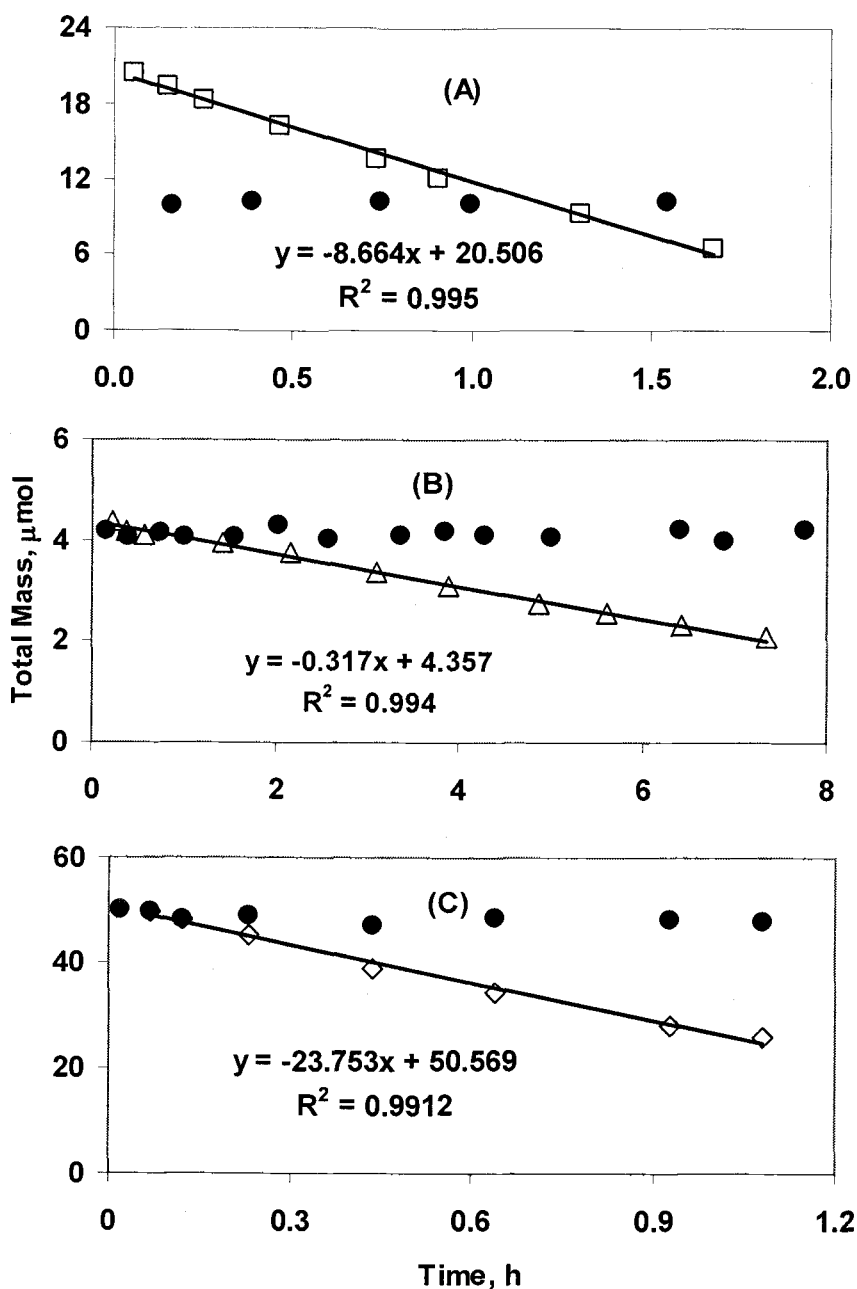


**Figure 4.4** Initial degradation rate of single compound by filter-attached *Graphium* sp. grown on propane. Filter-attached *Graphium* mycelia were grown on propane as described on materials and methods. 105 (A), 89 (B) and 63.8 (C) mg (dry weight) of harvested mycelia were incubated in sealed serum vials (164 ml). 500  $\mu\text{l}$  of 98% propane ( $\square$ ), 6  $\mu\text{l}$  MTBE ( $\triangle$ ) aqueous saturated solution, and 4  $\mu\text{l}$  of 99% TBF ( $\diamond$ ) were added respectively. No degradation of either compound took place in the killed control ( $\bullet$ ). Headspace samples were immediately analyzed by gas chromatography at the indicated times.

Several experiments at different initial concentrations for each compound were performed under the same conditions of inoculums, temperature, and sampling methods. Data was analyzed to obtain the kinetic constants by the methods already described.

A set of data for propane metabolism by filter-attached *Graphium sp.* grown on propane is shown on Figure 4.5 to illustrate how the kinetic constants were obtained. The solid line was the best fit using Equation 4.1 by non-linear least squares regression method using the statistical software SPLUS.

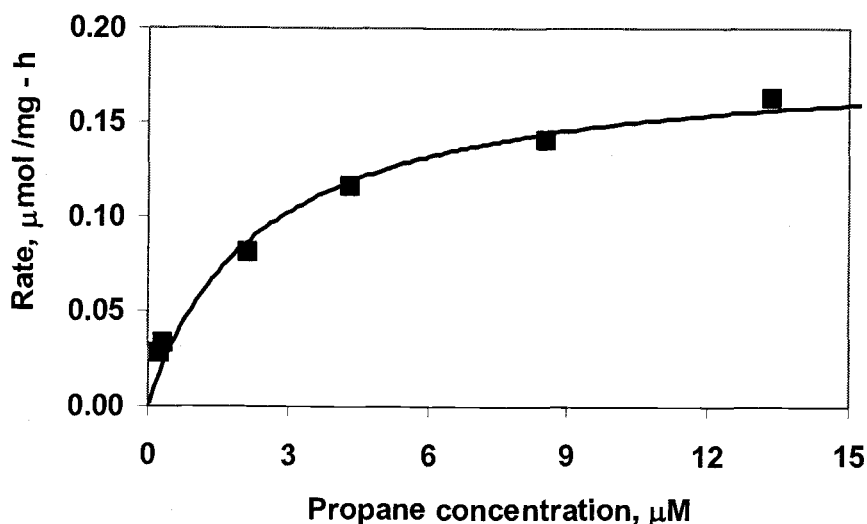


**Figure 4.5** NLSR method to determine  $k_{max}$  and  $K_s$  for propane. Initial degradation rates for various initial concentrations of Propane (■) and increasing biomass (mg dry mass). Harvested *Graphium sp.* grown on propane, as described in materials and methods, were placed in experimental sealed bottles (164 ml). Reactions were initiated by the addition of a known volume of propane. Metabolism of propane was determined by analyzing 100  $\mu\text{l}$  of headspace samples at the indicated times by gas chromatography. Solid line represents the best fit to equation 4.1 by non-linear least squares and SPLUS statistical software.



Data analysis for MTBE cometabolism are shown on Figure 4.6 to illustrate the Lineweaver-Burk plot method. The reciprocal of the initial degradation rate,  $v$ , ( $\mu\text{mol}/\text{mg dry mass}\cdot\text{h}$ ) was plotted versus the reciprocal of liquid concentration,  $S_L$ , ( $\text{mmol}/\text{L}$ ). The kinetic constants were determined from the slope and y-intercept as described by Equation 4.2.

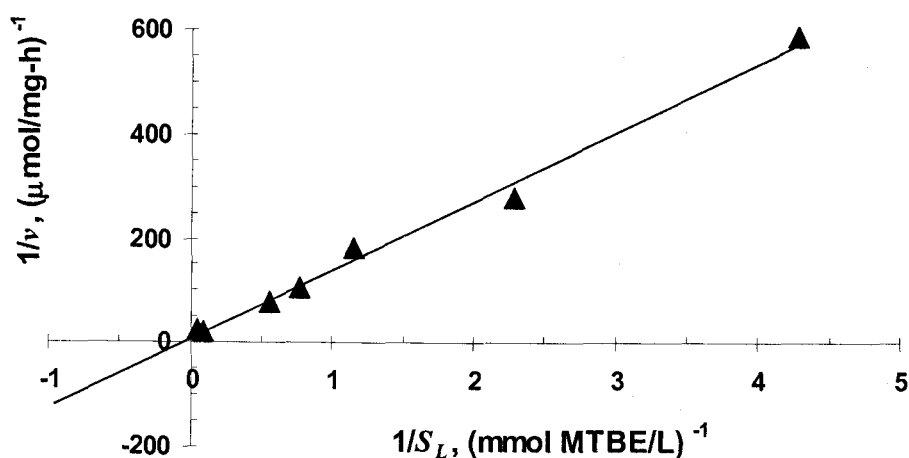


**Figure 4.6** Lineweaver-Burk plot method to determine  $k_{max}$  and  $K_s$  for MTBE. From slope =  $K_s/k_{max}$  and y-intercept =  $1/k_{max}$  as described by Equation 4.2. Initial degradation rates for various initial concentrations of MTBE ( $\blacktriangle$ ) and increasing biomass (mg dry weight).

Kinetic data for the cometabolism of TBF analyzed by the direct linear plot are shown in Figure 4.7. Experimental data pairs of aqueous concentration (x,0) and initial degradation rate (0,y) are plotted, joined with a straight line and extrapolated as previously described. Values of  $k_{max}$  and

$K_s$  were arranged in increasing order and the median of each represented the best estimates. In this case, the kinetic constants obtained for the TBF experimental data were  $0.52 \mu\text{mol/mg dry mass-h}$  for  $k_{max}$  and  $2.186 \text{ mmol/L}$  for  $K_s$ .

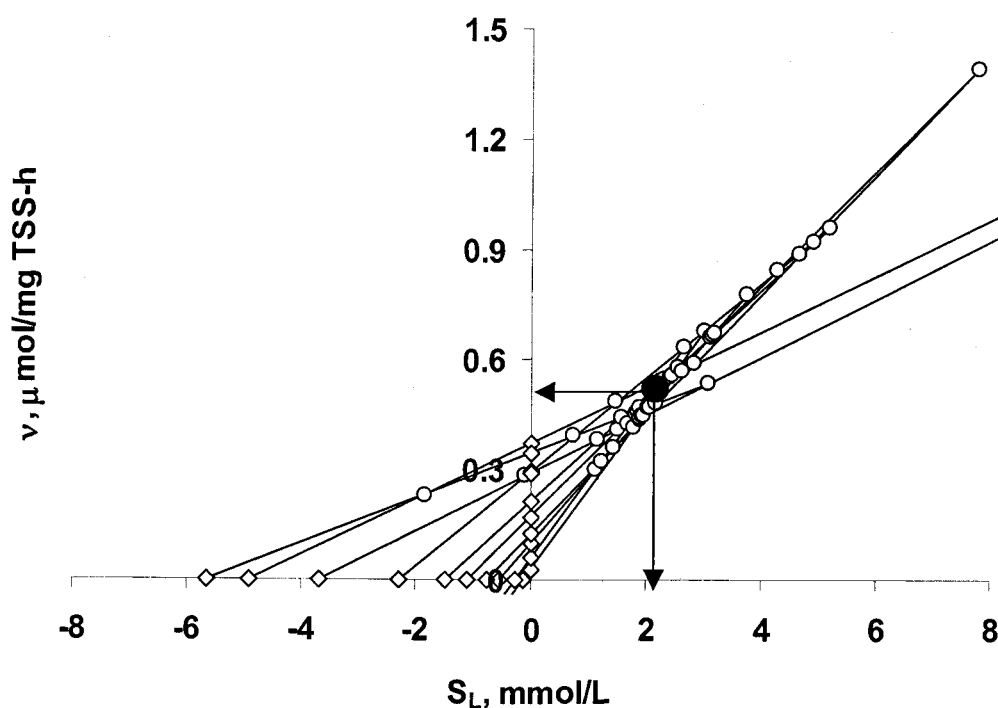


**Figure 4.7** Direct linear plot method to determine  $k_{max}$  and  $K_s$  for TBF. Experimental data is plotted by pairs ( $\diamond$ ) as described by Equation 3.3, joined and extrapolated. The small open symbols ( $\circ$ ) at the intersection of two lines represents a unique pair of  $k_{max}$  and  $K_s$  that satisfies those two sets of observations. The large solid circle ( $\bullet$ ) represents the median values as the best estimates for  $k_{max}$  and  $K_s$ .

Values of the kinetic constants, determined by the three methods, are summarized in Table 4.1. Values reported for the nonlinear least

squares method were obtained from the whole data set of individual experiments performed. For the reciprocal plot, the data were analyzed in two different ways: a) as a whole data set from individual experiments, and b) data from each individual experiment and then averaged. The standard deviation is in parenthesis. For the direct linear plot method, data of all individual experiments were analyzed as a whole set and the constants determined as the median values.

**Table 4.1** Kinetic coefficient values for filter-attached *Graphium sp.* grown on propane

	Propane		MTBE		TBF	
	$k_{max}$ $\mu\text{mol/mg-h}$	$K_s(10^{-3})$ mM	$k_{max}$ $\mu\text{mol/mg-h}$	$K_s$ mM	$k_{max}$ $\mu\text{mol/mg-h}$	$K_s$ mM
NLSR <sup>a</sup>	0.234 ( $\pm 0.029$ )	1.0 ( $\pm 0.44$ )	0.073 ( $\pm 0.007$ )	5.2 ( $\pm 1.45$ )	0.488 ( $\pm 0.034$ )	1.97 ( $\pm 0.33$ )
L-B Plot <sup>b</sup>	0.338	2.74	0.629	66	0.518	2.25
L-B Plot <sup>b1</sup>	0.241 (0.087)	1.93 (0.68)	0.10 (0.04)	11.8 (7.4)	0.518 ----	2.25 ----
D-L Plot <sup>c</sup>	0.202	1.3	0.070	4.54	0.523	2.19

<sup>a</sup> non-linear least squares. All data from individual experiments analyzed as a set ( $\pm$  shows 95% confidence interval)

<sup>b</sup> Lineweaver-Burk reciprocal plot. All data from individual experiments analyzed as a set

<sup>b1</sup> Lineweaver-Burk reciprocal plot. Average values of analyzed data from individual experiments (standard deviation).

<sup>c</sup> Direct linear plot. All data from individual experiments analyzed as a set, median value are reported.

For initial MTBE liquid concentration ranging from 20 – 200 mg/L and an average of 92 mg dry mass of *Graphium sp.* (per experimental bottle), the half-life of MTBE was estimated as 0.286 days. TBF had the highest degradation rate with an estimated half-life of 0.05 days.

The measured initial degradation rates for the metabolism of propane and the cometabolism of MTBE and TBF are shown in Figures 4.8, 4.9, and 4.10, respectively. The data were fit by non-linear least squares regression to Equation 4.1.

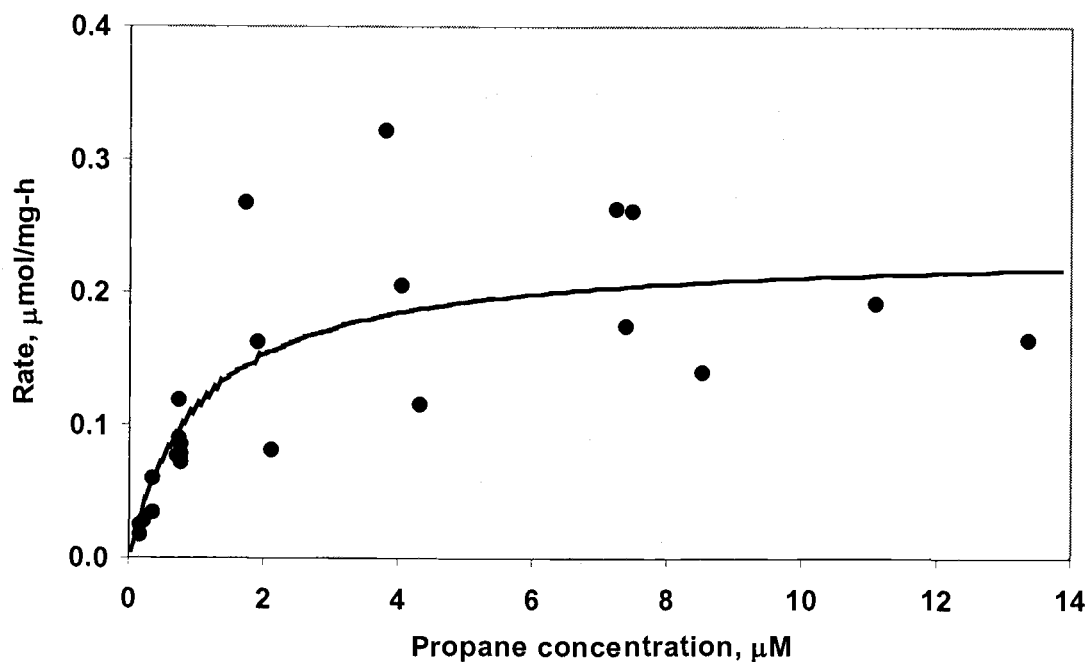


**Figure 4.8** Estimation of kinetic constants,  $k_{max}$  and  $K_s$ , for propane by NLSR. Initial degradation rate at various initial concentrations of Propane (●) and increasing biomass Solid line represents the best fit to Equation 4.1 by non-linear least squares and SPLUS statistical software.

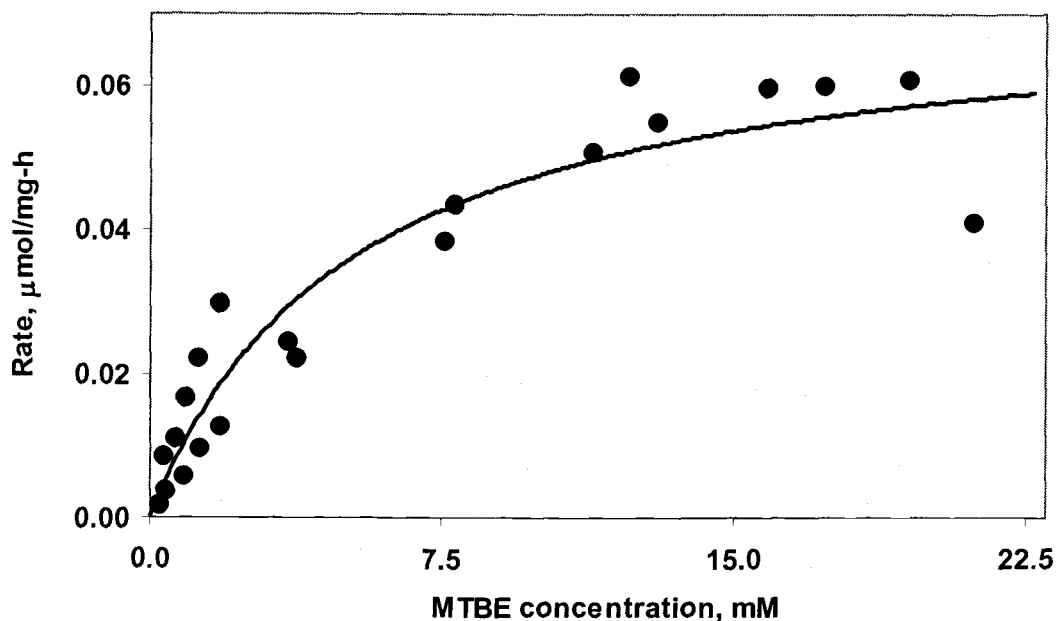


**Figure 4.9** Estimation of kinetic constants,  $k_{max}$  and  $K_s$  for MTBE by NLSR. Initial degradation rate at various initial concentrations of MTBE (●) and increasing biomass Solid line represents the best fit to Equation 4.1 by non-linear least squares and SPLUS statistical software.

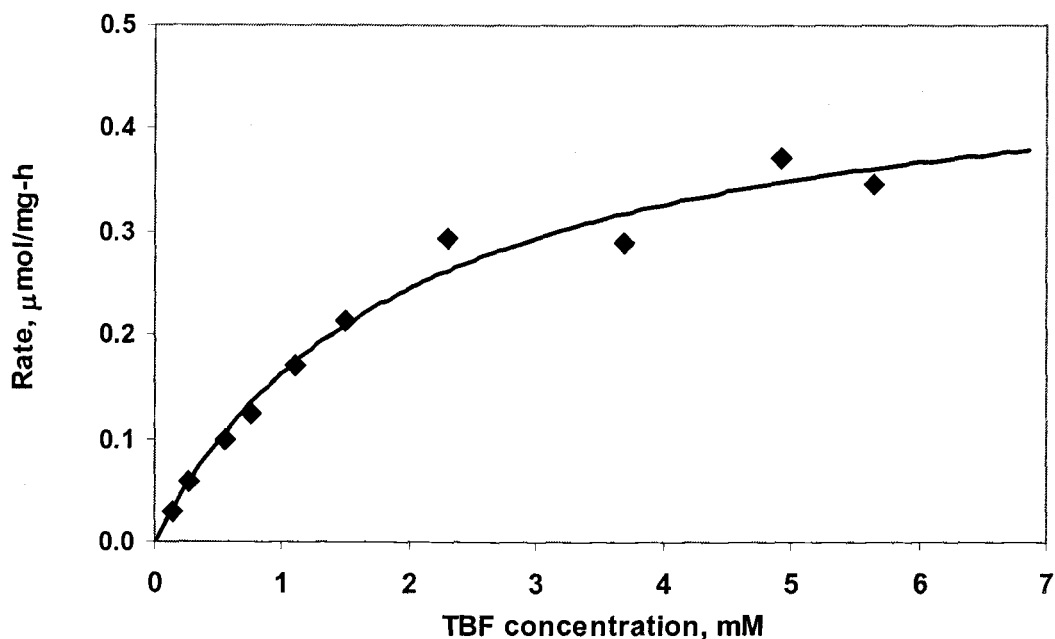


**Figure 4.10** Estimation of kinetic constants,  $k_{max}$  and  $K_s$ , for TBF by NLSR. Initial degradation rate at various initial concentrations of TBF (◆) and increasing biomass Solid line represents the best fit to Equation 4.1 by non-linear least squares and SPLUS software.

The slowest degradation rate was observed for TBA as already stated. Because of the nature of the experiment, in the filter-attached *Graphium sp.* culture, and TBA being fully miscible in water then the ability to accurately detect TBA in headspace sample was limited. Those experimental limitations prevented the determination of the kinetic constants for TBA oxidation.

Attempts to determine  $k_{max}$  and  $K_s$  by following the oxidation of TBA in the liquid phase were done, but were not successful. An experimental set-up of eight bottles was designed to follow TBA degradation in the liquid phase for a single initial concentration in all bottles. Three filters with harvested mycelia were incubated in each experimental bottle and 10  $\mu\text{l}$  of 0.116  $\mu\text{mol}/\mu\text{l}$  TBA stock solution were added to crimp-sealed bottles. The resulting initial concentration of TBA was calculated to be 25 mg/L. The bottles were equilibrated for one hour. Filters were removed from the experimental bottle and centrifuged to collect all liquid samples. Liquid samples were filtered to removed biomass present and 2  $\mu\text{l}$  were directly injected into the gas chromatogram. The bottles were sacrificed and analyzed over a period of 48 hours. No significant change in concentration was observed.

TBA oxidation rates were estimated from experiments originally designed for characterization of TBF degradation. Because of the rapid TBF degradation, large amounts of TBA accumulated and were detectable in

headspace samples. An approximate degradation rate for TBA was  $0.003 \pm 0.0005 \mu\text{mol/mg dry mass-h}$  from these TBF resting cells experiments.

## 4.5 Discussion

*Graphium sp.*, a fungal isolate, was tested for its potential to grow on *iso*-pentane with positive results as expected. However, liquid-suspension *Graphium sp.* cultures produced lower yields when grown on *iso*-pentane even at a five-fold inoculum for a period of 45 days as compared to yields obtained on propane grown liquid-culture.

*Graphium sp.* is one of the few fungal species that can grow on gaseous propane as a substrate (Zajic et al., 1969; Davies et al., 1974; Hardison et al., 1997), but cell yields (mg biomass/mg propane consumed) or degradation rates for batch tests were not found reported in the literature. Biomass yields in propane liquid-cultures as reported by Curry et. al., (1996) are comparable to our results ( 45 mg dry mass/100 ml). Hardison et. al., (1997) reported yields of *n*-butane grown liquid-culture of 0.49 mg dry mass/mg substrate ; this yield is about 13 % lower than the yield obtained in our propane-fed experiments (0.56 mg dry mass/100 ml). Yields for propane filter-attached culture used in experiments by Hardison et. al., (1997) were not reported. A yield of  $0.33 \pm 0.04 \text{ mg dry mass/mg propane}$

consumed for 5 days growth with  $2.5 \times 10^6$  initial conidia inocula was estimated from our results.

Propane-grown *Graphium sp.* cometabolically degraded MTBE to form TBF and TBA with higher degradation rates in the filter-attached cultures. MTBE, TBF, TBA alone did not support growth. Resting cell experiments (no substrate present) with propane-grown *Graphium sp.* harvested mycelia for both liquid and filter-attached cells under conditions of similar total MTBE mass added and degradation times were compared. Degradation rates for liquid culture were 4.11 versus 9.6 nmol MTBE/mg dry mass/h for the filter-attached culture. The differences are believed to be due to cell damage from culture manipulation during harvesting process.

Metabolism or cometabolism degradation rates of MTBE by a range of mixed and pure cultures have been already reported by several authors (Salanitro et al., 1994; Mo et al., 1997; Fortin et al., 1997; Fortin and Deshusses, 1999; Hardison et al., 1997; Hyman et al., 1998; Garnier et al., 1999; Deeb et al., 2000; Hanson et al., 1999; Steffan et al., 1997; Hyman and O'Reilly, 1999). In this work, the kinetic constants  $k_{max}$  and  $K_s$  for propane, MTBE and TBF were measured in systematic kinetic experiments by the filter-attached propane grown *Graphium sp.* at several (at least 10) initial concentrations and increasing mycelia biomass. The degradation rate for TBA could only be approximated because of experiment limitations.



In propane batch-kinetic tests, the biomass increase from propane degradation was less than 1% of initial biomass added and did not significantly affect the initial degradation rate. Kinetic constants were estimated from initial degradation rate at various propane concentrations as shown in Figure 4.5. The data were best fit to Equation 4.1 using NLSR. The degradation rates for MTBE and TBF were similarly obtained.

The estimated  $k_{max}$  values for MTBE and TBF, as compared to the propane maximal degradation rate, were as follows: MTBE was about three times smaller than for propane, whereas TBF was about two times greater than the value for propane. However,  $K_s$  values for MTBE and TBF were three orders of magnitude higher than the  $K_s$  for propane.  $k_{max}$  and  $K_s$  values were comparable when determined by NLSR and direct linear plots. On the other hand, the reciprocal plot method gave higher values for the kinetic constants, mainly due to sensitivity to extreme observations (outliers). Comparable values for the kinetic constants, by the reciprocal plot, was obtained when the data were analyzed for each individual experiment and then averaged (Table 4.1).

Because of the nature of the experimental set up, our estimations of liquid concentration are based on headspace injection. The presence of equilibrium conditions for MTBE, TBF, and TBA were confirmed by analyzing liquid samples at the end of the experiment.

Maximum degradation rates occurred in all the cases. Hardison et. al., (1997) reported a 10 nmol/mg-h for *Graphium sp.*, which is seven times smaller than the value obtained from our experiments (0.073  $\mu$ mol/mg-h) on propane. Our results suggested that the saturation of *Graphium sp.* for MTBE and TBF occurs at high concentrations (mM level), whereas the saturation for the growth substrate is reached at low concentrations ( $\mu$ M level). A high  $K_s$  for MTBE in mammalian microsomes was reported by (Brady et al., 1990) as 0.7 to 1.4 mM, similar to our findings.

MTBE and its breakdown products did not appear to be toxic to our culture. The addition of propane in bottles with MTBE stimulated the degradation of the remaining MTBE. These same observations were reported by Hardison et. al., (1997) for *n*-butane grown *Graphium sp.*, suggesting similarities in the enzyme system involved in the oxidation of the substrate and MTBE.

Aerobic cometabolism is a well-known process for the in-situ bioremediation of contaminated sites with chlorinated solvents (McCarty et al., 1998; Kim, 2000). Application of this concept with a filamentous fungus, *Graphium sp.*, that can utilize alkanes as a growth substrate offers an alternative for MTBE bioremediation. However, the high  $K_s$  values (e.g. low affinity) will make degradation of contaminants to low concentrations difficult. *Iso*-pentane was tested as a substrate because it is a major component of gasoline and is often present at spill-sites. However, low

yields and slow rates were observed suggesting that it may not be a practical substrate. However, more detailed studies with *Graphium* sp. in the presence of gasoline should be undertaken to determine if this culture could be applied successfully in the bioremediation of MTBE.

## 4.6 References

- Bradley, P. M., J. E. Landmeyer and F. H. Chapelle. 1999. Aerobic mineralization of MTBE and *tert*-butyl alcohol by stream-bed sediment microorganisms. *Environ. Sci. Technol.* 33: 1877 - 1879.
- Brady, J. F., F. Xiao, S. M. Hing and C. S. Yang. 1990. Metabolism of methyl *tertiary*-butyl ether by rat hepatic microsomes. *Arch. Toxicol.* 64: 197-200.
- Church, C. D., J. F. Panko and a. P. Trantnyek. 1999. Hydrolysis of *tert*-butyl formate: Kinetics, products and implications for the environmental impact of methyl *tert*-butyl ether. *Environ. Toxicol. Chem.* 18: 2789-2796.
- Cornish-Bowden, A. (1995). *Fundamentals of enzyme kinetics*. London, Portland Press. Ltd.
- Curry, S., L. Ciuffetti and M. Hyman. 1996. Inhibition of growth of a *Graphium* sp. on gaseous *n*-alkanes by gaseous *n*-alkynes and *n*-alkenes. *Appl. Environ. Microbiol.* 62: 2198-2200.
- Davies, J. S., J. E. Zajic and A. Wellman. 1974. Fungal oxidation of gaseous alkanes. *Dev. Ind. Microbiol.* 15: 256-262.
- Deeb, R. A., K. M. Scow and L. Alvarez-Cohen. 2000. Aerobic MTBE biodegradation: An examination of past studies, current challenges and future research directions. *Biodegradation* 11: 171 - 186.
- EPA, (1997). *Drinking Water Advisory: Consumer acceptability advice and health effects analysis on MTBE*.
- Finneran, K. T. and D. R. Lovley. 2001. Anaerobic degradation of methyl *tert*-butyl ether (MTBE) and *tert*-butyl alcohol (TBA). *Environ. Sci. Technol.* 35: 1785-1790.
- Fortin, N., M. Deshusses, J. Eweis, R. S. Hanson, K. Scow, D. P. Chang and E. Schroeder. (1997). Biodegradation of MTBE: Kinetics, metabolism of degradation by-products and role of oxygen release compounds. 1997 ACS Pacific Conference on Chemistry and Spectroscopy.

Fortin, N. Y. and M. A. Deshusses. 1999. Treatment of methyl *tert*-butyl ether vapors in biotrickling filters. 1: Reactor startup, steady-state performance, and culture characteristics. *Environ. Sci. Technol.* 33: 2980-2986.

Garnier, P. M., R. Auria, C. Augur and S. Revah. 1999. Cometabolic biodegradation of methyl *t*-butyl ether by *Pseudomonas aeruginosa* grown on pentane. *Appl. Microbiol. Biotechnol.* 51: 498-503.

Hanson, R. S., C. E. Ackerman and K. Scow. 1999. Biodegradation of methyl *tert*-butyl ether by a bacterial pure culture. *Appl. Environ. Microbiol.* 65: 4788 - 4792.

Hardison, L., S. Curry, L. Ciuffetti and M. Hyman. 1997. Metabolism of diethyl ether and cometabolism of methyl *tert*-butyl ether by a filamentous fungus, *Graphium sp.* *Appl. Environ. Microbiol.* 63: 3059-3067.

Hyman, M., P. Kwon, K. J. Williamson and K. O'Rilley. (1998). Cometabolism of MTBE by alkane-utilizing microorganisms. In G.B. Wickramanayake and R. Compounds. Batelle Press, Columbus, OH.

Hyman, M. and K. O'Reilly. (1999). Physiological and enzymatic features of MTBE-degrading bacteria. In situ bioremediation of petroleum hydrocarbon and other organic compounds. Batelle Press, Columbus. OH.

Jacobs, J., J. Guertin and C. Herron. (2000). MTBE: Effects on soil and groundwater resources. Lewis Publishers.

Kim, Y. 2000. Aerobic cometabolism of chlorinated aliphatic hydrocarbons by a butane-grown mixed culture: transformation abilities, kinetics and inhibition. Ph.D. Thesis. Oregon State University: Corvallis, OR.

Kim, Y., D. J. Arp and L. Semprini. 2002. A combined method for determining inhibition type, kinetic parameters, and inhibition coefficients for aerobic cometabolism of 1,1,1-Trichloroethane by a butane-grown mixed culture. *Biotechnology and Bioengineering* 77: 564-576.

Mackay, D. and W. Ying. 1981. Critical review of Henry's Law constants for chemicals of environmental interest. *J. Phys. Chem.* 10: 1175-1195.

McCarty, P., M. Goltz, G. Hopkins, M. Dolan, J. Allan, B. Kawakami and T. Carrothers. 1998. Full scale evaluation of in-situ cometabolic degradation of Trichloroethylene in groundwater through toluene injection. Environ. Sci. Technol. 32: 88-100.

Mo, K., O. Lora, A. E. Wanken and M. Javammardian. 1997. Biodegradation of methyl *t*-butyl ether by pure bacterial cultures. Appl. Microbiol. Biotechnol 47: 69-72.

Salanitro, J., C. Chou, H. Wisniewski and T. Vipond. (1998). Perspectives on MTBE degradation and the potential for in-situ aquifer bioremediation. Southern Regional Conference on the Nat. G.W. Association.

Salanitro, J., L. Diaz, M. Williams and H. Wisniewski. 1994. Isolation of a bacterial culture that degrades methyl *tert*-butyl ether. Appl. Microbiol. 60: 2593-2596.

Squillace, P. J., J. S. Zogorski, W. G. Weber and V. Price. 1996. Preliminary assessment of the occurrence and possible sources of MTBE in groundwaters in the United States, 1993 -1994. Environ. Sci. Technol. 30: 721-30.

Steffan, J., K. McClay, S. Vainberg, C. Condee and D. Zhang. 1997. Biodegradation of the gasoline oxygenates methyl *tert*-butyl ether and *tert*-amyl methyl ether by propane-oxidizing bacteria. Appl. Environ. Microbiol. 63: 4216-4222.

White, G., N. Russell and E. Tidswell. 1996. Bacterial scission of ether bonds. Microbiol. Rev. 60: 744-752.

Yeh, C. K. and J. T. Novak. 1994. Anaerobic biodegradation of gasoline oxygenates in soil. Water Environ. Res. 66: 744-752.

Zajic, J. E., B. Volesky and A. Wellman. 1969. Growth of *Graphium* sp. on natural gas. Can. J. Microbiol. 15: 1231-1236.

## Chapter 5

**“MTBE Kinetics by Alkane Grown *Mycobacterium vaccae*  
and *Graphium sp.*”**

**Adriana Martínez-Prado, Kristin Skinner, Lynda M. Ciuffetti  
and Kenneth J. Williamson**

**Submitted to**

**Battelle  
Remediation of Chlorinated and Recalcitrant Compounds  
The Third International Conference**

## 5.1 Abstract

A bacterial strain, *Mycobacterium vaccae* JOB 5, and a fungal isolate, *Graphium* sp., when cultured on either propane or *iso*-pentane, aerobically cometabolized MTBE. *Tert*-butyl formate (TBF) and *tert*-butyl alcohol (TBA) were identified as metabolites. Biokinetic coefficients ( $K_s$  and  $k_{max}$ ) were estimated and competitive inhibition was observed between the substrates, MTBE and TBA in both systems. High concentrations of TBF inhibited propane oxidation in *Graphium* sp. After TBF concentrations were reduced, propane oxidation immediately occurred. Propane, *iso*-pentane, TBA, and MTBE oxidation were inhibited by acetylene, whereas TBF was not. TBF was the only compound degraded under anoxic conditions, with both microbes, but at a slower rate than under aerobic conditions. Results suggest that at least two different enzymes are involved in this metabolic pathway. Inhibition assays showed that acetylene acts as a reversible inhibitor for both microbes. In *M. vaccae*, the trace composition of the liquid media influenced irreversibility of inhibition. Experiments are being conducted to compare the degradation of MTBE in growth-batch reactors for *iso*-pentane grown bacteria with predicted degradation rates based upon previously determined biokinetic constants. Metabolic patterns in *M. vaccae* were similar to those in *Graphium* sp.



## 5.2 Introduction

A branched-alkyl ether, methyl *tert*-butyl ether (MTBE) has been added to gasoline for over twenty years. While originally used to increase octane ratings, MTBE is now used primarily as a means to introduce oxygen into the combustion process. In localities that do not meet ambient air quality standards, The Clean Air Act of 1990 mandates the use of so-called "reformulated gasoline". Currently, oxygenates are added to the majority of US gasoline and 85% of all reformulated gasoline contains MTBE. Leaks from underground storage tanks have resulted in MTBE being the second most common groundwater pollutant in the US (Squillace et al., 1996). Because MTBE can hydrogen bond with water, it is highly soluble and acts as a non-retarded species. Although MTBE has been identified as a possible human carcinogen, concentrations of MTBE found in the environment do not pose a significant threat to public health. However, because very low concentrations of MTBE render drinking water unpalatable, MTBE contamination is an emerging environmental threat. In 1997, the US EPA issued a drinking-water advisory of 40  $\mu\text{g/L}$  for MTBE (EPA, 1997). More recently, widespread public concern about the distribution of MTBE in the environment has prompted many states to phase out the use of MTBE in reformulated gasoline.

A tertiary carbon structure and an ether linkage render MTBE resistant to natural attenuation in the environment. However, some propane-oxidizing microorganisms can cometabolically oxidize MTBE. Cometabolism is defined as the transformation of a non-growth supporting substrate in the presence of a growth-supporting substrate. Such enzymatic activity has been observed for microorganisms grown on individual aliphatic components of gasoline such as *iso*-pentane (Hyman et al., 1998; Hyman and O'Reilly, 1999). This suggests that substrates present within gasoline itself can support the growth of MTBE oxidizing organisms. MTBE breakdown products vary under either aerobic or anaerobic conditions. TBA and TBF are commonly reported as the intermediates of aerobic MTBE oxidation (Hardison et al., 1997; Garnier et al., 1999). Others have shown that carbon dioxide (CO<sub>2</sub>) is directly produced (Bradley et al., 2001). Anaerobic degradation of MTBE and TBA produces methane (CH<sub>4</sub>) and CO<sub>2</sub> (Finneran and Lovley, 2001).

*Graphium* sp., a soil-borne ascomycete has very different biological properties from those of *M. vaccae*, a gram-positive bacterium. Previous studies have shown that *M. vaccae* and *Graphium* sp. aerobically cometabolize MTBE (Hardison et al., 1997; Hyman et al., 1998; Hyman and O'Reilly, 1999) suggesting that these two microbes could compliment each other for *in situ* bioremediation applications. This study addresses the practicality of this scenario by determining the metabolic behavior of each

microbe in the presence of different metabolites generated by the MTBE oxidation pathway.

### 5.3 Materials and methods

MTBE (99.8%), propane (98%), acetylene (99.6%), *iso*-pentane (99.5%), *tert*-butyl formate (TBF) (99%), and *tert*-butyl alcohol (TBA) (99%), were obtained from Aldrich Chemical Company Co. All other chemicals were at least of reagent grade.

*Graphium sp.* (ATCC 58400) was grown under constant illumination for 6-10 days on potato dextrose agar plates at 25 °C. Conidia were harvested from the mycelial growth and quantified for inoculation. Liquid suspension cultures were grown in 700-ml glass bottles in 100-ml mineral salts medium (MSM), as previously described (Curry et al., 1996). Bottles were inoculated with  $1 \times 10^6$  conidia, and sealed. Then, one of two growth substrates, propane gas (10% v/v headspace) or *iso*-pentane (0.05% v/v headspace) was injected into the sealed bottle. Liquid suspension cultures were incubated for 7 days at  $25 \pm 0.5$  °C at 125 rpm on a rotary shaker. Pressure was equilibrated to 1 atm by adding pure oxygen to maintain aerobic conditions along the incubation period. Filter-attached cultures were

prepared as previously described (Hardison et al. 1997), but were inoculated with  $2.5 \times 10^6$  conidia. After inoculation, the filter attached cultures were placed into a tight-sealing container with two septum inserted into the lid. The 7.8-L container was closed and the edges wrapped with parafilm to prevent leaks. Propane was injected into the container at 15% (v/v). Pure oxygen was added as needed to maintain aerobic conditions. The container was incubated as described for 5 days at  $25 \pm 1$  °C.

*Mycobacterium vaccae* JOB5 (ATCC 29678) was grown in the *Xantobacter* Py2 medium (Hamamura et al., 1999) with the addition of iron (1ml/L of Fe-EDTA solution) and micronutrient solution (1ml/L). Cultures were prepared and grown under the same conditions as *Graphium* sp., except that the experimental system contained 1:1 (liquid:gas) volume ratio to which propane (60 ml) or *iso*-pentane (300  $\mu$ l) were added. Bottles were placed in a 200-rpm shaker at 30 °C. Cells were harvested at an optical density ( $OD_{600}$ ) ranging from 0.84 to 0.86.

The degradation of *n*-alkanes, MTBE, TBF, TBA, and acetylene was monitored with a gas chromatograph fitted with a flame ionization detector (GC-FID). Headspace or liquid samples were taken and analyzed directly. Appropriate external standard curves were developed for each chemical. Previously reported dimensionless Henry's Law coefficients (Mackay and Ying, 1981; Church et al., 1999; Garnier et al., 1999) were used to calculate

concentrations in the liquid phase at equilibrium. Oxygen consumption and CO<sub>2</sub> were monitored with a gas chromatograph fitted with a thermal conductivity detector (GC-TCD). Biomass production was calculated as total suspended solids (TSS) for *M. vaccae* JOB5 and as dry mass for *Graphium* sp.

Kinetic and inhibition studies under aerobic conditions were performed as follows. *M. vaccae* cultures were harvested by centrifugation (6000 x g for 15 min), washed three times with fresh Py2 medium, and concentrated. Propane, *iso*-pentane MTBE, TBF, or TBA was added as needed. All experimental bottles consisted of 5-ml liquid and 22.8-ml gas. Bottles were placed in a rotary shaker (200 rpm) at 20 °C. Liquid and headspace samples were taken and consumption of compounds was measured over time as described above. *Graphium* sp. liquid suspension cultures were harvested by gentle vacuum filtration and washed 3 times with 100-ml MSM. Mycelia were resuspended in 50-ml of fresh MSM in a sterile 700-ml bottle. Bottles were sealed with screw caps fitted with butyl rubber septa. MTBE was added to the bottles and shaken in a rotary table (125 rpm). Filter-attached cultures growing in glass petri plates were removed from the container after five days of growth. Mycelial mats growing on the glass filters were carefully transferred to 164-ml sterile serum vial bottles. Multiple filters were placed in one bottle, without overlap, to

increase fungal biomass. After the fungus was added to the bottle, the gas phase was calculated to be 157 to 163 ml and the liquid phase was between 1.3 to 6.5 ml, depending on the treatment. Serum vial bottles were sealed with a Teflon stopper and an aluminum crimp seal. Substrates were added as needed. Filter attached cultures were not shaken during the experiment.

Anaerobic conditions were created by purging bottles with nitrogen treated in a tube furnace at 600 °C for 45 minutes. Headspace samples were analyzed by GC-TCD to confirm that anaerobic conditions were established. Substrates were added to the bottles as needed. To re-establish aerobic conditions, bottles were opened and equilibrated with the ambient atmosphere under sterile conditions, recapped, and compounds of interest were readded to the bottles. The substrate(s) were reinjected and the consumption of the substrate was followed over time to quantitate the recovery of enzyme activity.

The consumption of propane, *iso*-pentane, MTBE, TBF, and TBA in the presence of acetylene was followed over time. In *M. vaccae*, concentrations of 2.2% and 4.5% (v/v) acetylene (either commercial or produced from calcium carbide) for two different media; 10 mM phosphate buffer and Py2 media were used to test the influence of acetylene on propane oxidation. In *Graphium* sp., only 0.5% commercial acetylene (v/v) was tested in MSM. Consumption of the substrate was followed for a fixed

period of time by analyzing headspace samples. Bottles were purged with  $N_2$  for 15 min to remove the acetylene. After purging, bottles were opened in a sterile environment to allow for oxygen equilibration with the atmosphere and recapped. The substrate(s) was reinjected and the consumption of the substrate was measured over time to quantitate the recovery of enzyme activity.

An abiotic control and a killed cell control were included in each experiment. The abiotic control was identical to an experimental treatment except no biomass was present. The killed cell control for *M. vaccae* consisted of cells poisoned with 10% pure  $HgCl_2$ ; filter-attached *Graphium* sp. cultures were autoclaved at 130 °C for 30 min.

## 5.4 Results

*M. vaccae* and *Graphium* sp. were tested for their potential to grow on propane and *iso*-pentane as substrates. The yields for *M. vaccae* were  $0.80 \pm 0.01$  and  $0.61 \pm 0.01$  mg TSS/mg substrate consumed for propane and *iso*-pentane, respectively. For *Graphium* sp. grown in liquid suspension, the yields were  $0.56 \pm 0.05$  (7 days growth and  $1 \times 10^6$  conidia) and 0.35 (45 days and  $5 \times 10^6$  conidia) mg dry mass/mg substrate consumed for propane and *iso*-pentane, respectively. Filter-attached

cultures grown on propane yielded  $0.33 \pm 0.04$  mg dry mass/mg propane (5 days growth and  $2.5 \times 10^6$  conidia). This approach was not studied for isopentane because of the slow growth rate and low mycelial yield, even when initial conidia concentrations were increased five-fold.

Propane grown *Graphium* sp. liquid-suspension cultures yielded low MTBE oxidation rates. The maximum initial rates for 5 and 10  $\mu$ mole addition were 1.8 and 6.7 nmole MTBE/h/mg dry mass, respectively. When *Graphium* sp. was grown in liquid suspension culture, the biomass was manipulated during harvesting (filtering, rinsing, and resuspending). It was hypothesized that the low rates could be attributed to excessive cell manipulation. To avoid excessive cell damage, the *Graphium* sp. kinetic experiments were completed with propane grown filter-attached cultures. TBF and TBA were two intermediates identified from MTBE cometabolism. TBA was further degraded to  $\text{CO}_2$ . No growth was observed when MTBE, TBF, or TBA was used as the sole source of carbon and energy for either culture.

Non-linear least squares regression (NLSR) was used to determine the kinetic parameters by fitting the initial degradation rate measured at different concentrations to the differential form of Michaelis–Menten Equation 5.1 listed below.



$$\frac{dM}{dt} = - \frac{k_{\max} \left( \frac{M}{V_L + V_G * H_{cc}} \right)}{K_s + \left( \frac{M}{V_L + V_G * H_{cc}} \right)} \quad (5.1)$$

Where  $k_{\max}$  = maximal velocity rate ( $\mu\text{mol}/\text{mg TSS-h}$ );  $K_s$  = half- saturation coefficient ( $\mu\text{M}$ ),  $M$  = total mass of compound ( $\mu\text{mol}$ );  $V_L$  = liquid volume (L),  $V_G$  = headspace volume (L),  $X$  = Biomass (mg dry mass or mg TSS/L) and  $H_{cc}$  = Henry's law constant (dimensionless).

The kinetic constants are summarized in Table 5.1 with their 95% confidence interval (C.I.). For *Graphium sp.*, an approximate degradation rate for TBA,  $0.003 \pm 0.0005 \mu\text{mol}/\text{mg dry mass-h}$ , was estimated from TBF degradation experiments.

No significant degradation of propane, MTBE, or TBA was observed in either culture under anaerobic conditions. TBF was degraded, but at a slower rate than under aerobic conditions. The degradation rate under aerobic conditions was 1.6 and 2.4 times faster for *M. vaccae* and *Graphium sp.*, respectively. When aerobic conditions were re-established, an immediate consumption of MTBE and TBA took place and the rate of TBF degradation substantially increased. As an example, the percentage of each compound consumed is summarized in Table 5.2.

**Table 5.1** Kinetic constants with their 95% C.I. by NLSR

Compound	$k_{max}$ ( $\mu\text{mol/mg} \cdot \text{h}$ )	$K_s$ ( $\text{mg/L}$ )
<i>Mycobacterium vaccae</i>		
Propane	$0.173 \pm 0.011$	$0.194 \pm 0.035$
MTBE	$0.062 \pm 0.002$	$14 \pm 2$
TBF	$0.73 \pm 0.034$	$28 \pm 4$
TBA	$0.049 \pm 0.004$	$34 \pm 10$
<i>Graphium sp.</i>		
Propane	$0.234 \pm 0.029$	$0.047 \pm 0.002$
MTBE	$0.0725 \pm 0.007$	$458 \pm 128$
TBF	$0.489 \pm 0.034$	$200 \pm 34$

**Table 5.2** Degradation (%) under anaerobic conditions with propane-grown cultures after 24 hours exposure

Compound	<i>M. vaccae</i>	<i>Graphium sp.</i>
Propane	7	4
MTBE	9	8
TBF	97	75
TBA	0*	0**
* 80 % TBA Accumulation		
** 60 % TBA Accumulation		

The influence of acetylene on the degradation of propane, MTBE, TBF, and TBA was evaluated. Propane, MTBE, and TBA degradation were totally inhibited by the presence of acetylene in both microbial systems.

This suggested that the same family of enzymes is responsible for the oxidation of all three compounds. The TBF degradation rate was not affected by the presence of acetylene in either microbe.

In *M. vaccae*, complete inhibition of propane oxidation was observed. Concentration, source of acetylene, and media composition did not influence these results. After purging acetylene from the system and readdition of the substrate, enzyme activity recovered and proceeded at a slower rate until complete consumption. In the presence of 10 mM phosphate buffer, complete inactivation was observed. When comparing substrate oxidation in the absence of acetylene the oxidation rate in the Py2 media was about 2.2 times faster when compared to that in the phosphate buffer.

An example of the results obtained from acetylene inhibition assays in filter-attached *Graphium sp.* cultures is shown in Figure 5.1. Propane oxidation did not occur in the presence of acetylene. After 100 minutes of acetylene exposure, bottles were purged and propane was readded. The cultures metabolized propane at approximately the same rate as the propane only control. Heat-killed controls did not metabolize propane, MTBE, TBA or TBF.

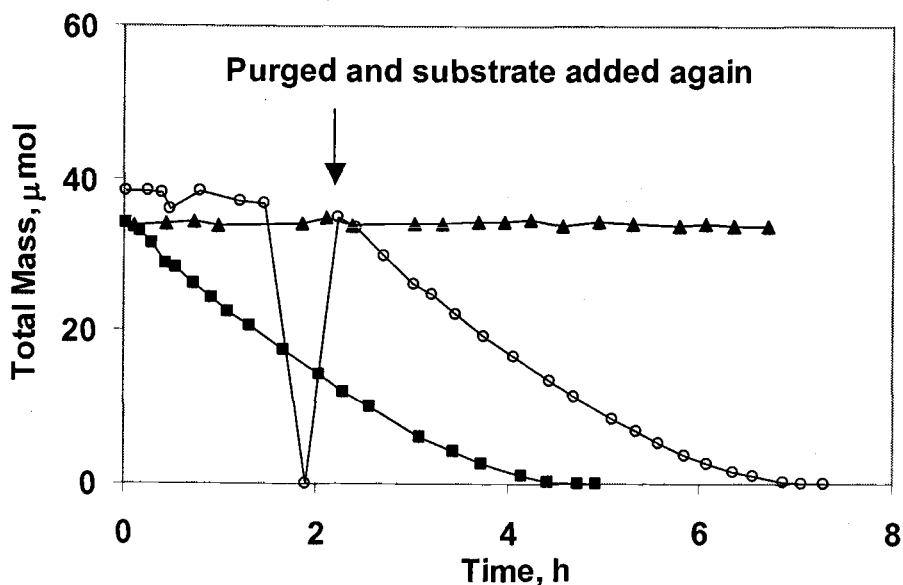


**FIGURE 5.1** Acetylene influence on propane oxidation by *Graphium* sp. Propane (◆), Propane + Acetylene (○), and Killed Control (▲)

Growth batch reactor experiments with *M. vaccae* were designed as described in materials and methods with the exception that *iso*-pentane and MTBE were added at the same time. Consumption of the substrates in triplicate bottles was followed for 100 h. Consumption of *iso*-pentane slightly slowed because of the presence of MTBE. During the first 30 h, MTBE oxidation was not significant because the presence of *iso*-pentane competitively inhibited MTBE oxidation and initial low biomass. MTBE reached its maximum oxidation rate after 50 h, and all MTBE was consumed after 56 h. TBF and TBA were detected in all samples with the

corresponding accumulation of TBA. After MTBE and TBF were consumed, TBA was completely consumed within 74 h. The consumption rate for MTBE, TBF, and TBA was faster than those observed in the kinetic experiments.

## 5.5 Discussion

Although *M. vaccae* is a prokaryote whose lifestyle, lifecycle, and growth habit are markedly different from those of a eukaryotic filamentous fungus, both microbes showed similar behavior in regard to their *n*-alkane oxidation pathways and MTBE cometabolism. Experiments further suggested that both microbes cometabolically degrade MTBE to form TBF and TBA when grown on *n*-alkanes (Hardison et al., 1997; Steffan et al., 1997) The fungal enzymes that participate in this pathway behaved similarly to those in *M. vaccae* under aerobic conditions, anaerobic conditions, and in the presence of acetylene. Both *M. vaccae* and liquid suspension *Graphium* sp. cultures produced higher yields when grown on propane as compared to yields obtained from *iso*-pentane. MTBE, TBF, and TBA did not support growth of either microbe.

The presence of propane lowered the rates of reaction for MTBE and TBA oxidation in both organisms. These experiments clearly showed that

propane competitively inhibited TBA and MTBE oxidation (data not shown). TBF degradation rates were not influenced by the presence of propane. Reaction rates were TBF > propane > MTBE > TBA in both cultures. The  $k_{max}$  for all compounds, except TBF, were higher in *Graphium sp.* The  $K_s$  was higher for propane, but not for MTBE or TBF in *M. vaccae*.

Experimental design limitations prevented the determination of biokinetic coefficients for TBA oxidation *Graphium sp.* filter-attached cultures. Attempts to determine  $K_s$  and  $k_{max}$  by following the oxidation of TBA in the liquid phase were not successful. Because TBA is totally miscible in water, the ability to accurately detect TBA in headspace samples is limited. However, estimates of TBA oxidation rates were calculated from experiments originally designed for TBF degradation. Because the TBF hydrolysis rate is very rapid and because this reaction yields TBA, large amounts of TBA accumulated resulting in detection in headspace samples. After complete consumption of TBF, the TBA concentration was measured over time to estimate TBA oxidation rates.

*M. vaccae* and *Graphium sp.* cultures showed qualitatively identical results under anaerobic conditions. No oxidation of propane, MTBE, or TBA took place, whereas TBF was consumed, but at a slower rate than in aerobic treatments. These results imply that at least two different enzymes, a monooxygenase, and a hydrolytic enzyme, are present in the degradation

pathway. Collectively, these results suggest that *M. vaccae* and *Graphium sp.* cometabolically degrade MTBE via similar metabolic pathways.

Abiotic hydrolysis of TBF occurred, but did not significantly contribute to the overall hydrolysis reaction. An abiotic hydrolysis rate constant was estimated (data not shown) over a wide concentration range at pH 7.5. Abiotic TBF hydrolysis followed first order kinetics, and the half-life ( $T_{1/2}$ ) was calculated to be  $11.43 \pm 0.80$  days. These results are comparable to previously reported values (Church et al., 1999).

Previous studies have concluded that a propane monooxygenase (PMO) is responsible for MTBE and alkane oxidation in both *Graphium sp.* and *M. vaccae*. (Hardison et al., 1997; Steffan et al., 1997). Studies have shown that acetylene inhibits *n*-alkane activity in both organisms (Curry et al., 1996; Hamamura et al., 1999), and acts as an inactivator of several monooxygenases (Hamamura et al., 1999; Prior and Dalton, 1985). Our results showed that enzymatic activity in both *M. vaccae* and *Graphium sp.* recovered after incubation with acetylene. Once acetylene was removed from the system, cells reinitiated oxidation activity, which suggests that acetylene acts as a reversible inhibitor in the presence of growth medium. On the other hand, acetylene irreversibly inactivated the PMO when Py2 medium was replaced with a phosphate buffer in *M. vaccae* experiments. No transformation of acetylene was observed. Further experiments may explain the significance of these results. One hypothesis is that the

enzymes are able to replace their heme cofactor that is covalently bound to acetylene, as  $\text{Fe}^{2+}$  is available in the Py2 media, but not in the phosphate buffer. Inactivation assays were not conducted with *Graphium sp.* filter-attached cultures because it is not practical to replace the MSM media with phosphate buffer as the liquid phase is contained within the filters that harbor the *Graphium sp.* biomass.

The kinetic coefficients determined for single compounds were used to model the growth batch reactor with a good fit for *iso*-pentane oxidation. An acceptable fit was achieved, but with a faster rate for MTBE and its breakdown products in the batch reactor. Interactions among MTBE, TBF, and TBA in a 1:1 ratio were qualitatively tested. These results showed that oxidation rates for both MTBE and TBA notably decreased when both were present. The presence of TBF further decreased MTBE and TBA oxidation rates. However, MTBE and TBA did not significantly influence TBF degradation. In these experiments, both *M. vaccae* and *Graphium sp.* were shown to degrade MTBE to environmentally significant levels via a very similar alkane oxidation pathway and showed that both microbes are efficient with respect to degradation of MTBE and its degradation products.



## **5.6 Acknowledgements**

This project was supported by a grant from the Western Region Hazardous Substance Research Center funded by the US EPA and by the Country of Mexico through Consejo Nacional de Ciencia y Tecnología (CONACyT) and Instituto Tecnológico de Durango (ITD). The authors also wish to thank Dr. Michael Hyman at North Carolina State University for helpful insight and advice.

## 5.7 References

- Bradley, P. M., J. E. Landmeyer and F. H. Chapelle. 2001. Widespread potential for microbial MTBE degradation in surface-water sediments. *Environ. Sci. Technol.* 35: 658 - 662.
- Church, C. D., P. G. Tratnyek, J. F. Pankow, J. E. Landmeyer, A. L. Baehr, M. A. Thomas and M. Schirmer. 1999. Effects of environmental conditions on MTBE degradation in model column aquifers. *Proceedings of the Technical Meeting of USGS Toxic Substances Hydrology Program*. 3: 93-101.
- Curry, S., L. Ciuffetti and M. Hyman. 1996. Inhibition of growth of a *Graphium* sp. on gaseous *n*-alkanes by gaseous *n*-alkynes and *n*-alkenes." *Appl. Env. Microbiol.* 62: 2198-2200.
- EPA, 1997. Drinking Water Advisory: Consumer acceptability advice and health effects analysis on MTBE.
- Finneran, K. T. and D. R. Lovley. 2001. Anaerobic degradation of methyl *tert*-butyl ether (MTBE) and *tert*-butyl alcohol (TBA). *Env. Sci. Technol.* 35: 1785-1790.
- Garnier, P. M., R. Auria, C. Augur and S. Revah. 1999. Cometabolic biodegradation of methyl *t*-butyl ether by *Pseudomonas aeruginosa* grown on pentane. *Appl. Microbiol. Biotechnol.* 51: 498-503.
- Hamamura, N., R. T. Storfa, L. Semprini and D. Arp. 1999. Diversity in butane monooxygenases among butane-grown bacteria. *Appl. Env. Microbiol.* 65: 4586-4593.
- Hardison, L., S. Curry, L. Ciuffetti and M. Hyman. 1997. Metabolism of diethyl ether and cometabolism of methyl *tert*-butyl ether by a filamentous fungus, *Graphium* sp. *Appl. Environ. Microbiol.* 63: 3059-3067.
- Hyman, M., P. Kwon, K. J. Williamson and K. O'Rilley. 1998. Cometabolism of MTBE by alkane-utilizing microorganisms. In G.B. Wickramanayake *Proceedings of the first Int. Conference on Remediation and Recalcitrant Compounds* 3: 321-326. Battelle Press, Columbus, OH.

Hyman, M. and K. O'Reilly. 1999. Physiological and enzymatic features of MTBE-degrading bacteria. In situ bioremediation of petroleum hydrocarbon and other organic compounds. 5: 7-12, Battelle Press, Columbus. OH.

Mackay, D. and W. Ying. 1981. Critical review of Henry's Law constants for chemicals of environmental interest. J. Phys. Chem. 10: 1175-1195.

Prior, S. D. and H. Dalton. 1985. Acetylene as a suicide substrate and active site probe for methane monooxygenase from *Methylococcus capsulatus* (Bath). FEMS Microbiol. Lett. 29: 105-109.

Squillace, P. J., J. S. Zogorski, W. G. Wilber and V. Price. 1996. Preliminary assessment of the occurrence and possible sources of MTBE in groundwaters in the United States, 1993 -1994. Environ. Sci. Technol. 30: 1721-1730.

Steffan, J., K. McClay, S. Vainberg, C. Condee and D. Zhang. 1997. Biodegradation of the gasoline oxygenates methyl *tert*-butyl ether and *tert*-amyl methyl ether by propane-oxidizing bacteria. Appl. Environ. Microbiol. 63: 4216-4222.

## Chapter 6

### Conclusions and Engineering Significance

The findings of this research, its significance, and conclusions are summarized and briefly discussed in this chapter.

#### **6.1 Degradation Kinetics of Methyl *tert*-Butyl Ether (MTBE) and its Breakdown Products by Propane and *Iso*-pentane Grown *Mycobacterium vaccae* JOB5**

**Conclusions:** Resting cell and growth batch reactor experiments demonstrated that *iso*-pentane and propane grown *Mycobacterium vaccae* JOB5 cultures were capable of degrading MTBE, TBF, and TBA via cometabolism under aerobic conditions. TBF and TBA were identified as the MTBE-oxidation metabolites in both alkane systems. MTBE, TBF, and TBA did not support growth. Degradation rates went from high to low in the following order: TBF > propane > MTBE > TBA, and TBF > *iso*-pentane > MTBE > TBA for the propane and *iso*-pentane-grown system, respectively. TBF abiotic hydrolysis rate was estimated and did not significantly affect the overall biodegradation rate. Methods used to determine the kinetic coefficients offered comparable values. Our results suggested competitive inhibition among the substrates and MTBE and TBA.

We were able to identify competitive inhibition of *iso*-pentane on MTBE degradation by performing inhibition studies at three different *iso*-pentane concentrations. Degradation rates observed in growth batch reactor were higher than the ones obtained from single compound experiments. Stella modeling predicted comparable biomass production and degradation of *iso*-pentane and MTBE, but with slower degradation for TBA. MTBE, TBF and TBA were degraded to non-detectable levels.

## **6.2 Degradation of Methyl *tert*-Butyl Ether (MTBE) and its Breakdown Products by Propane and *iso*-pentane Grown *Mycobacterium vaccae* JOB5: Cometabolism and Inhibition**

**Conclusions:** Batch experiments demonstrated that *Mycobacterium vaccae* JOB5 was not able to degrade *iso*-pentane, propane, MTBE, and TBA under anaerobic conditions. Similar experiments showed that degradation of *iso*-pentane, propane, MTBE, and TBA were inhibited by the presence of acetylene under aerobic conditions. On the other hand, TBF was degraded under anaerobic conditions, but at a slower rate than under aerobic conditions. TBF degradation was identical in the presence or absence of acetylene under aerobic conditions. Acetylene inhibition was shown to be reversible; reversibility was influenced by the trace composition of the liquid media (Py2 media versus phosphate solution). This suggested

that a nutrient or trace element in the Py2 media protects the enzyme from losing its degradation capacity. Our results supported the hypothesis that at least two different enzymes appear to be involved in the degradation process: one for the oxidation of propane, *iso*-pentane, MTBE, and TBA; and a second one responsible for the transformation of TBF, most likely a hydrolase. Similar metabolic patterns were observed in the transformation of MTBE, independently of which alkane was used as a growth substrate.

### **6.3 Kinetics of MTBE, TBF, and TBA Aerobic Cometabolism by an Alkane Grown Fungal Isolate, *Graphium sp.***

**Conclusions:** A fungal isolate, *Graphium sp.*, was found able to grow on *iso*-pentane as a growth substrate when cultured in liquid suspension, but offered low mycelial yields and slow rates. Fungal liquid suspension and filter-attached cultures grown on propane were found capable of cometabolizing MTBE under aerobic conditions with the latter offering higher degradation rates. TBF and TBA were the breakdown products of MTBE-oxidation. MTBE, TBF, and TBA were not used as a carbon and energy source. Propane-grown filter-attached culture was used to determine the kinetic coefficients for propane, MTBE, and TBF with three different methods. NLSR and direct linear plot offered comparable results. An approximate degradation rate of TBA oxidation was estimated from TBF

experiments. The maximal degradation rate observed in this system was TBF > propane > MTBE > TBA. Degradation of MTBE, TBF and TBA was possible to non-detectable levels.

#### **6.4 MTBE Kinetics by Alkane Grown *Mycobacterium vaccae* and *Graphium sp.***

**Conclusions:** Two different microbes, *Mycobacterium vaccae* and *Graphium sp.*, showed similar behavior in regard to their alkane oxidation and MTBE cometabolism. Both propane-grown microbial systems were compared. Experiments further suggested that both microbes cometabolically degraded MTBE to form TBF and TBA when grown on propane. The fungal enzymes that participate in this pathway behaved similarly to those in *M. vaccae* under aerobic conditions, anaerobic conditions, and in the presence of acetylene. *M. vaccae* and *Graphium sp.* cultures showed qualitatively identical results under anaerobic conditions. No oxidation of propane, MTBE, or TBA took place, whereas TBF was consumed, but at a slower rate than in aerobic treatments. Our results showed that enzymatic activity in both *M. vaccae* and *Graphium sp.* recovered after incubation with acetylene. Once acetylene was removed from the system, cells reinitiated oxidation activity, which suggests that

acetylene acts as a reversible inhibitor in growth media. These results imply that at least two different enzymes, a monooxygenase and a hydrolytic enzyme, are present in the degradation pathway. Collectively, these results suggest that *M. vaccae* and *Graphium* sp. cometabolically degrade MTBE via similar metabolic pathways. Reaction rates were TBF > propane > MTBE > TBA in both cultures. The  $k_{max}$  for all compounds, except TBF, were higher in *Graphium* sp. The  $K_s$  was higher for propane, but not for MTBE or TBF in *M. vaccae*.

**General Conclusions:** The presence of an alkane (propane or *iso*-pentane) monooxygenase in both microorganisms (*Mycobacterium vaccae* JOB5 and *Graphium* sp.) was indicated by the following results: 1) oxygen was required for the oxidation of propane or *iso*-pentane; and 2) propane and *iso*-pentane oxidation was inhibited by the presence of acetylene. Both cultures oxidized propane at similar rates and exhibited a strong affinity for propane (low  $K_s$  values). Both cultures were capable of cometabolizing MTBE and the same metabolites, TBF, and TBA, were identified and degraded to non-detectable levels. Based on similar experiments, our results suggested that the same alkane monooxygenase is the responsible for the cometabolism of MTBE and TBA; degradation of both required oxygen and was inhibited by acetylene. Furthermore, the presence of the



substrate decreased the degradation rate of MTBE and TBA suggesting competitive inhibition and preference for the substrate due to its high affinity.

The presence of a second enzyme, a hydrolase, in both microorganisms (*Mycobacterium vaccae* and *Graphium sp.*) was indicated by the following results: 1) TBF, a MTBE-oxidation metabolite, was degraded to TBA under either aerobic or anaerobic conditions; 2) TBF was not inhibited by the presence of acetylene; and 3) propane was a weak inhibitor in the degradation of TBF.

Acetylene was shown to act as a reversible inhibitor in both cultures when tested on growth media; oxidation activity was reinitiated once acetylene was removed. The reversibility was influenced by media composition in the bacterial system. Acetylene acted as an inactivator when tested in the presence of the phosphate solution. Our hypothesis is that a trace element, present in the growth media, may protect the enzyme from losing its oxidation activity.

Nonlinear least squares regression and direct linear plot methods were used to estimate kinetic coefficients and provided comparable results. These kinetic coefficients were used to model metabolism of *iso*-pentane, biomass production, and cometabolism of MTBE and TBA in *iso*-pentane growth batch reactors for the bacterial system; degradation rates observed were faster than the ones determined from kinetic experiments.

Experimental data were fit with STELLA; however, adjustments were required to account for reducing energy consumption. Energy generating substrates such as propane and *iso*-pentane regenerate reductant such as NAD(P)H, whereas cometabolic substrates such as MTBE do not (Dalton and Stirling, 1982). Cometabolic rates occurring in the absence of a growth supporting substrate can be reduced or stopped because of that reductant limitation. Competitive inhibition among substrates and co-substrates becomes an issue because cometabolic rates can also be reduced due to the presence of the primary substrate (Alvarez & Speitel, 2001). To avoid competitive inhibition, the use of alternate energy substrates such as propanol for propane oxidizers has been suggested because they are not oxidized by oxygenases (Stirling and Dalton, 1989).

## 6.5 Engineering significance

MTBE is an important research topic as methods are being sought to remove it from the environment. Some states, such as California, and the federal government have decided to phase out MTBE. In the meantime, the cleanup cost associated with MTBE contamination will increase. Millions of dollars will be spent in cleanup and water treatment if MTBE remains as a fuel additive (Wilson et al., 2001).

Detailed study of microorganisms capable of degrading contaminants of environmental interest, as well as their intermediates, is needed for the further development of bioremediation applications. Cometabolism has been successfully applied in the remediation of several compounds. The production of oxygenases by alkane oxidizers suggests that cometabolism offers a biological strategy for MTBE bioremediation.

An *iso*-pentane and propane-grown bacterial system and a propane-grown fungal system evaluated in this study were found suitable of degrading MTBE and its breakdown products to non-detectable levels. Maximum degradation rate for both propane-grown systems were comparable, whereas the *iso*-pentane grown bacterial system was about 3 times higher than those. Our results are comparable or higher than those observed by Fortin et al., (1999); Hardison et al., (1997); Garnier et al., (1999); and Koenigsberg et al., (1999); but lower than Salanitro et al., (1994); Deeb et al., (2000); Hyman et al., (1998); and Steffan et al., (1997).

Propane and *iso*-pentane as a growth substrate are advantageous in in-situ bioremediation. The former has been used successfully in the bioremediation of chlorinated aliphatic hydrocarbons (Tovanabootr, 1997) and is not a regulated chemical. *iso*-pentane itself is a major component of gasoline, thus no addition is required. Our results suggest that similar approach can be applied to the bioremediation of MTBE from gasoline-spills contamination.

However, more detailed kinetic studies are suggested to evaluate the interaction of substrates, MTBE, TBF, and TBA in the presence of gasoline during the cometabolism process and to clearly identify inhibition relationships. Such information may lead to a better understanding of this complex system and to better model in-situ conditions. Development of models are needed particularly to convince public, site owners, and regulators that implementation of aerobic cometabolism is an effective bioremediation strategy.

## Bibliography

Alvarez-Cohen, L. and G. E. S. Jr. 2001. Kinetics of aerobic cometabolism of chlorinated solvents. *Biodegradation* 12: 105-126.

Bradley, P. M., F. H. Chapelle and J. E. Landmeyer. 2001. Methyl *tert*-butyl ether mineralization in surface-water sediment microcosms under denitrifying conditions. *Appl. Environ. Microbiol.* 67: 1975-1978.

Bradley, P. M., J. E. Landmeyer and F. H. Chapelle. 1999. Aerobic mineralization of MTBE and *tert*-butyl alcohol by stream-bed sediment microorganisms. *Environ. Sci. Technol.* 33: 1877 - 1879.

Bradley, P. M., J. E. Landmeyer and F. H. Chapelle. 2001. Widespread potential for microbial MTBE degradation in surface-water sediments. *Environ. Sci. Technol.* 35: 658 - 662.

Brady, J. F., F. Xiao, S. M. Hing and C. S. Yang. 1990. Metabolism of methyl *tertiary*-butyl ether by rat hepatic microsomes. *Arch. Toxicol.* 64: 197-200.

Burleigh-Flayer, H. D., J. S. Chun and W. J. Kintigh. (1992). Methyl *tertiary*-butyl ether vapor inhalation oncogenicity study in CD1 mice. Export, PA, Bushy Run Research Center.

Chang, H. L. and L. Alvarez-Cohen. 1996. Biodegradation of individual and multiple chlorinated aliphatic hydrocarbons by methane-oxidizing cultures. *Appl. Environ. Microbiol.* 62: 3371-3377.

Chun, J. S., H. D. Burleigh-Flayer and W. J. Kintigh. (1992). Methyl *tertiary*-butyl ether: vapor inhalation oncogenicity study in Fischer 344 rats. Export, PA, Bushy Run Research Center.

Church, C. D., J. F. Panko and a. P. Trantnyek. 1999. Hydrolysis of *tert*-butyl formate: Kinetics, products and implications for the environmental impact of methyl *tert*-butyl ether. *Environ. Toxicol. Chem.* 18: 2789-2796.

Church, C. D., P. G. Tratnyek, J. F. Pankow, J. E. Landmeyer, A. L. Baehr, M. A. Thomas and M. Schirmer. (1999). Effects of environmental conditions on MTBE degradation in model column aquifers. U. S. Geological Survey : 93 - 101.

Cornish-Bowden, A. (1995). Fundamentals of enzyme kinetics. London, Portland Press. Ltd.

Curry, S., L. Ciuffetti and M. Hyman. 1996. Inhibition of growth of a *Graphium* sp. on gaseous *n*-alkanes by gaseous *n*-alkynes and *n*-alkenes. Appl. Environ. Microbiol. 62: 2198-2200.

Dalton, H. and D. I. Stirling. 1982. Co-Metabolism. Phil. Trans. Roy. Soc. Lond. B. 297: 481-496.

Davies, J. S., J. E. Zajic and A. Wellman. 1974. Fungal oxidation of gaseous alkanes." Dev. Ind. Microbiol. 15: 256-262.

Deeb, R. A., H.-Y. Hu, J. R. Hanson, K. M. Scow and L. Alvarez-Cohen. 2001. Substrate interactions in BTEX and MTBE mixtures by an MTBE-degrading isolate." Environ Sci. Technol. 35: 312-317.

Deeb, R. A., K. M. Scow and L. Alvarez-Cohen. 2000. Aerobic MTBE biodegradation: An examination of past studies, current challenges and future research directions." Biodegradation 11: 171 - 186.

Dupasquier, D., S. Revha and R. Auria. 2002. Biofiltration of methyl *tert*-butyl ether vapors by cometabolism with pentane: Modeling and experimental approach. Environ. Sci. Technol. 36: 247-253.

EPA, (1997). Drinking Water Advisory: Consumer acceptability advice and health effects analysis on MTBE.

Eweis, J., D. P. Chang, E. Schroeder, K. Scow, R. Morton and R. Caballero. (1997). Meeting the challenge of of MTBE biodegradation. 90th Annual Meeting and Exhibition of the Air and Waste Management Association, Toronto, Canada.

Finneran, K. T. and D. R. Lovley. 2001. "Anaerobic degradation of methyl *tert*-butyl ether (MTBE) and *tert*-butyl alcohol (TBA)." Environ. Sci. Technol. 35: 1785-1790.

Fortin, N., M. Deshusses, J. Eweis, R. S. Hanson, K. Scow, D. P. Chang and E. Schroeder. (1997). Biodegradation of MTBE: Kinetics, metabolism of degradation by-products and role of oxygen release compounds. 1997 ACS Pacific Pacific Conference on Chemistry and Spectroscopy.

Fortin, N. Y. and M. A. Deshusses. 1999. Treatment of methyl *tert*-butyl ether vapors in biotrickling filters. 1: Reactor startup, steady-state performance, and culture characteristics." Environ. Sci. Technol. 33: 2980-2986.

Fortin, N. Y. and M. A. Deshusses. 1999. Treatment of methyl *tert*-butyl ether vapors in biotrickling filters. 2: Analysis of the rate limiting step and behavior under transient conditions. Environ. Sci. Technol. 33: 2987-2991.

Garnier, P. M., R. Auria, C. Augur and S. Revah. 1999. Cometabolic biodegradation of methyl *t*-butyl ether by *Pseudomonas aeruginosa* grown on pentane. Appl. Microbiol. Biotechnol. 51: 498-503.

Gornall, G., C. J. Bardawill and M. David. 1949. Determination of serum proteins by means of the biuret reaction. J. Biol. Chem. 177: 751-766.

Grosjean, E., D. Grosjean, R. Guanawardena and R. Rasmussen. 1998. Ambient concentrations of ethanol and methyl *tert*-butyl ether in Porto Allegre, Brazil, March 1996 to April 1997. Environ. Sci. Technol. 32: 736 - 742.

Hamamura, N., C. Page, T. Long, L. Semprini and D. Arp. 1997. Chloroform cometabolism by butane-grown CF8, *Pseudomonas butanorova* and *Mycobacterium vaccae* JOB5 and methane-grown *Methylosinus trichosporium* OB3b. Appl. Environ. Microb. 63: 3607-3613.

Hamamura, N., R. T. Storfa, L. Semprini and D. Arp. 1999. Diversity in butane monooxygenases among butane-grown bacteria. Appl. Environ. Microbiol. 65: 4586-4593.

Hanson, J., K. M. Scow, M. Bruns and T. Brethour (1996). Characterization of MTBE-degrading bacterial isolates and associated consortia. MTBE Workshop, Univ. Calif., Davis.

Hanson, R. S., C. E. Ackerman and K. Scow. 1999. Biodegradation of methyl *tert*-butyl ether by a bacterial pure culture. Appl. Environ. Microbiol. 65: 4788 - 4792.

Hardison, L., S. Curry, L. Ciuffetti and M. Hyman. 1997. Metabolism of diethyl ether and cometabolism of methyl *tert*-butyl ether by a filamentous fungus, *Graphium* sp. Appl. Environ. Microbiol. 63: 3059-3067.

Haston, Z. C. and P. L. McCarty. 1999. Chlorinated ethene half-velocity coefficients ( $K_s$ ) for reductive dehalogenation. Environ. Sci. Technol. 33: 223-226.

Henry, S. M. and Grbic-Galic. 1991. Influence of endogenous and exogenous electron donors and trichloroethylene oxidation toxicity on trichloroethylene oxidation by methanotrophic cultures from a groundwater aquifer. Appl. Environ. Microbiol. 57: 236-244.

Hill, T. 1982. Hydrolysis and oxidation processes in the environment. Environ. Toxicol. Chem. 1: 135 - 141.

Hunkeler, D., B. J. Bulter, R. Aravena and F. Barker. 2001. Monitoring biodegradation of methyl *tert*-butyl ether (MTBE) using compound-specific carbon isotope analysis. Environ. Sci. Technol. 35: 676 - 681.

Hurt, K. L., J. T. Wilson, F. P. Beck and J. S. Cho. (1999). Anaerobic biodegradation of MTBE in a contaminated aquifer. Fifth International in situ and on-site bioremediation symposium, Monterrey, Ca., Battelle.

Hyman, M., P. Kwon, K. J. Williamson and K. O'Riley. (1998). Cometabolism of MTBE by alkane-utilizing microorganisms. In G.B. Wickramanayake and R. Compounds, Batelle Press, Columbus, OH.

Hyman, M. and K. O'Reilly. (1999). Physiological and enzymatic features of MTBE-degrading bacteria. In situ bioremediation of petroleum hydrocarbon and other organic compounds. Batelle Press, Columbus. OH.

Hyman, M. R. and D. J. Arp. 1987. Quantification and removal of some contaminating gases from acetylene to study gas-utilizing enzymes and microorganisms. Appl. Environ. Microbiol. 53: 298-303.

Jacobs, J., J. Guertin and C. Herron. (2000). MTBE: Effects on soil and groundwater resources. Lewis Publishers.

Jensen, J. M. and E. Arvin. (1990). Solubility and degradability of the gasoline additive MTBE. Methyl *tert*-butyl ether, and gasoline compounds in water. Dordrecht, Netherlands, Kluwer Academic Publisher.



Kenner, W. K. and D. J. Arp. 1993. Kinetic studies of ammonia monooxygenase inhibition in *Nitrosomonas europaea* by hydrocarbons and halogenated hydrocarbons in an optimized whole-cell assay. *Appl. Environ. Microbiol.* 59: 2501-2510.

Kim, Y. 2000. Aerobic cometabolism of chlorinated aliphatic hydrocarbons by a butane-grown mixed culture: transformation abilities, kinetics and inhibition. Ph.D. Thesis. Oregon State University: Corvallis, OR.

Kim, Y., D. J. Arp and L. Semprini. 2002. A combined method for determining inhibition type, kinetic parameters, and inhibition coefficients for aerobic cometabolism of 1,1,1-Trichloroethane by a butane-grown mixed culture. *Biotechnology and Bioengineering* 77: 564-576.

Koenigsberg, S., C. Sandefur, W. Mahaffey, M. Deshusses and N. Fortin. (1999). Peroxygen mediated bioremediation of MTBE. Fifth International In Situ and On-Site Bioremediation Symposium. Monterrey, Ca., Battelle.

Kwon, P. O. 1998. A study of in-situ bioremediation of methyl *tert*-butyl ether (MTBE) through cometabolic processes by alkane-utilizing microorganisms Project report. Oregon State University: Corvallis, OR.

Landmeyer, J. E., F. H. Chapelle, H. H. Herlong and P. M. Bradley. 2001. Methyl *tert*-butyl ether biodegradation by indigenous aquifer microorganisms under natural and artificial oxic conditions. *Environ. Sci. Technol.* 35: 1118 - 1126.

Leethem, J. T. 2001. In situ chemical oxidation of MTBE and BTEX in soil and groundwater: A case study. *AEHS, Contaminated Soil, Sediment and Groundwater. The magazine of Environmental Assessment & Remediation*: 54-58.

Mackay, D. and W. Ying. 1981. Critical review of Henry's Law constants for chemicals of environmental interest. *J. Phys. Chem.* 10: 1175-1195.

McCarty, P., M. Goltz, G. Hopkins, M. Dolan, J. Allan, B. Kawakami and T. Carrothers. 1998. Full scale evaluation of in-situ cometabolic degradation of Trichloroethylene in groundwater through toluene injection. *Environ. Sci. Technol.* 32: 88-100.

Mill, T. 1982. Hydrolysis and oxidation processes in the environment. *Environ. Toxicol. Chem.* 1: 135-141.

- Missen, R. W., C. A. Mims and B. A. Saville. (1999). Chemical reaction engineering and kinetics. John Wiley & Sons, Inc.
- Mo, K., O. Lora, A. E. Wanken and M. Javammardian. 1997. Biodegradation of methyl *t*-butyl ether by pure bacterial cultures. Appl. Microbiol. Biotechnol 47: 69-72.
- Nichols, E. M., M. D. Einarson and S. C. Beadle. 2000. Strategies for characterizing subsurface releases of gasoline containing MTBE. American Petroleum Institute: 1 - 8.
- Oyama, J. and J. Foster. 1965. Bacterial oxidation of cycloparaffinic hydrocarbons. Antonie van Leeuwenhoek 31: 45-65.
- Park, K. and R. Cowan. (1997). Biodegradation of gasoline oxygenates. Fourth International In Situ and On-Site Bioremediation Symposium.
- Perry, J. J. 1980. Propane utilization by microorganisms. J. of Bacteriology. 26: 89 - 115.
- Philips, W. E. and J. J. Perry. 1974. Metabolism of *n*-butane and 2-butanol by *Mycobacterium vaccae*. J. of Bacteriology 120: 987 - 989.
- Prior, S. D. and H. Dalton. 1985. Acetylene as a suicide substrate and active site probe for methane monooxygenase from *Methylococcus capsulatus* (Bath). FEMS Microbiol Lett. 29: 105-109.
- Pruden, A., M. T. Suidan, A. D. Venosa and G. J. Wilson. 2001. Biodegradation of methyl *tert*-butyl ether under various substrate conditions. Environ. Sci. Technol. 35: 4235 - 4241.
- Reuter, J. E., B. C. Allen, R. C. Richards, J. F. Pankow, C. L. Goldman, R. L. Scholl and J. S. Seyfried. 1998. Concentrations, sources and fate of the gasoline oxygenate methyl *tert*-butyl ether (MTBE) in a multiple use lake. Environ. Sci. Technol. 32: 3666 - 3672.
- Rungkamol, D. 2001. Aerobic cometabolism of 1,1,1-Trichloroethane and other chlorinated aliphatic hydrocarbons by indigenous and bioaugmented butane-utilizers in Moffett field microcosms. M.S. Thesis. Oregon State University: Corvallis, OR.

Salanitro, J., C. Chou, H. Wisniewski and T. Vipond. (1998). Perspectives on MTBE degradation and the potential for in-situ aquifer bioremediation. Southern Regional Conference on the Nat. G.W. Association.

Salanitro, J., L. Diaz, M. Williams and H. Wisniewski. 1994. Isolation of a bacterial culture that degrades methyl *tert*-butyl ether. Appl. Microbiol. 60: 2593-2596.

Salanitro, J., G. Spinnler, P. Maner, H. Wisniewski and P. Johnson. (1999). Potential for MTBE bioremediation-in situ inoculation of specialized cultures. Conference on petroleum hydrocarbons and organic chemicals in ground water: prevention, detection and remediation, Houston, TX.

Salanitro, J. and H. Wisniewski. (1996). Observations on the biodegradation and bioremediation potential of methyl *tert*-butyl ether. 17th Annual Meeting of the Society of Environmental Toxicology and Chemistry.

Salanitro, J. P., P. C. Johnson, G. E. Spinnler, P. M. Maner, H. L. Wisniewski and C. Bruce. 2000. Field-scale demonstration of enhanced MTBE bioremediation through Aquifer Bioaugmentation and Oxygenation. Environ. Sci. Technol. 34: 4152 - 4162.

Salanitro, J. P., G. E. Spinnler, P. M. Maner and K. A. Lyons. 2001. Enhanced bioremediation of MTBE (Bioremedy) at retail gas stations. AEHS, Contaminated Soil, Sediment and Groundwater. The magazine of Environmental Assessment & Remediation: 47-49.

Semprini, L., R. L. Ely and M. M. Lang. 1998. Modeling of cometabolism for the in-situ biodegradation of Trichloroethylene and other chlorinated aliphatic hydrocarbons. Bioremediation 1: 89-134.

Soo, C. J. and J. T. Wilson. (1999). Hydrocarbon and MTBE removal rates during natural attenuation application. Battelle Conference, In situ and On site Bioremediation.

Squillace, P., J. F. Pankow and J. Zogorski. (1998). Environmental behavior and fate of methyl *tert*-butyl ether (MTBE). The Southwest Focused Groundwater Conference, Anaheim, California, National Ground Water Association.

Squillace, P. J., J. S. Zogorski, W. G. Weber and V. Price. 1996. Preliminary assessment of the occurrence and possible sources of MTBE in groundwaters in the United States, 1993 -1994. *Environ. Sci. Technol.* 30: 721-30.

Steffan, J., K. McClay, S.Vainberg, C. Condee and D. Zhang. 1997. Biodegradation of the gasoline oxygenates methyl *tert*-butyl ether and *tert*-amyl methyl ether by propane-oxidizing bacteria. *Appl. Environ. Microbiol.* 63: 4216-4222.

Stephens, G. M. and H. Dalton. 1986. The role of terminal and subterminal oxidation pathways in propane metabolism by bacteria. *J. of Gen. Microbiol.* 132: 2453 - 2462.

Stirling, D. I. and H. Dalton. 1979. The fortuitous oxidation and cometabolism of various carbon compounds by whole-cell suspensions of *Mehylococcus capsulatus* (Bath). *FEMS Microbiol Lett.* 5: 315-318.

Stocking, A. J., R. A. Deeb, A. E. Flores, W. Stringfellow, J. Talley, R. Brownell and M. C. Kavanaugh. 2000. Bioremediation of MTBE: A review from a practical perspective. *Biodegradation* 11: 187-201.

Sulita, J. M. and M. R. Mormille. 1993. Anaerobic biodegradation of known and potential gasoline oxygenates in the terrestrial sub-surface. *Environ. Sci. Technol.* 27: 976-978.

Tovanabootr, A. 1997. Aerobic cometabolism of chlorinated aliphatic hydrocarbons by subsurface microbes grown on methane, propane, and butane from McClellan Air Force Base. M.S. Thesis. Oregon State University: Corvallis, OR.

Wackett, L. P., G. A. Brusseau, S. R. Householder and R. S. Hanson. 1989. Survey of microbial oxygenase: Trichloroethylene degradation by propane oxidizing bacteria. *Appl. Environ. Microbiol.* 55: 2960 - 2964.

White, G., N. Russell and E. Tidswell. 1996. Bacterial scission of ether bonds. *Microbiol. Rev.* 60: 744-752.

Wilson, B. H., H. Shen, D. Pope and S. Schmelling. (2001). Cost of MTBE remediation. The Sixth International In Situ and On-Site Bioremediation Symposium, San Diego, California, Battelle Press.

Yeh, C. K. and J. T. Novak. 1994. Anaerobic biodegradation of gasoline oxygenates in soil. *Water Environ. Res.* 66: 744-752.

Yeh, C. K. and J. T. Novak. 1995. The effect of hydrogen peroxide on the degradation of methyl and ethyl *tert*-butyl ether in soils. *Water Environ. Res.* 67: 828 - 834.

Zajic, J. E., B. Volesky and A. Wellman. 1969. Growth of *Graphium sp.* on natural gas. *Can. J. Microbiol.* 15: 1231-1236.

Zhang, Q., L. C. Davis and L. E. Erickson. 2001. Transport of methyl *tert*-butyl ether through alfalfa plants. *Environ. Sci. Technol.* 35: 725 - 731.

Zogorski, J., A. Morduchowist, A. Baehr, B. Bauman, D. Conrad, R. Drew, N. Korte, W. Lapham, J. Pankow and E. Washington. 1996. Fuel Oxygenates and Water Quality: Current Understanding of Sources, Occurrence in Natural Waters, Environmental Behavior, Fate, and Significance. Washington, D.C., Interagency oxygenated fuel assessment, office of science and technology policy, executive office of the President.

Zogorski, J., A. Morduchowist, A. Baehr, B. Bauman, D. Conrad, R. Drew, N. Korte, W. Lapham, J. Pankow and E. Washington. 1997. Fuel Oxygenates and Water Quality. Washington, D.C., Interagency oxygenated fuel assessment, office of science and technology policy, executive office of the President.

## **APPENDICES**

## Appendix A

### Gas chromatography analysis

#### A.1 Propane and *iso*-pentane

The degradation of both *n*-alkanes, propane and *iso*-pentane, was monitored by injecting a 100  $\mu$ l headspace sample into a Hewlett Packard gas chromatograph (Model HP6890) fitted with a flame ionization detector (GC-FID). A 30 m x 0.45 mm I.D., 2.55  $\mu$ m DB-MTBE column was used (Agilent Technology, Willmington, DE) at an oven temperature of 65 °C, gas flowrates for helium, hydrogen and air were 15, 35, and 250 ml/min, respectively. A chemstation was connected to the GC providing the corresponding a report of the peak areas for the gaseous analysis by comparison with a standard curve, through a chromatogram. Standard curves were prepared with external standards for each compound.

### **A.1.1 Propane**

Standard curve preparation: A 310-ml serum bottle was crimped with aluminum seal fitted with butyl stoppers. A volume of 75 ml headspace was withdrawn from the sealed bottle and replaced with 98% propane; bottle was incubated at the desired experimental temperature. Headspace samples of 20, 40, 60, 80 and 100  $\mu$ l were taken with a 100- $\mu$ l gas-tight syringe (Hamilton 81000, with cemented needle) and injected into the GC-FID. The standard curve was generated by plotting the peak area versus mass injected.

### **A.1.2 iso-pentane**

Standard curve preparation: A 160-ml serum bottle was crimped with aluminum seal fitted with butyl stoppers. A volume of 30  $\mu$ l of 99.5% *iso*-pentane, trapped between 2 volumes of 10- $\mu$ l of water, was added to the sealed bottle with a 50- $\mu$ l sample-lock syringe (Hamilton 80956), bottle was incubated at the desired experimental temperature. Headspace samples of 20, 40, 60, 80 and 100  $\mu$ l were taken with a 100- $\mu$ l gas-tight syringe



(Hamilton 81000, with cemented needle) and injected into the GC-FID. The standard curve was generated by plotting the peak area versus mass injected.

## **A.2 MTBE, TBF, and TBA**

MTBE, TBF and TBA were monitored by liquid or headspace sample injection, using two different gas chromatographs.

### **A.2.1 Liquid injection samples**

MTBE, TBF and TBA were monitored by injecting 2  $\mu$ l into a Hewlett Packard gas chromatograph (Model HP5890A) fitted with a flame ionization detector (GC-FID). A 3' x 1/8" stainless steel column packed with Porapak Q (80/100 mesh) (Alltech Associates, Inc., Deerfield, IL) was used at an oven temperature of 135 °C, and a detector temperature of 220 °C. Helium was used as the carrier gas with a 40 ml/min flow rate. A Hewlett Packard integrator (HP 3390A) was connected to the GC providing a report with the integrated peak area for the liquid injection analysis. Corresponding concentration of any sample was estimated by comparing with a standard curve prepared with external standards for each of the three compounds.

Standard curve preparation: Different volumes of autoclaved Py2 media were added to sterile 27.8-ml glass vials (Supelco, Bellefonte, PA) and were crimped with aluminum seals fitted with butyl stoppers. A given amount of either stock or aqueous saturated solution (depending on the concentration range) of MTBE, TBF or TBA was added. The final volume in all bottles was 5 ml. The bottle was shaken for at least 30 min to allow equilibration at 200 rpm in a 20 or 25 °C room.

Liquid samples of 2  $\mu$ l were taken, from all prepared bottles, with a 10- $\mu$ l liquid tight syringe (Hamilton 80030) and injected into the gas chromatograph. Plotting the peak area for each compound versus the corresponding liquid concentration generated the standard curves

### **A.2.2 Headspace injection samples**

MTBE, TBF and TBA were also monitored by using the same method and GC-FID as for propane and *iso*-pentane analysis described at the beginning of this section.

Standard curves preparation: Three 164-ml serum bottles, one for each compound, were crimped with aluminum seal fitted with butyl stoppers. Volumes of 5- $\mu$ l of 99.8% MTBE, 6.5- $\mu$ l of 99% TBF, and 10 - $\mu$ l of 99% TBA

were added to its corresponding bottle. Bottles were incubated at the desired experimental temperature. Headspace samples of 20, 40, 60, 80 and 100  $\mu\text{l}$  were taken with a 100- $\mu\text{l}$  gas-tight syringe (Hamilton 81000, with cemented needle) and injected into the GC-FID. The standard curves were generated by plotting the peak area versus mass injected.

Compounds were detected at different retention times in both GC. Table A.1 summarizes the retention times for all five compounds.

**Table A.1** Retention time (min) of compounds analyzed by gas chromatography

Compound name	Headspace injection	Liquid injection
Propane	0.88	1.4
<i>I</i> so-pentane	1.20	1.9
MTBE	1.65	2.9
TBF	2.10	4.7
TBA	1.32	7.8

## Appendix B

### Culturing *Graphium sp.*

#### B.1 Stock cultures

Long-term stocks are maintained on PDA (Potato Dextrose Agar) slants. Seal test tubes well with parafilm and store in a container at 4 °C. New slants need to be prepared every 8 months, using the most recent slants as inoculums. To prepare *working stocks*, inoculate a PDA plate using a long-term slant as the inoculum. Streak the plate with a sterile wooden applicator and incubate at 25 °C under constant illumination for 5 to 7 days. Using a sterile scalpel, cut a small (~ 2 mm<sup>2</sup>) square out of the mycelia-covered agar, and place it fungus-side down in the center of a new PDA plate. The mycelia will grow outwards in a circle, with the newest growth always at the outer edge. Once the fungus has grown to about 5 cm diameter, wrap the plate with parafilm and store at 4 °C. To routinely inoculate plates for harvesting conidia, use a sterile wooden applicator to scrape approximately 1 cm<sup>2</sup> area from the edge of the working stock, and spread on a PDA plate. The working stock plates typically last 3. When the new growth from the working stock is depleted prepare another. When

inoculating plates for conidia, spread with the applicator to cover a majority of the agar surface. Incubate plates lid side up at 25 °C under constant illumination. Shake excess condensation off the lids if a lot accumulates. Grow plates 8 -11 days for maximal conidial production- conidia will make the cultures appear slightly gray/brown.

## **B.2 Harvesting of conidia**

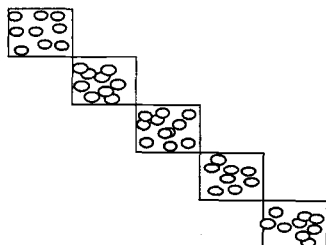
Process performed under sterile conditions.

1. Flood a healthy-growing plate with 8 ml of DI water + Tween<sup>a</sup>, more or less depending on how well the plate grew. Using a sterile rubber policeman, scrape the entire surface of the plate lightly to dislodge conidia.
2. Pour the solution into a 250-ml beaker covered with one layer of cheesecloth secured with a rubber band (all sterile). If the conidial solution in the beaker is a definite golden color (indicating lots of conidia), use an additional 1-2 ml Tween<sup>a</sup> solution to rinse the agar plate and filter through the cheesecloth.

<sup>a</sup> Tween solution. Add several drops of Tween 20 to 500 ml of deionized water (dH<sub>2</sub>O), shake and autoclave.

3. Discard the cheesecloth. Swirl the beaker to keep conidia in suspension and, using a sterile Pasteur pipet, transfer a drop of the suspension to a haemocytometer. The haemocytometer is called a "Levy Chamber", and is 1/400 sq. mm, and 1/10 mm deep. It has 2 grids, and each grid is a square divided into 25 smaller squares. Count conidia (5 squares diagonally) twice and take the average of the 2 values, multiply this number by 5 and then multiply by  $10^4$  (which is the dilution factor for volume of grid).

**Example of a calculation:**



Count 1 = 45

Count 2 = 47

Average value = 46

$46 \times 5 \times 10^4 = 2.3 \times 10^6$  conidia/ml

Inoculum desired =  $2 \times 10^6$  conidia

Volume required = 870  $\mu$ l

If there are too many conidia to count, dilute the suspension and take another sample.

4. Conidia can now be used to inoculate liquid culture or filters.

### B.3 Mineral salts growth medium

- a) 10 g/100 ml  $(\text{NH}_4)_2\text{SO}_4$  10 ml/L
- b) 1 g/100 ml  $\text{CaCl}_2$  10 ml/L
- c) 5 g/100 ml  $\text{MgSO}_4 \cdot 7\text{H}_2\text{O}$  10 ml/L
- d) 1 g/100 ml  $\text{NaCl}$  10 ml/L
- e) 3.6 mM  $\text{FeCl}_3$  + 50 mM EDTA 1 ml/L  
 (pH = 7.0). Prepare the EDTA  
 solution & add  $\text{FeCl}_3$  powder to it
- f) 10%  $\text{K}_2\text{HPO}_4$  (pH = 7)\* 10 ml/L
- \* Autoclave this solution separately, add after autoclaving.
- g) Trace Elements \*\* 1 ml/L

#### \*\* Trace element solution (for *Xanthobacter*)

Solution	stock solution mg/L	Concentration of stock mM
$\text{FeSO}_4 \cdot 7\text{H}_2\text{O}$	4500	22.6
$\text{MnCl}_2 \cdot 4\text{H}_2\text{O}$	300	1.52
$\text{ZnSO}_4 \cdot 7\text{H}_2\text{O}$	148	0.514
$\text{H}_3\text{BO}_3$	62	1.0

continued.....	stock solution mg/L	Concentration of stock mM
$\text{Na}_2\text{MoO}_4 \cdot 7\text{H}_2\text{O}$	147	0.45
$\text{NiCl}_2 \cdot 6\text{H}_2\text{O}$	24	0.10
$\text{Cu}_2\text{Cl}_2 \cdot 2\text{H}_2\text{O}$	17	0.10
$\text{Co}_2\text{Cl}_2 \cdot 6\text{H}_2\text{O}$	24	0.10

Prepare trace element solution in 1 liter of  $\text{dH}_2\text{O}$  containing 5 ml HCl.

Culturing technique and solution preparation was adapted from Hardison et al., (1997) and Curry et al., (1997).

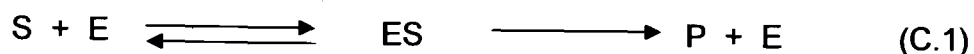


## Appendix C

### Model Development and STELLA Modeling

#### C.1 Metabolism of propane and *iso*-pentane and cometabolism of MTBE, TBF, and TBA

The rates of propane and *iso*-pentane metabolism, and MTBE, TBF, and TBA cometabolism were described by Michaelis-Menten/Monod kinetics (Missen. et al., 1999), which is based on the kinetics of the general enzyme-catalyzed reaction represented in Equation C.1.



This is a two-step mechanism with the first step being a rapid reversible formation of an enzyme-substrate complex (ES), followed by a slow step to form the product (P) to reproduce the enzyme. The general Michaelis-Menten/Monod expression is expressed as:

$$\frac{dM}{dt} = -\frac{k_{\max} X C_L}{K_s + C_L} V_L \quad (\text{C.2})$$

where:

$M$  = Total Mass of propane, *iso*-pentane, MTBE, TBF, or TBA,  $\mu\text{mol}$

$t$  = time, day

$X$  = Active microbial concentration, mg TSS/L

$C_L$  = Propane, *iso*-pentane, MTBE, TBF, and TBA concentration in liquid phase,  $\mu\text{mol/L}$

$k_{\max}$  = Maximum specific rate of propane, *iso*-pentane, MTBE, TBF, and TBA,  $\mu\text{mol/mg TSS-h}$

$K_s$  = Half-saturation coefficient for propane, *iso*-pentane, MTBE, TBF, and TBA,  $\mu\text{mol/L}$ .

$V_L$  = Liquid volume, L

Degradation rates were measured relative to the aqueous phase concentration. The mass balance of all five compounds in the experimental bottles can be expressed in terms of total mass as described by Equation C.3.

$$M = C_L V_L + C_G V_G \quad (\text{C.3})$$

where:

$V_G$  = Gas (Headspace) volume, L

$C_G$  = Propane, *iso*-pentane, MTBE, TBF, and TBA concentration in the gas phase,  $\mu\text{mol/L}$

The equilibrium between the two phases (gas and liquid) was assumed based on Henry's Law. The unitless Henry's coefficient ( $H_{cc}$ ) was used to describe the distribution of all five compounds between the two phases and is described by Equation C.4

$$H_{cc} = \frac{C_G}{C_L} \quad (\text{C.4})$$

Combining Equations C.3 and C.4 gives an expression in terms of the liquid phase concentration.

$$C_L = \frac{M}{V_L + V_G H_{cc}} \quad (\text{C.5})$$

Substituting Equation C.5 into C.2 yields Equation C.6

$$\frac{dM}{dt} = - \frac{k_{\max} X \left( \frac{M}{V_L + V_G H_{cc}} \right)}{K_s + \left( \frac{M}{V_L + V_G H_{cc}} \right)} V_L \quad (\text{C.6})$$

Equation C.6 applies for both substrate and co-substrate degradation as a function of time when a single compound is tested.  $M$ ,  $k_{\max}$ , and  $K_s$  would represent the total initial mass, maximum degradation rate coefficient and half-saturation coefficient for the single compound being tested, respectively.

### C.1.1 Inhibition

Competitive inhibition was observed among the substrates, propane and *iso*-pentane, and co-substrates MTBE and TBA. A competitive inhibitor binds to the enzyme and competes directly with the co-substrate for the same binding site of the enzyme. With competitive inhibition  $k_{\max} = k_{\max}^{app}$  (apparent, inhibitor present) while  $K_s^{app}$  (apparent) increases with increasing inhibitor concentration ( $I_L$ ).

Equation C.6 is modified to account for competitive inhibition resulting in Equation C.7, where  $I_L$  is the concentration of the inhibitor ( $\mu\text{mol/L}$ ) and  $K_{ic}$  is the inhibition (competitive) constant ( $\mu\text{mol/L}$ ).

$$\frac{dM_c}{dt} = - \frac{k_{\max c} \left( \frac{M_c}{V_L + V_G H_{ccc}} \right)}{K_{sc} \left( 1 + \frac{I_L}{K_{ic}} \right) + \left( \frac{M_c}{V_L + V_G H_{ccc}} \right)} (XV_L) \quad (\text{C.7})$$

The subscript c refers to co-substrate (MTBE and TBA). The concentration of the inhibitor  $I_L$  (which in this case is the substrate) can be also expressed in terms of total mass by  $I_L = \left( \frac{M_s}{V_L + V_G H_{ccs}} \right)$ , where  $M_s$  is the total mass of the inhibitor ( $\mu\text{mol}$ ) and  $H_{ccs}$  is the Henry's coefficient of the inhibitor, yielding Equation C.8.

$$\frac{dM_c}{dt} = - \frac{k_{\max c} \left( \frac{M_c}{V_L + V_G H_{ccc}} \right)}{K_{sc} \left( 1 + \frac{\frac{M_s}{V_L + V_G H_{ccs}}}{K_{ic}} \right) + \left( \frac{M_c}{V_L + V_G H_{ccc}} \right)} (XV_L) \quad (\text{C.8})$$

### C.1.2 Microbial growth

Microbial growth of the cultures (*Mycobacterium vaccae* and *Graphium sp.*) was also expressed by Monod kinetics as a function of substrate consumption (propane or *iso*-pentane) and cell decay.

$$\left(\frac{dX}{dt}\right) = Y\left(\frac{dM_{\text{substrate}}}{dt V_L}\right) - bX \quad (\text{C.9})$$

where:

$Y =$  Cellular yield from propane or *iso*-pentane, mg TSS/ $\mu\text{mol}$  substrate consumed.

$b =$  Cell decay rate,  $\text{day}^{-1}$

If Equation C.6 is expressed in terms of primary substrate, then:

$$\frac{dM_s}{dt} = - \frac{k_{\max s} X \left( \frac{M_s}{V_L + V_G H_{\text{ccs}}} \right)}{K_{ss} + \left( \frac{M_s}{V_L + V_G H_{\text{ccs}}} \right)} V_L \quad (\text{C.10})$$

Substituting Equation C.10 into C.9,

$$\frac{dX}{dt} = Y \frac{k_{\max s} X \left( \frac{M_s}{V_L + V_G H_{ccs}} \right)}{K_{ss} + \left( \frac{M_s}{V_L + V_G H_{ccs}} \right)} - bX \quad (\text{C.11})$$

When the cometabolism of a co-substrate is evaluated in the absence of the substrate, energy would be depleted affecting cell activity. If no energy is available, transformation of the remaining compounds would cease. If kinetic coefficients are estimated accurately, fitting of cometabolism experimental data can be done by adjusting the activity loss of the cells from the loss of energy by incorporating the energy loss (E) as equivalent to cell decay.

$$\frac{dX}{dt} = Y \frac{k_{\max s} X \left( \frac{M_s}{V_L + V_G H_{ccs}} \right)}{K_{ss} + \left( \frac{M_s}{V_L + V_G H_{ccs}} \right)} - (b + E)X \quad (\text{C.12})$$

A combination of these equations can be solved to model metabolism of substrates, biomass production, and cometabolism of co-substrates in the presence or absence of the growth supporting substrate by numerical integration in STELLA® using a fourth-order Runge-Kutta method. The different cases are listed in Table C.1.

**Table C.1** Equations used in STELLA modeling for the degradation of substrate and cometabolism of MTBE, TBF, and TBA

Case	Equation				
	C.6	C.8	C.10	C.11	C.12
Metabolism of substrate			✓	✓	
Cometabolism of MTBE or TBA <sup>a</sup>		✓	✓	✓	
Cometabolism of MTBE or TBA <sup>b*</sup>	✓				✓
Cometabolism of TBF <sup>a*</sup>	✓			✓	
Cometabolism of TBF <sup>b*</sup>	✓				✓

<sup>a</sup> in the presence of the substrate

<sup>b</sup> in the absence of the substrate

\* no inhibition

## C.2 Bacterial system modeling

### C.2.1 Low initial biomass concentration

Experiments involving biomass growth of *M. vaccae* JOB5, isopentane metabolism and cometabolism of MTBE, TBF, and TBA were analyzed using data obtained from growth batch reactors experiment and modeling with STELLA® software. The interactions modeled and the



equations for the simulation in STELLA<sup>®</sup> shown in Figures C.1 and C.2, respectively. Results are discussed in Chapter 2.

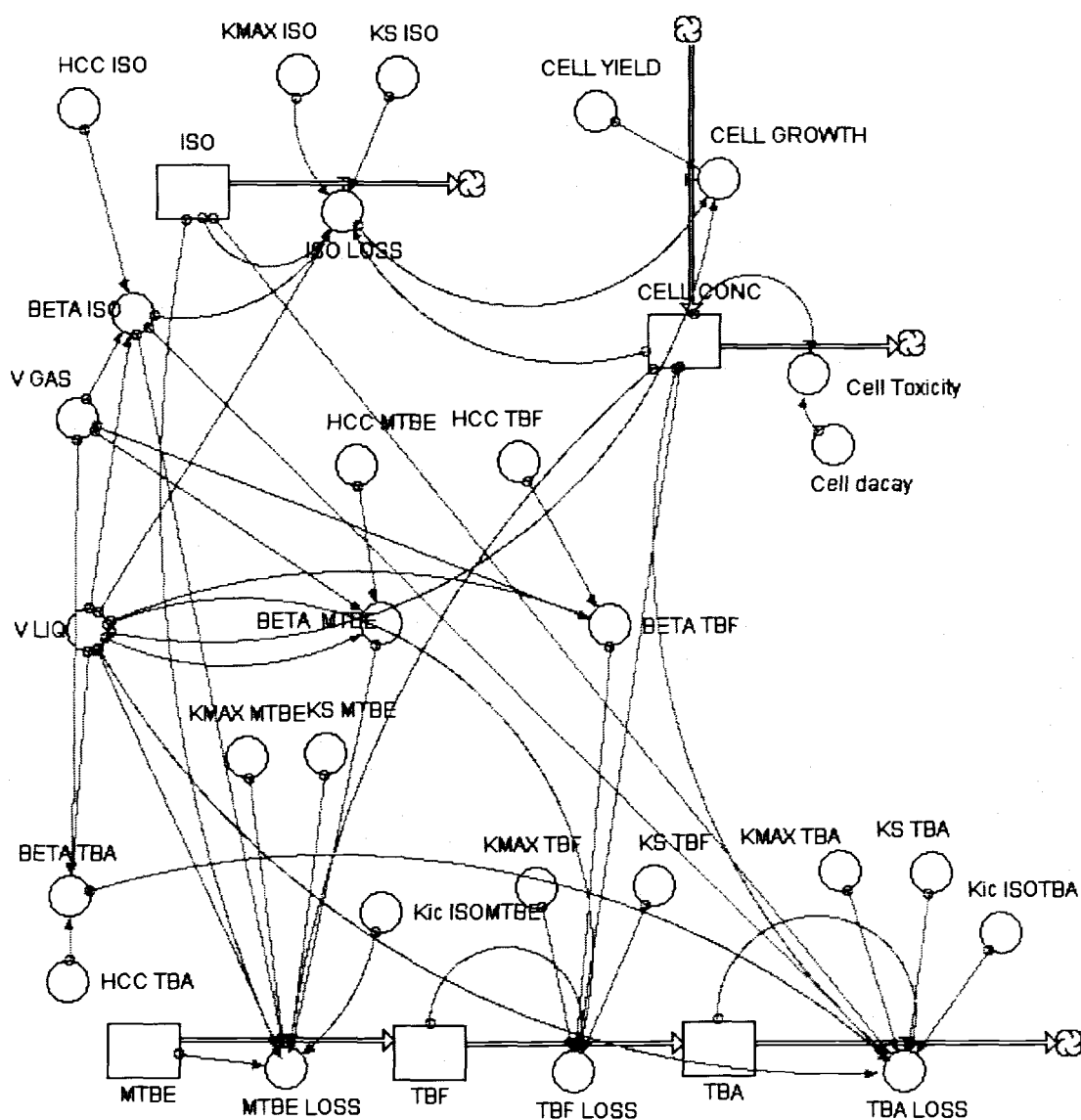


**Figure C.1** Diagram for STELLA simulation. Metabolism of *iso*-pentane and cometabolism of MTBE, TBF, and TBA by *Mycobacterium vaccae* in growth batch reactor

$$\text{CELL\_CONC}(t) = \text{CELL\_CONC}(t - dt) + (\text{CELL\_GROWTH} - \text{Cell\_Toxicity}) * dt$$

dt

$$\text{INIT CELL\_CONC} = 21$$

INFLOWS:

$$\text{CELL\_GROWTH} = \text{CELL\_YIELD} * \text{ISO\_LOSS} / \text{V\_LIQ}$$

OUTFLOWS:

$$\text{Cell\_Toxicity} = \text{Cell\_decay} * \text{CELL\_CONC}$$

$$\text{ISO}(t) = \text{ISO}(t - dt) + (- \text{ISO\_LOSS}) * dt$$

$$\text{INIT ISO} = 2920$$

OUTFLOWS:

$$\text{ISO\_LOSS} =$$

$$(\text{CELL\_CONC} * \text{V\_LIQ} * \text{KMAX\_ISO} * \text{BETA\_ISO} * \text{ISO}) / (\text{KS\_ISO} + \text{BETA\_ISO} * \text{ISO})$$

$$\text{MTBE}(t) = \text{MTBE}(t - dt) + (- \text{MTBE\_LOSS}) * dt$$

$$\text{INIT MTBE} = 145$$

OUTFLOWS:

$$\text{MTBE\_LOSS} =$$

$$(\text{CELL\_CONC} * \text{V\_LIQ} * \text{KMAX\_MTBE} * \text{BETA\_MTBE} * \text{MTBE}) / ((\text{KS\_MTBE} * (1 + \text{BETA\_ISO} * \text{ISO} / \text{Kic\_ISOMTBE}) + \text{MTBE} * \text{BETA\_MTBE}))$$

$$\text{TBA}(t) = \text{TBA}(t - dt) + (\text{TBF\_LOSS} - \text{TBA\_LOSS}) * dt$$

$$\text{INIT TBA} = 0$$

INFLOWS:

$$\text{TBF\_LOSS} =$$

$$(\text{CELL\_CONC} * \text{V\_LIQ} * \text{KMAX\_TBF} * \text{BETA\_TBF} * \text{TBF}) / (\text{KS\_TBF} + \text{BETA\_TBF} * \text{TBF})$$

OUTFLOWS:

$$\text{TBA\_LOSS} =$$

$$(\text{CELL\_CONC} * \text{V\_LIQ} * \text{KMAX\_TBA} * \text{BETA\_TBA} * \text{TBA}) / ((\text{KS\_TBA} * (1 + \text{BETA\_ISO} * \text{ISO} / \text{Kic\_ISOTBA}) + \text{BETA\_TBA} * \text{TBA}))$$

**Figure C.2** Equations for model simulation in STELLA. Metabolism of isopentane and cometabolism of MTBE, TBF, and TBA by *iso*-pentane-grown *Mycobacterium vaccae* in growth batch reactor.

$$\text{TBF}(t) = \text{TBF}(t - dt) + (\text{MTBE\_LOSS} - \text{TBF\_LOSS}) * dt$$

INIT TBF = 0

INFLOWS:

MTBE\_LOSS =

$$(\text{CELL\_CONC} * \text{V\_LIQ} * \text{KMAX\_MTBE} * \text{BETA\_MTBE} * \text{MTBE}) / ((\text{KS\_MTBE} * (1 + \text{BETA\_ISO} * \text{ISO} / \text{Kic\_ISOMTBE}) + \text{MTBE} * \text{BETA\_MTBE}))$$

OUTFLOWS:

TBF\_LOSS =

$$(\text{CELL\_CONC} * \text{V\_LIQ} * \text{KMAX\_TBF} * \text{BETA\_TBF} * \text{TBF}) / (\text{KS\_TBF} + \text{BETA\_TBF} * \text{TBF})$$

$$\text{BETA\_ISO} = 1 / (\text{V\_LIQ} + \text{V\_GAS} * \text{HCC\_ISO})$$

$$\text{BETA\_TBA} = 1 / (\text{V\_LIQ} + \text{V\_GAS} * \text{HCC\_TBA})$$

$$\text{BETA\_TBF} = 1 / (\text{V\_LIQ} + \text{V\_GAS} * \text{HCC\_TBF})$$

$$\text{BETA\_MTBE} = 1 / (\text{V\_LIQ} + \text{V\_GAS} * \text{HCC\_MTBE})$$

$$\text{Cell\_decay} = 0.075$$

$$\text{CELL\_YIELD} = 0.044$$

$$\text{HCC\_ISO} = 55.55$$

$$\text{HCC\_MTBE} = 0.0217$$

$$\text{HCC\_TBA} = 0.0001$$

$$\text{HCC\_TBF} = 0.024$$

$$\text{Kic\_ISOMTBE} = 14.67$$

$$\text{Kic\_ISOTBA} = 7$$

$$\text{KMAX\_ISO} = 31.104$$

$$\text{KMAX\_MTBE} = 4.8$$

$$\text{KMAX\_TBA} = 1.64$$

$$\text{KMAX\_TBF} = 10.08$$

$$\text{KS\_ISO} = 14.67$$

$$\text{KS\_MTBE} = 164$$

$$\text{KS\_TBA} = 94.4$$

$$\text{KS\_TBF} = 140$$

$$\text{V\_GAS} = 0.35$$

$$\text{V\_LIQ} = 0.35$$

**Figure C.2, Continued.**

### **C.2.2 Independent solution and Fortran code**

Equations C.8, C.10, and C.11 were solved independently to compare and check for the modeling results provided by STELLA.

Let:

$$\alpha = Yk_{\max, s} \quad \text{C.13)}$$

$$\gamma = K_{ss}(V_L + V_G H_{cs}) \quad \text{C.14)}$$

$$\beta = k_{\max, s} V_L \quad \text{(C.15)}$$

$$\delta = b \quad \text{(C.16)}$$

Substituting Equation C.13 through C.15 into C.10 and C.11 yielded Equations C.17 and C.18

$$\frac{dM_s}{dt} = -\frac{\beta XM_s}{\gamma + M_s} \quad \text{(C.17)}$$

$$\frac{dX}{dt} = \frac{\alpha XM_s}{\gamma + M_s} - \delta X = \frac{\alpha XM_s - \delta \gamma X - \delta XM_s}{\gamma + M_s} \quad \text{(C.18)}$$

Dividing C.18 by C.17, then:

$$\frac{dX}{dM_s} \frac{dt}{dt} = \left[ \frac{(\alpha - \delta)XM_s - \delta \gamma X}{\gamma + M_s} \right] \left[ \frac{\gamma + M_s}{\beta XM_s} \right] \quad \text{(C.19)}$$

$$\frac{dX}{dM_s} = \frac{\delta - \alpha}{\beta} + \left( \frac{\delta\gamma}{\beta} \right) \left( \frac{1}{M_s} \right) \quad (\text{C.20})$$

Integrating equation C.20 yields Equation C.22

$$\int_{X_0}^X dX = \left( \frac{\delta - \alpha}{\beta} \right) \int_{M_{s_0}}^{M_s} dM_s - \frac{\delta\gamma}{\beta} \int_{M_{s_0}}^{M_s} \frac{1}{dM_s} dM_s \quad (\text{C.21})$$

$$X = \left( \frac{\delta - \alpha}{\beta} \right) (M_s - M_{s_0}) + \frac{\delta\gamma}{\beta} \ln \left( \frac{M_s}{M_{s_0}} \right) + X_0 \quad (\text{C.22})$$

Equation C.22 applies for:

$$\begin{aligned} M_s &= M_{s_0} \quad \text{when} \quad X = X_0 \quad \text{at} \quad t = 0 \\ X &= X_{max} \quad \text{when} \quad 0 < M_s << M_{s_0} \quad \text{at} \quad t = \text{finite} \end{aligned}$$

Figure C.3 shows the linear relationship of biomass produced as a function of *iso*-pentane consumed in the growth batch reactor. A very good agreement was obtained between the experimental data and the computed results with Equation C.22. Computed values were obtained using the values listed in Table C.2.

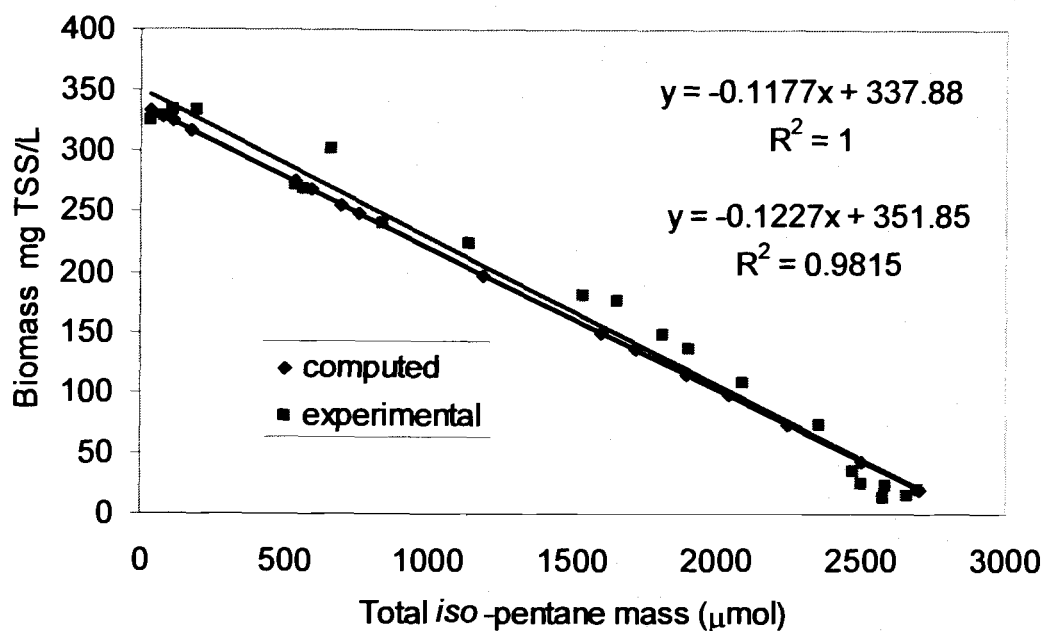


**Figure C.3** Production of *Mycobacterium vaccae* in growth batch reactor. Metabolism of *iso*-pentane and cometabolism of MTBE, TBF, and TBA by

**Table C.2** Parameters used in computation of biomass from *iso*-pentane metabolism in growth batch reactor

Parameter	Units	Comments
$X_0 = 20$	mg TSS/L	Measured at $t = 0$
$M_0 = 2700$	$\mu\text{mol/L}$	<i>iso</i> -pentane added at $t = 0$
$Y = 0.044$	mg TSS/ $\mu\text{mol}$ -d	Determined experimentally
$k_{max} = 27$	$\mu\text{mo iso/mg TSS} - \text{d}$	Determined experimentally
$K_s = 14.67$	$\mu\text{mol iso/L}$	Determined experimentally
$V_L = V_G = 0.35$	L	Volume in experimental bottle
$b = 0.075$	1/d	Assumed, typical value
$H_{cc} = 55.55$	dimensionless	Literature value

In order to solve C.8, a new equation was generated as a function of C.17 and C.18 as follows:

Let:

$$\phi = K_{\max c} V_L \quad (\text{C.23})$$

$$\eta = (V_L + V_G H_{ccc}) \quad (\text{C.24})$$

$$\varepsilon = K_{sc} \quad (\text{C.25})$$

$$\rho = K_{ic} (V_L + V_G H_{cc}) \quad (\text{C.26})$$

Substituting Equation C.23 through C.26 into C.8 yields Equation C.27:

$$\frac{dM_c}{dt} = - \frac{\phi \frac{M_c}{\rho}}{\varepsilon \left( 1 + \frac{M_s}{\rho} \right) + \frac{M_c}{\eta}} \quad (\text{C.27})$$

Rearranging terms, we obtain

$$\frac{dM_c}{dt} = - \frac{\phi M_c X}{\varepsilon \eta + \frac{\varepsilon \eta}{\rho} M_s + M_c}$$

where:

$$f(t) = \phi X(t) \quad \text{and} \quad g(t) = \varepsilon \eta + \frac{\varepsilon \eta}{\rho} M_s(t)$$

then,

$$\frac{dM_c}{dt} = -f(t) + \frac{g(t)f(t)}{g(t) + M_c} \quad (\text{C.28})$$

A Fortran code was written to solve Equations C.17 and C.18 independently and the values obtained were used to solve Equation C.28 using a fourth-order Runge-Kutta method (see Figure C.4). Substrate metabolism, biomass production, and cometabolism of MTBE were computed as a function of time with these 3 independent equations and results obtained were identical to the values obtained from STELLA as shown in Figure C.5.



\*\*\*\*\*  
 \*\*\*\*\*ABSTRACT \*\*\*\*\*

THIS PROGRAM USES A 4TH ORDER RUNGE-KUTTA METHOD TO INTEGRATE A SET OF THREE FIRST ORDER ODE'S. THE USER SUPPLIES THE INITIAL CONDITION AND THE FINAL VALUE OF T, AS WELL AS THE EQUATIONS FOR F (T, MS, MC, X). THIS PROGRAM CALCULATE THE DEGRADATION OF ISO-PENTANE (SUSTRATE), MICROBIAL GROWTH OF MYCOBACTERIUM VACCAE JOB5, AND THE COMETABOLISM OF METHYL TERT-BUTYL ETHER (CO-SUSTRATE)

\*\*\*\*\* NOMENCLATURE \*\*\*\*\*  
 \*\*\*\*\*

DT- THE STEP SIZE

DMSDT- THE DERIVATIVE OF MS WITH RESPECT TO T

DMCDT- THE DERIVATIVE OF MC WITH RESPECT TO T

DXDT- THE DERIVATIVE OF X WITH RESPECT TO T

K1MS- K1 IN EQUATION 10 (Selwyn Hollis, 2002)

K2MS- K2 IN EQUATION 10 (Selwyn Hollis, 2002)

K3MS- K3 IN EQUATION 10 (Selwyn Hollis, 2002)

K4MS- K4 IN EQUATION 10 (Selwyn Hollis, 2002)

K1MC- K1 IN EQUATION 10 (Selwyn Hollis, 2002)

K2MC- K2 IN EQUATION 10 (Selwyn Hollis, 2002)

K3MC- K3 IN EQUATION 10 (Selwyn Hollis, 2002)

K4MC- K4 IN EQUATION 10 (Selwyn Hollis, 2002)

K1X- K1 IN EQUATION 10 (Selwyn Hollis, 2002)

K2X- K2 IN EQUATION 10 (Selwyn Hollis, 2002)

K3X- K3 IN EQUATION 10 (Selwyn Hollis, 2002)

K4X- K4 IN EQUATION 10 (Selwyn Hollis, 2002)

T- THE INDEPENDENT VARIABLE

TMAX- THE FINAL VALUE OF TIME

MS- THE DEPENDENT VARIABLE

MC- THE DEPENDENT VARIABLE

X- THE DEPENDENT VARIABLE

\*\*\*\*\*  
 \*\*\*\*\*

**Figure C.4** Fortran code. Biomass production, metabolism of *iso*-pentane and cometabolism of MTBE by *Mycobacterium vaccae* in growth batch reactor

```
*****
*****
```

# DOUBLE PRECISION

```
T,MS,MC,X,DMSDT,DMCDT,DXDT,K1MS,K2MS,K3MS,K4MS,K1MC,K2MC
,K3MC,K4MC
```

```
DOUBLE PRECISION K1X,K2X,K3X,K4X,T1,MS1,MC1,X1
```

```
T=0.0
```

```
MS=2700.0
```

```
MC=145.0
```

```
X=20.0
```

```
TMAX=4.0
```

```
DT=0.05
```

```
1 CALL FUNCTMS(T,MS,MC,X,DMSDT)
```

```
CALL FUNCTMC(T,MS,MC,X,DMCDT)
```

```
CALL FUNCTX(T,MS,MC,X,DXDT)
```

```
WRITE(6,10)T,MS,MC,X
```

```
10 FORMAT( 4H T=,E14.7,3X,4H MS=,E14.7,3X,4H MC=,E14.7,3X,4H
X=,E14.7)
```

```
K1MS=DMSDT
```

```
K1MC=DMCDT
```

```
K1X=DXDT
```

```
MS1=MS+DMSDT*DT/2.0
```

```
MC1=MC+DMCDT*DT/2.0
```

```
X1=X+DXDT*DT/2.0
```

```
T1=T+DT/2.0
```

```
CALL FUNCTMS(T1,MS1,MC1,X1,DMSDT)
```

```
CALL FUNCTMC(T1,MS1,MC1,X1,DMCDT)
```

```
CALL FUNCTX(T1,MS1,MC1,X1,DXDT)
```

```
K2MS=DMSDT
```

```
K2MC=DMCDT
```

```
K2X=DXDT
```

```
MS1=MS+DMSDT*DT/2.0
```

```
MC1=MC+DMCDT*DT/2.0
```

```
X1=X+DXDT*DT/2.0
```

```
CALL FUNCTMS(T1,MS1,MC1,X1,DMSDT)
```

```
CALL FUNCTMC(T1,MS1,MC1,X1,DMCDT)
```

```
CALL FUNCTX(T1,MS1,MC1,X1,DXDT)
```

```
K3MS=DMSDT
```

```
K3MC=DMCDT
```

**Figure C.4 Continued**

```

K3X=DXDT
MS1=MS+DMSDT*DT
MC1=MC+DMCDT*DT
X1=X+DXDT*DT
T1=T+DT
CALL FUNCTMS(T1,MS1,MC1,X1,DMSDT)
CALL FUNCTMC(T1,MS1,MC1,X1,DMCDT)
CALL FUNCTX(T1,MS1,MC1,X1,DXDT)
K4MS=DMSDT
K4MC=DMCDT
K4X=DXDT
MS=MS+DT*(K1MS+2.0*K2MS+2.0*K3MS+K4MS)/6.0
MC=MC+DT*(K1MC+2.0*K2MC+2.0*K3MC+K4MC)/6.0
X=X+DT*(K1X+2.0*K2X+2.0*K3X+K4X)/6.0
T=T+DT
IF(T.LT.TMAX)GO TO 1
WRITE(6,10)T,MS,MC,X
STOP
END

```

\*\*\*\*\* ABSTRACT \*\*\*\*\*

THESE SUBROUTINES CALCULATES THE DERIVATIVE OF MS,MC,X  
WITH RESPECT TO T.  
THE USER SUPPLIES THE EQUATION FOR DMSDT,DMCDT,DXDT.

\*\*\*\*\*

```

SUBROUTINE FUNCTMS(T,MS,MC,X,DMSDT)
DOUBLE PRECISION T,MS,MC,X,DMSDT
DOUBLE PRECISION BETA,GAMMA,KMAX,KS,VL,VG,HCC
KMAX=27.0
KS=14.67
VG=0.35
VL=0.35
HCC=55.55
BETA=KMAX*VL
GAMMA=KS*(VL+VG*HCC)
DMSDT=-BETA*X*MS/(GAMMA+MS)
RETURN
END

```

**Figure C.4 Continued**

```

SUBROUTINE FUNCTX(T,MS,MC,X,DXDT)
DOUBLE PRECISION T,MS,MC,X,DXDT
DOUBLE PRECISION
ALPHA,DELTA,GAMMA,YIELD,KMAX,KS,VL,VG,HCC,B
KMAX=30.0
KS=14.67
VG=0.35
VL=0.35
HCC=55.55
B=0.075
YIELD=0.044
ALPHA=YIELD*KMAX
GAMMA=KS*(VL+VG*HCC)
DELTA=B
DXDT=ALPHA*X*MS/((GAMMA+MS)-DELTA*X
RETURN
END

```

```

SUBROUTINE FUNCTMC(T,MS,MC,X,DMCDT)
DOUBLE PRECISION T,MS,MC,X,DMCDT
DOUBLE PRECISION KMAXC,KIC,KS,KSC,VL,VG,HCC,HCCC
DOUBLE PRECISION PHI,RHO,XHI,ETHA
KMAXC=4.8
KIC=14.67
KSC=164.0
VG=0.35
VL=0.35
HCC=55.55
HCCC=0.0217
PHI=KMAXC*VL
RHO=KIC*(VL+VG*HCC)
XHI=KSC
ETHA=VL+VG*HCCC
DMCDT=-
PHI*RHO*X*MC/((XHI*RHO*ETHA+XHI*ETHA*MS+RHO*MC)
RETURN
END

```

**Figure C.4 Continued**

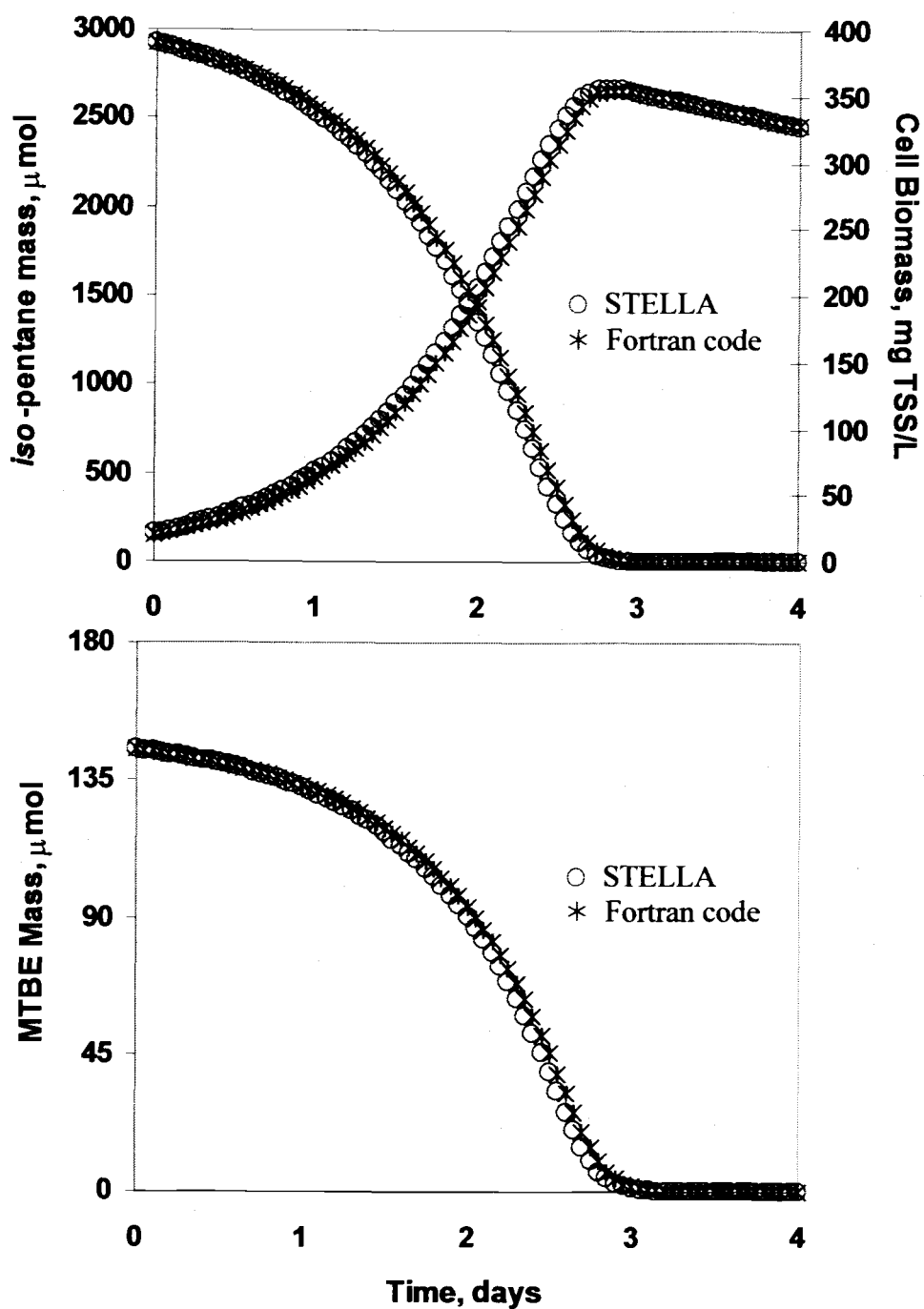


**Figure C.5** Growth batch reactor modeling with STELLA and Fortran code. Metabolism of *iso*-pentane, biomass production, and cometabolism of MTBE.

### C.2.3 High initial biomass concentration

*iso*-pentane metabolism and cometabolism of MTBE, TBF, and TBA, by harvested and concentrated bacterial cells, was also model with STELLA. Figure C.6 shows a good agreement between the experimental data and the predicted results from modeling for the metabolism of *iso*-pentane. Degradation of 3.5  $\mu\text{mol}$  *iso*-pentane by an initial biomass concentration of 490 mg TSS/L was followed with time.

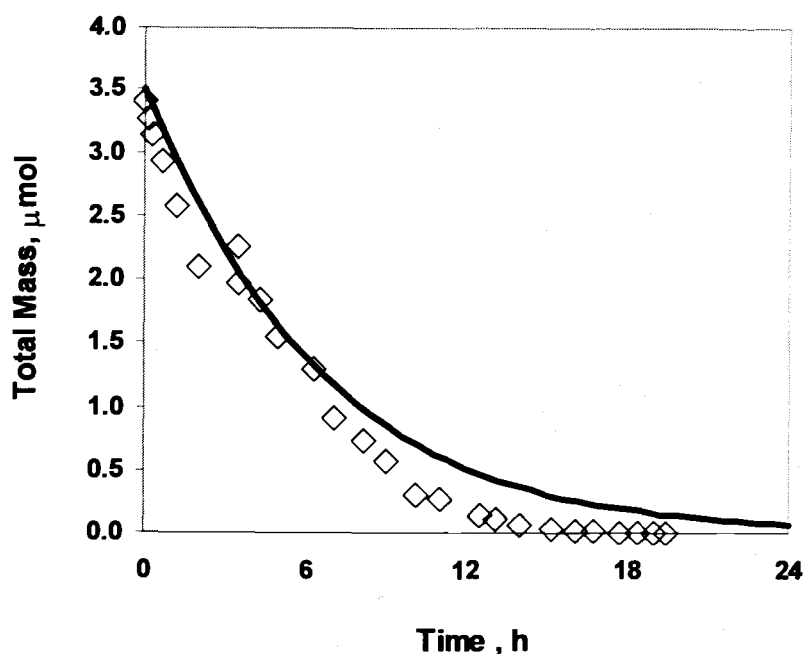


**Figure C.6** Metabolism of *iso*-pentane by concentrated *iso*-pentane grown *M. vaccae* cells. Experimental data and STELLA modeling are represented by the open diamonds and the solid line, respectively.

Kinetic coefficients used in STELLA to model experimental data are as listed in Table 2.6: Yield = 0.044 mg TSS/ $\mu$ mo *iso* consumed;  $k_{max-iso}$  = 30  $\mu$ mol *iso*/mgTSS-d;  $K_{s-iso}$  = 14.67  $\mu$ mol/L; cell decay = 0.075 1/day (typical value);  $V_{LIQ}$  = 0.005 L ;  $V_{GAS}$  = 0.0228 L.

The cometabolism of MTBE, TBF, and TBA by *iso*-pentane grown bacterial culture, in the absence of the substrate, was also modeled as shown in Figures C.7. Degradation of 3.8  $\mu$ mol MTBE, and TBF and TBA produced from MTBE oxidation were followed with time. Kinetic coefficients for MTBE, TBF, and TBA used in STELLA are as listed in Table 2.2: ; cell decay = 0.075 1/day (typical value);  $V_{LIQ}$  = 0.005 L ;  $V_{GAS}$  = 0.0228 L and initial biomass concentration of 490 mg TSS/L. To account for energy depletion E was adjusted and the best fit was obtained at 0.15 1/h.

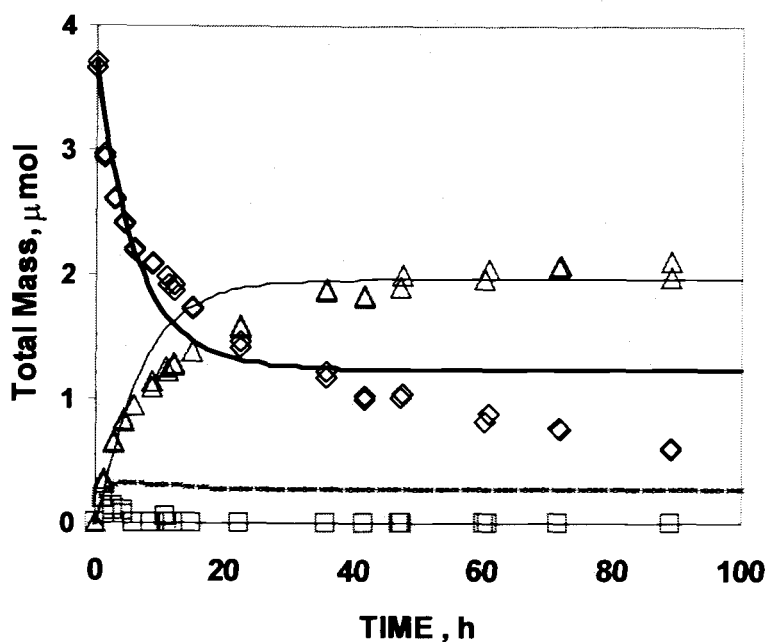


**Figure C.7** Cometabolism of MTBE, TBF, and TBA by concentrated *iso*-pentane grown *M. vaccae* cells. Experimental data of MTBE ( $\diamond$ ), TBF ( $\square$ ), and TBA ( $\triangle$ ) and STELLA modeling are represented by the solid lines. respectively

Another example for the cometabolism of 4  $\mu\text{mol}$  TBF, by *iso*-pentane grown *M. vaccae* culture, in the absence of the substrate, is shown in Figure C.8. Kinetic coefficients for MTBE, TBF, and TBA used in STELLA are as listed in Table 2.2; cell decay = 0.075 1/day (typical value);  $V_{\text{LIQ}} = 0.005 \text{ L}$ ;  $V_{\text{GAS}} = 0.0228 \text{ L}$  and initial biomass concentration of 490 mg TSS/L. The best fit was obtained when E term was adjusted to 0.08 1/h.



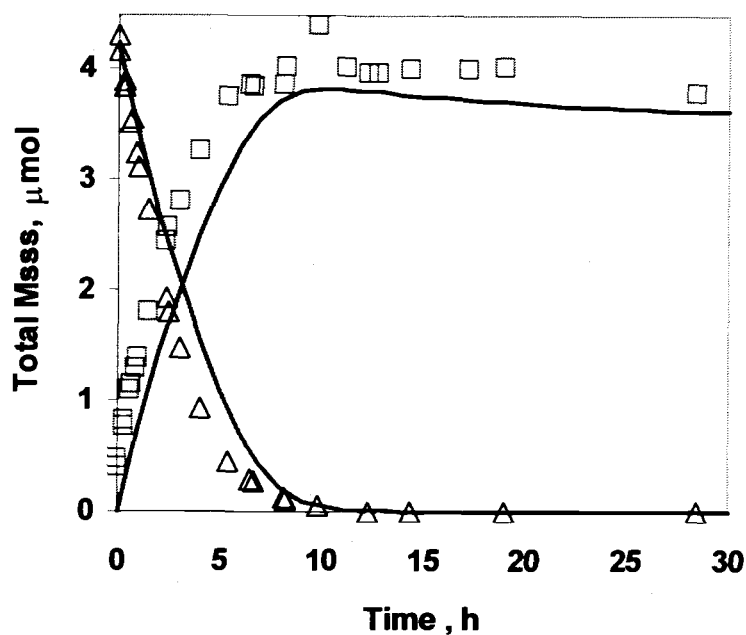


**Figure C.8** Cometabolism of TBF, and TBA by concentrated *iso*-pentane grown *M. vaccae* cells. Experimental data of TBF ( $\Delta$ ), and TBA ( $\square$ ) and STELLA modeling are represented by the solid lines.

### C.3 Fungal system modeling

MTBE and TBF cometabolism by propane-grown *Graphium sp* (filter-attached culture) was modeled with STELLA<sup>®</sup>. Experimental data was obtained from resting cell experiments. The diagram generated and the Equations for the model simulation in STELLA<sup>®</sup> are shown in figures C.9 and C.10, and C.11 and C.12, respectively.

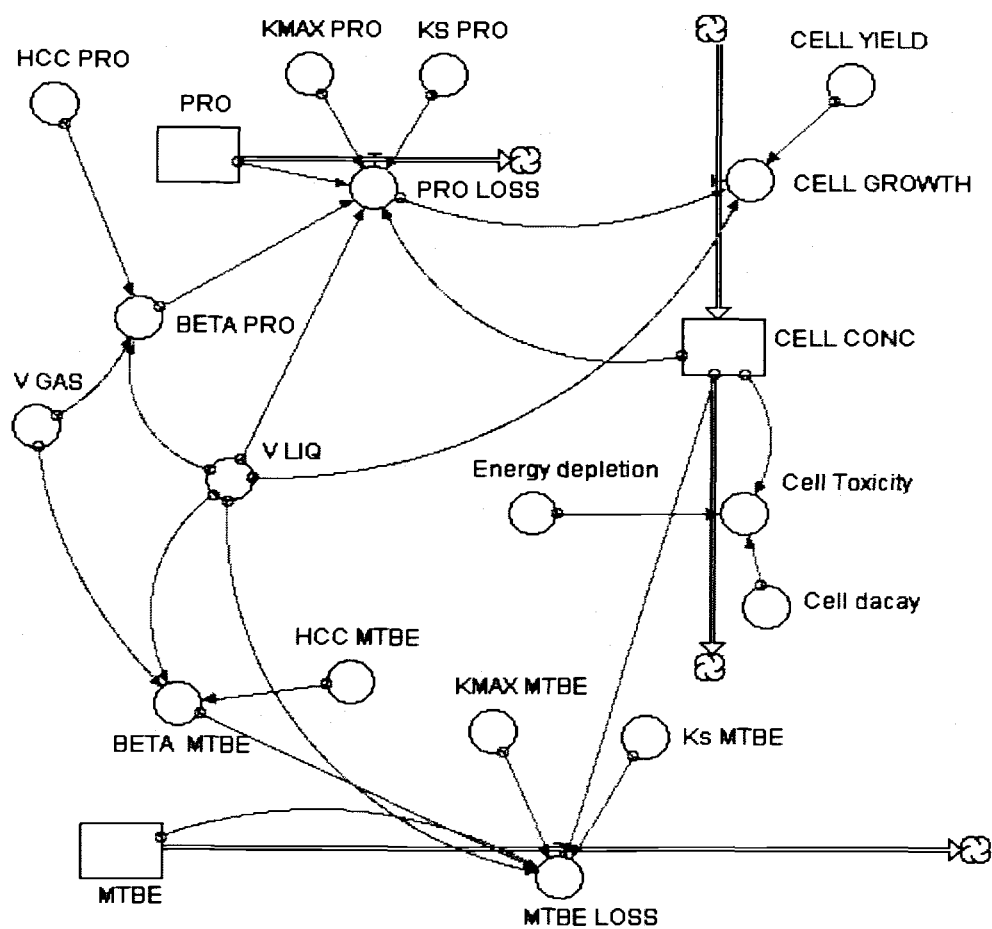


**Figure C.9** STELLA simulation diagram for the cometabolism of MTBE by propane-grown *Graphium* sp. (Filter-attached culture).

$$\text{CELL\_CONC}(t) = \text{CELL\_CONC}(t - dt) + (\text{CELL\_GROWTH} - \text{Cell\_Toxicity}) * dt$$

$$\text{INIT CELL\_CONC} = 9430$$

INFLOWS:

$$\text{CELL\_GROWTH} = \text{CELL\_YIELD} * \text{PRO\_LOSS} / V\_LIQ$$

OUTFLOWS:

$$\text{Cell\_Toxicity} = (\text{Cell\_decay} + \text{Energy\_depletion}) * \text{CELL\_CONC}$$

$$\text{MTBE}(t) = \text{MTBE}(t - dt) + (- \text{MTBE\_LOSS}) * dt$$

$$\text{INIT MTBE} = 18$$

OUTFLOWS:

$$\text{MTBE\_LOSS} = \text{CELL\_CONC} * V\_LIQ * K_{\text{MAX\_MTBE}} * \text{BETA\_MTBE} * \text{MTBE} / (\text{K}_{\text{S\_MTBE}} + \text{BETA\_MTBE} * \text{MTBE})$$

$$\text{PRO}(t) = \text{PRO}(t - dt) + (- \text{PRO\_LOSS}) * dt$$

$$\text{INIT PRO} = 0.001$$

OUTFLOWS:

$$\text{PRO\_LOSS} =$$

$$(\text{CELL\_CONC} * V\_LIQ * K_{\text{MAX\_PRO}} * \text{BETA\_PRO} * \text{PRO}) / (\text{K}_{\text{S\_PRO}} + \text{BETA\_PRO} * \text{PRO})$$

$$\text{BETA\_PRO} = (1/V\_LIQ + V\_GAS * H_{\text{CC\_PRO}})$$

$$\text{BETA\_MTBE} = 1/(V\_LIQ + V\_GAS * H_{\text{CC\_MTBE}})$$

$$\text{Cell\_decay} = 0.00313$$

$$\text{CELL\_YIELD} = 0.01455$$

$$\text{Energy\_depletion} = 0$$

$$\text{HCC\_MTBE} = 0.0221$$

$$\text{HCC\_PRO} = 28.89$$

$$K_{\text{MAX\_MTBE}} = 0.073$$

$$K_{\text{MAX\_PRO}} = 0.234$$

$$K_{\text{S\_MTBE}} = 5200$$

$$K_{\text{S\_PRO}} = 1.07$$

$$V\_GAS = 157.5/1000$$

$$V\_LIQ = 6.5/1000$$

**Figure C.10** Equations for model simulation in STELLA®. Cometabolism of MTBE by propane-grown *Graphium* sp. (Filter-attached culture).

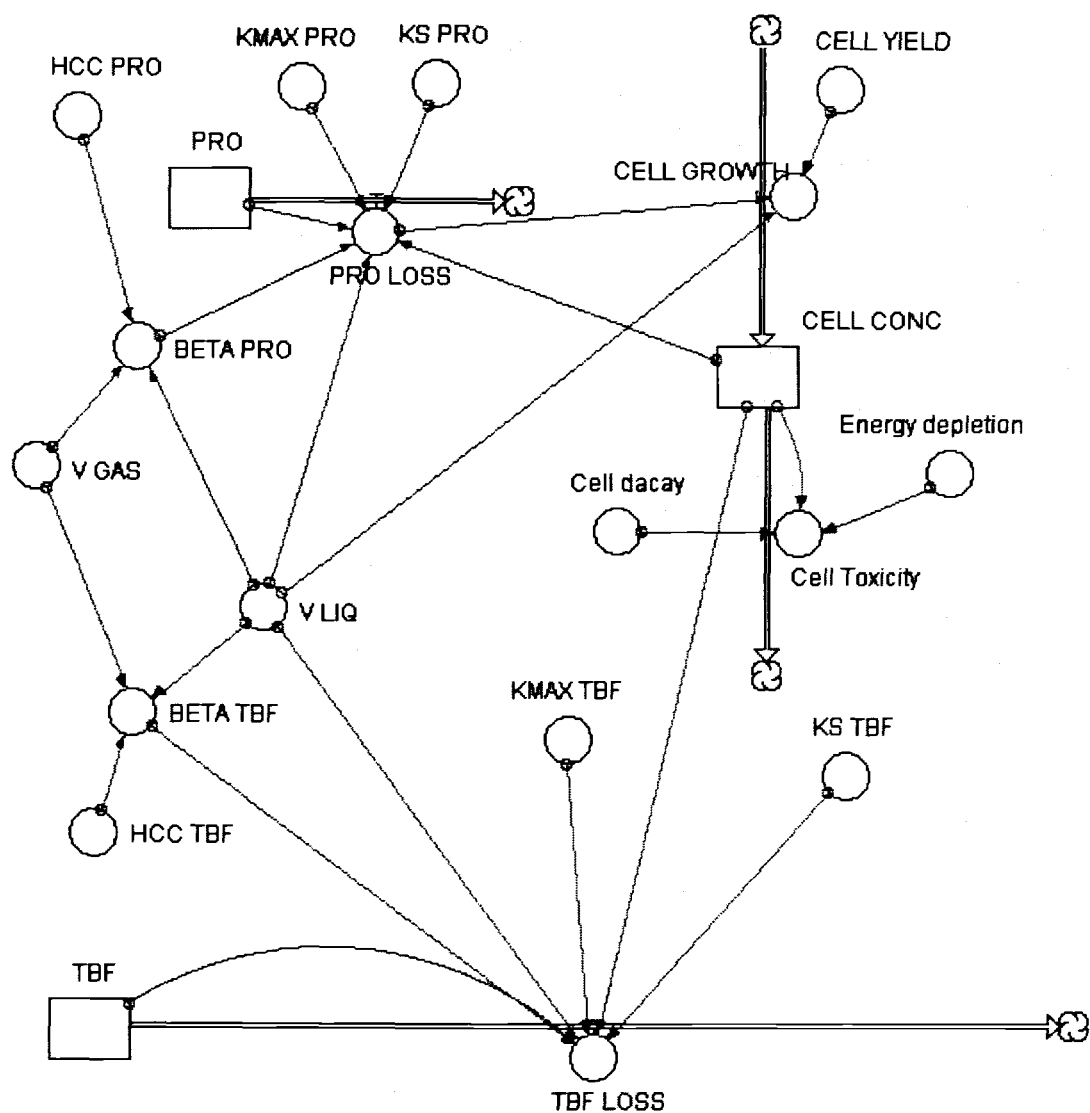


**Figure C.11** STELLA simulation diagram for the cometabolism of TBF by propane-grown *Graphium* sp. (Filter-attached culture).

$$\text{CELL\_CONC}(t) = \text{CELL\_CONC}(t - dt) + (\text{CELL\_GROWTH} - \text{Cell\_Toxicity}) * dt$$

$$\text{INIT CELL\_CONC} = 10564$$

INFLOWS:

$$\text{CELL\_GROWTH} = \text{CELL\_YIELD} * \text{PRO\_LOSS} / V\_LIQ$$

OUTFLOWS:

$$\text{Cell\_Toxicity} = (\text{Cell\_dacay} + \text{Energy\_depletion}) * \text{CELL\_CONC}$$

$$\text{PRO}(t) = \text{PRO}(t - dt) + (- \text{PRO\_LOSS}) * dt$$

$$\text{INIT PRO} = 0.01$$

OUTFLOWS:

$$\text{PRO\_LOSS} =$$

$$(\text{CELL\_CONC} * V\_LIQ * KMAX\_PRO * BETA\_PRO * \text{PRO}) / (KS\_PRO + BETA\_PRO * \text{PRO})$$

$$\text{TBF}(t) = \text{TBF}(t - dt) + (- \text{TBF\_LOSS}) * dt$$

$$\text{INIT TBF} = 8.6$$

OUTFLOWS:

$$\text{TBF\_LOSS} =$$

$$(\text{CELL\_CONC} * V\_LIQ * KMAX\_TBF * BETA\_TBF * \text{TBF}) / (KS\_TBF + BETA\_TBF * \text{TBF})$$

$$\text{BETA\_PRO} = (1 / V\_LIQ + V\_GAS * HCC\_PRO)$$

$$\text{BETA\_TBF} = 1 / (V\_LIQ + V\_GAS * HCC\_TBF)$$

$$\text{Cell\_dacay} = 0.00313$$

$$\text{CELL\_YIELD} = 0.01455$$

$$\text{Energy\_depletion} = 0$$

$$\text{HCC\_PRO} = 28.89$$

$$\text{HCC\_TBF} = 0.024$$

$$\text{KMAX\_PRO} = 0$$

$$\text{KMAX\_TBF} = 0.488$$

$$\text{KS\_PRO} = 0$$

$$\text{KS\_TBF} = 1970$$

$$V\_GAS = 157.5 / 1000$$

$$V\_LIQ = 3.9 / 1000$$

**Figure C.12** Equations for model simulation in STELLA®. Cometabolism of TBF by propane-grown *Graphium* sp. (Filter-attached culture).

The cometabolism of MTBE by propane-grown *Graphium sp.*, in the absence of the substrate, was modeled as shown in Figure C.13. Degradation of 18 and 250  $\mu\text{mol}$  of MTBE was followed with time. Input values for STELLA modeling are summarized in Table C.3. Data was modeled at three different conditions: with constants as determined from kinetic data, adjusting  $k_{\text{max-MTBE}}$ , and adjusting  $K_{\text{s-MTBE}}$ . The best fit, for either low or high MTBE mass, was when  $k_{\text{max}} = 2.7 k_{\text{max}} (\text{lab})$ .

**Table C.3** Parameters used in STELLA modeling for MTBE cometabolism by propane-grown *Graphium sp.* (filter-attached culture)

Estimated from Kinetic Experiments	UNITS
Yield = 0.01455 $k_{\text{max-propane}} = 0.234$ $K_{\text{s-propane}} = 1.07$ $k_{\text{max-MTBE}} = 0.073$ $K_{\text{s-MTBE}} = 5200$	mg dry mass/ $\mu\text{mol}$ propane $\mu\text{mol}$ propane/mg dry mass-h $\mu\text{mol}$ propane /L $\mu\text{mol}$ MTBE/mg dry mass-h $\mu\text{mol}$ MTBE/L
<b>Low MTBE Mass Case</b>  MTBE mass = 18 X = 61.3 $V_{\text{Liq}} = 0.0065$ $V_{\text{Liq}} = 0.1575$ b = 0.0031 (assumed)	$\mu\text{mol}$ mg dry mass L L 1/h
<b>High MTBE Mass Case</b>  MTBE mass = 250 X = 59.3 $V_{\text{Liq}} = 0.0065$ $V_{\text{Liq}} = 0.1575$ b = 0.0031 (assumed)	$\mu\text{mol}$ mg dry mass L L 1/h

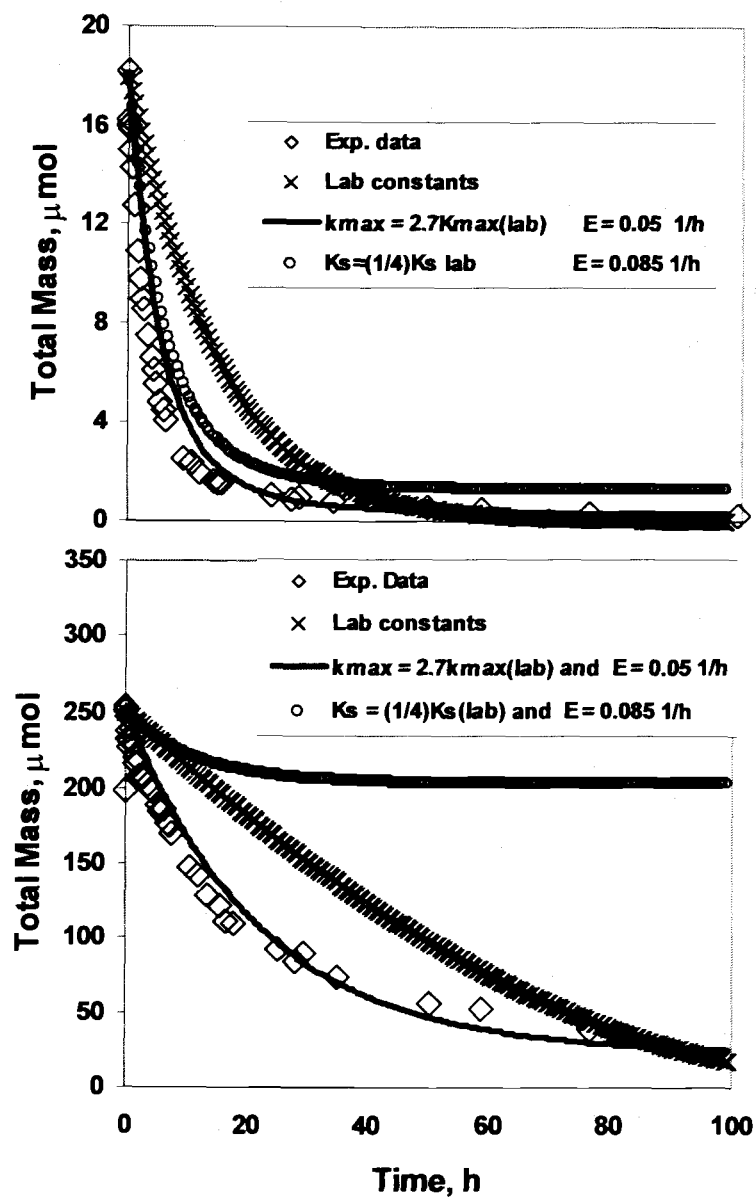


**Figure C.13** Cometabolism of MTBE by propane-grown *Graphium* sp. (filter-attached). MTBE experimental data ( $\diamond$ ), and STELLA modeling for three different cases as listed.

The cometabolism of TBF by propane-grown *Graphium sp.* (filter-attached), in the absence of the substrate, was modeled and results are as shown in Figure C.14. Degradation of 8.6 and 56  $\mu\text{mol}$  of TBF was followed with time. Input values for STELLA modeling are summarized in Table C.4 for these two cases. No adjustment was required, predicted data match experimental data perfectly, at either low or high TBF mass.

**Table C.4** Parameters used in STELLA modeling for TBF cometabolism by propane-grown *Graphium sp.* (filter-attached culture).

Estimated from Kinetic Experiments	UNITS
Yield = 0.01455 $k_{\text{max-propane}} = 0.234$ $K_{s\text{-propane}} = 1.07$ $k_{\text{max-TBF}} = 0.488$ $K_{s\text{-TBF}} = 1970$	mg dry mass/ $\mu\text{mol}$ propane $\mu\text{mol}$ propane/mg dry mass-h $\mu\text{mol}$ propane /L $\mu\text{mol}$ TBF/mg dry mass-h $\mu\text{mol}$ TBF/L
<b>Low TBF Mass Case</b>  TBF mass = 8.6 $X = 41.2$ $V_{\text{Liq}} = 0.0039$ $V_{\text{Liq}} = 0.160$ $b = 0.0031$ (assumed)	$\mu\text{mol}$ mg dry mass L L 1/h
<b>High TBF Mass Case</b>  MTBE mass = 56 $X = 70$ $V_{\text{Liq}} = 0.0065$ $V_{\text{Liq}} = 0.1575$ $b = 0.0031$ (assumed)	$\mu\text{mol}$ mg dry mass L L 1/h



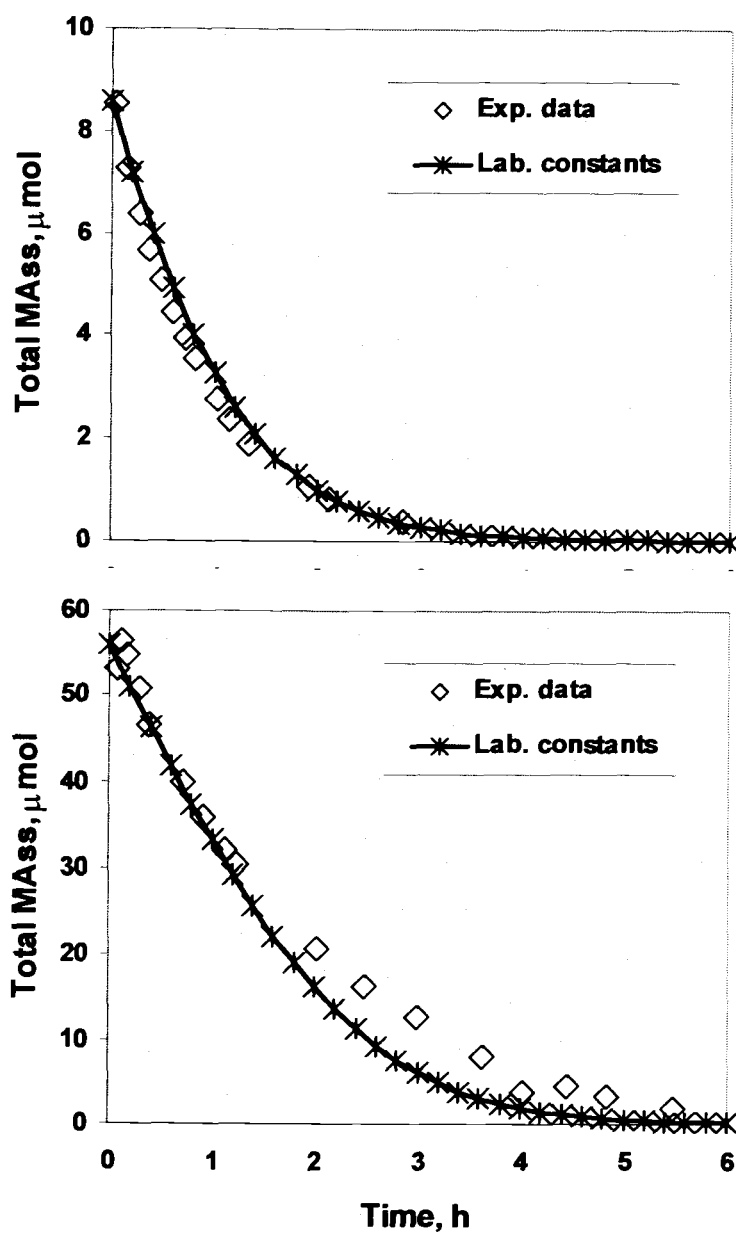


**Figure C.14** Cometabolism of TBF by propane-grown *Graphium* sp. (filter-attached culture). TBF experimental data ( $\diamond$ ), and STELLA modeling with kinetic constants as determined from kinetic experiments.

## Appendix D

### Visual Basic program for the direct linear plot method

#### D.1 Instructions

##### Entering the data:

In the Data sheet

Start in the first row (do not label the columns).

Enter the values for X (Liquid concentration in mg/L) in the first column.

(positive values, the program will make them negative).

Enter the values for Y (rate in  $\mu\text{mol/mg TSS-h}$ ) in the second column.

Make sure there is nothing else in these columns, only your values.

##### Solving:

Click "Solve" to solve and get median values based on sorted results.

The corresponding plot is provided in "Plot" sheet.

##### Results:

In the Results by pairs sheet.

Each row represents a intersection of two equations.

The rows are sorted according to the value of X of this intersection.

The first and second columns are the row number (in Data sheet).

of the data points used for that intersection.

The third column is the value of X.

The fourth column is the value of Y.

In the Results sorted sheet.

Values are treated differently depending on which quadrant the lines crossed

If on first or second quadrant, no treatment is needed.

If on third quadrant, make values positive.

The first column is the value of X.

The second column is the value of Y.

Columns for X and Y have been sorted independently.

**For another analysis:**

Click "Delete data" to erase all values in Data and Results sheets.

As suggestion, keep a file for each analysis.

**Important notes:**

Do not change the names of the sheets or the program will not work.

## D.2 Visual Basic program

```
Option Explicit
Option Base 1
DefDbl A-Z
```

```
Type TypeSolution
    Data1 As Integer
    Data2 As Integer
    X As Double
    Y As Double
End Type
```

```
Private Enum SortConstants
    SortByX
    SortByY
End Enum
```

```
Dim X(), Y()
Dim N As Integer, C As Integer
Dim i As Integer, j As Integer, k As Integer
Dim Solution() As TypeSolution
Dim SwapTemp As TypeSolution
Dim Xmed, Ymed
Dim Xmin(), Xmax()
'Dim Slope(), Intercept()
```

```
Sub Solve()
    Dim Chrt As Chart
    Dim z As Object
    Dim N
    ' GET DATA
    Worksheets("Data").Activate
    If IsEmpty(Cells(1, 1).Value) Then
        MsgBox "No data to analyze", vbInformation
        Exit Sub
    End If
    Do
```

```

k = k + 1
ReDim Preserve X(k), Y(k)
X(k) = -Cells(k, 1).Value
Y(k) = Cells(k, 2).Value
Loop Until IsEmpty(Cells(k + 1, 1).Value)

```

' Number of data pairs and number of solutions (combinations of 2 taken from N)

```

N = k
C = Combinations(N, 2)
ReDim Solution(C)

```

'Set initial limits for plotting

```

ReDim Xmin(N), Xmax(N)
For i = 1 To N
    Xmin(i) = X(i)
    Xmax(i) = 0
Next i

```

' Solve all C systems of equations

```

k = 0
For i = 1 To N - 1
    For j = i + 1 To N
        k = k + 1
        With Solution(k)
            .Data1 = i
            .Data2 = j
            .X = X(i) * X(j) * (Y(i) - Y(j)) / (X(j) * Y(i) - X(i) * Y(j))
            .Y = Y(i) * (1 - .X / X(i))
            'Check limits for plotting
            If .X < Xmin(i) Then Xmin(i) = .X
            If .X < Xmin(j) Then Xmin(j) = .X
            If .X > Xmax(i) Then Xmax(i) = .X
            If .X > Xmax(j) Then Xmax(j) = .X
        End With
    Next j
Next i

```

```
' Sort data by X
SortData SortByX
```

```
' Dump results to "Results by pairs" sheet
Worksheets("Results by pairs").Activate
Worksheets("Results by pairs").Cells.ClearContents
For k = 1 To C
  With Solution(k)
    Cells(k, 1).Formula = .Data1
    Cells(k, 2).Formula = .Data2
    Cells(k, 3).Formula = .X
    Cells(k, 4).Formula = .Y
  End With
Next k
```

```
'Make negative values positive, only if both X and Y are negative
For i = 1 To C
  With Solution(i)
    If .X < 0 And .Y < 0 Then
      .X = -.X
      .Y = -.Y
    End If
  End With
Next i
```

```
'Sort again by X - necessary because sign changes
SortData SortByX
```

```
' Dump results to "Results sorted" worksheet
' Dump first column (X values)
Worksheets("Results sorted").Activate
Worksheets("Results sorted").Cells.ClearContents
For k = 1 To C
  With Solution(k)
    Cells(k, 1).Formula = .X
  End With
Next k
```

```
' Find median value of X
If (C Mod 2) = 0 Then
```

```

'Even number of values, take average...
Xmed = (Solution(C / 2).X + Solution(C / 2 + 1).X) / 2
Else
'Odd number of values, take central one...
Xmed = Solution((C + 1) / 2).X
End If

' Sort data by Y
SortData SortByY

' Dump second column (Y values)
For k = 1 To C
  With Solution(k)
    Cells(k, 2).Formula = .Y
  End With
Next k

' Find median value of Y
If (C Mod 2) = 0 Then
  'Even number of values, take average...
  Ymed = (Solution(C / 2).Y + Solution(C / 2 + 1).Y) / 2
Else
  'Odd number of values, take central one...
  Ymed = Solution((C + 1) / 2).Y
End If

' Display median
MsgBox "Median values are" & vbNewLine & vbNewLine _
  & " X = " & Format$(Xmed) & vbNewLine _
  & " Y = " & Format$(Ymed), vbInformation

'Dump plot information
Sheets("Plot data").Select
Sheets("Plot data").Cells.Clear
Range("A1").Select

'Dump median
Cells(1, 1).Formula = "Median X"
Cells(1, 2).Formula = "Median Y"
Cells(2, 1).Formula = Xmed
Cells(2, 2).Formula = Ymed

```

```

For i = 1 To N
    Cells((i - 1) * 4 + 4, 1).Formula = "Line #" & i
    Cells((i - 1) * 4 + 4, 2).Formula = "Slope"
    Cells((i - 1) * 4 + 4, 3).Formula = "Intercept"
    Cells((i - 1) * 4 + 4, 4).Formula = "X1 & X2"
    Cells((i - 1) * 4 + 4, 5).Formula = "Y1 & Y2"
    Cells((i - 1) * 4 + 5, 2).Formula = -Y(i) / X(i)
    Cells((i - 1) * 4 + 5, 3).Formula = Y(i)
    Cells((i - 1) * 4 + 5, 4).Formula = Xmin(i)
    Cells((i - 1) * 4 + 6, 4).Formula = Xmax(i)
    Cells((i - 1) * 4 + 5, 5).FormulaR1C1 = "=RC[-3]*RC[-1]+RC[-2]"
    Cells((i - 1) * 4 + 6, 5).FormulaR1C1 = "=R[-1]C[-3]*RC[-1]+R[-1]C[-2]"
Next i

```

'Original data points, for plot...

```

Sheets("Data").Select
Range("A1").Select
For i = 1 To N
    Cells(i, 4).Formula = X(i)
    Cells(i, 5).Formula = 0
    Cells(i, 7).Formula = 0
    Cells(i, 8).Formula = Y(i)
Next i

```

'Create chart

```

Charts.Add
' Set Chrt = Charts(ActiveChart.Name)

```

With ActiveChart

.ChartType = xlXYScatter

.SetSourceData Source:=Sheets("Plot Data").Range("A2:B2"),

PlotBy:=xlColumns

.HasTitle = False

.HasLegend = False

.ApplyDataLabels Type:=xlDataLabelsShowNone, LegendKey:=False

.Location Where:=xlLocationAsObject, Name:="Plot"

End With

With ActiveChart.Axes(xlCategory)

.HasTitle = True

.AxisTitle.Characters.Text = "S<sub>L</sub>, mg/L"

.HasMajorGridlines = False



```
.HasMinorGridlines = False
End With
```

```
With ActiveChart.Axes(xlValue)
    .HasTitle = True
    .AxisTitle.Characters.Text = "v,  $\mu$ mol/mg TSS-h"
    .HasMajorGridlines = False
    .HasMinorGridlines = False
End With
```

```
With ActiveChart.PlotArea
    .Border.LineStyle = xlLineStyleNone
    .Interior.ColorIndex = 2
End With
```

```
ActiveChart.ChartArea.Border.LineStyle = xlLineStyleNone
```

```
ActiveChart.SeriesCollection(1).Delete
```

```
' Series for median
```

```
'Series for solution points
```

```
ActiveChart.SeriesCollection.Add _
    Source:=Worksheets("Results by pairs").Range("C1:D" & C), _
    rowcol:=xlColumns, serieslabels:=False, _
    categorylabels:=True, Replace:=False
```

```
With ActiveChart.SeriesCollection(1)
```

```
.Border.LineStyle = xlNone
.MarkerBackgroundColorIndex = 2
.MarkerForegroundColorIndex = 1
.MarkerStyle = xlCircle
.MarkerSize = 6
.Shadow = False
```

```
End With
```

```
ActiveChart.SeriesCollection.Add _
    Source:=Worksheets("Plot data").Range("A2:B2"), _
    rowcol:=xlColumns, serieslabels:=False, _
    categorylabels:=True, Replace:=False
```

```
With ActiveChart.SeriesCollection(2)
```

```
.Border.LineStyle = xlNone
.MarkerBackgroundColorIndex = 32
.MarkerForegroundColorIndex = 1
.MarkerStyle = xlCircle
```

```
.MarkerSize = 8
.Shadow = False
End With
```

```
ActiveChart.SeriesCollection.Add _
    Source:=Worksheets("Data").Range("D1:E" & N), _
    rowcol:=xlColumns, serieslabels:=False, _
    categorylabels:=True, Replace:=False
With ActiveChart.SeriesCollection(3)
    .Border.LineStyle = xlNone
    .MarkerBackgroundColorIndex = 2
    .MarkerForegroundColorIndex = 1
    .MarkerStyle = xlMarkerStyleDiamond
    .MarkerSize = 6
    .Shadow = False
End With
```

```
ActiveChart.SeriesCollection.Add _
    Source:=Worksheets("Data").Range("G1:H" & N), _
    rowcol:=xlColumns, serieslabels:=False, _
    categorylabels:=True, Replace:=False
With ActiveChart.SeriesCollection(4)
    .Border.LineStyle = xlNone
    .MarkerBackgroundColorIndex = 2
    .MarkerForegroundColorIndex = 1
    .MarkerStyle = xlMarkerStyleDiamond
    .MarkerSize = 6
    .Shadow = False
End With
```

```
' Add lines
For j = 1 To N
    ActiveChart.SeriesCollection.Add _
        Source:=Worksheets("Plot data").Range("D" & ((j - 1) * 4 + 5) & "E" &
        ((j - 1) * 4 + 6)), _
        rowcol:=xlColumns, serieslabels:=False, _
        categorylabels:=True, Replace:=False
    With ActiveChart.SeriesCollection(j + 4)
        .Border.ColorIndex = 1
        .Border.Weight = xlThin
        .Border.LineStyle = xlContinuous
```

```

        .MarkerStyle = xlNone
        .Smooth = False
        .Shadow = False
    End With
Next j
End Sub

```

```

Public Sub DeleteAll()
    Dim Obj As Object
    With Worksheets("Results by pairs")
        .Activate
        .Cells.ClearContents
        .Cells(1, 1).Select
    End With
    With Worksheets("Results sorted")
        .Activate
        .Cells.ClearContents
        .Cells(1, 1).Select
    End With
    With Worksheets("Data")
        .Activate
        .Cells.ClearContents
        .Cells(1, 1).Select
    End With
    With Worksheets("Plot data")
        .Activate
        .Cells.ClearContents
        .Cells(1, 1).Select
    End With
    'Erase charts, if any
    For Each Obj In Charts
        Obj.Delete
    Next
    Worksheets("Instructions").Activate
    MsgBox "All data and results have been erased"
End Sub

```

```

Private Sub SortData(SortBy As SortConstants)
    Select Case SortBy
        Case SortByX

```

```
For i = 1 To C - 1
  For j = i + 1 To C
    If Solution(j).X < Solution(i).X Then
      SwapTemp = Solution(i)
      Solution(i) = Solution(j)
      Solution(j) = SwapTemp
    End If
  Next j
Next i
Case SortByY
  For i = 1 To C - 1
    For j = i + 1 To C
      If Solution(j).Y < Solution(i).Y Then
        SwapTemp = Solution(i)
        Solution(i) = Solution(j)
        Solution(j) = SwapTemp
      End If
    Next j
  Next i
End Select
End Sub
```

### D.3 Example

TBF kinetic data (see Table D.1), for the propane-grown filter-attached *Graphium sp.*, is used to illustrate an example of estimation of the kinetic constants by the direct linear plot method.

**Table D.1** TBF experimental data  
(filter-attached *Graphium sp.*)

ID	Biomass (mg)	C <sub>liq</sub> (mg/L)	RATE ( $\mu\text{mol/mg-h}$ )
F1	10.3	14.149	0.0298
F2	11.5	27.495	0.0581
F3	23.8	55.932	0.0985
F4	38	77.644	0.1236
F5	41.2	112.29	0.1720
F6	57.8	153.01	0.2146
F7	70.9	234.83	0.2941
F8	67.3	376.77	0.2907
F9	63.8	502.39	0.3723
F10	70	576.79	0.3455

Pairs of data are plotted, aqueous concentration (x,0) and initial degradation rate (0,y) , joined with a straight line and extrapolated. Each line is represented by an equation of a line ( $y = mx + b$ ), slope and intercept for each line are summarized in Table D.2.

Coordinates are obtained, solving simultaneous equations, for any two lines that intersect. Results obtained are summarized in Table D.3. Line

# represents the line numbers where each pair of lines crossed, and x and y are the coordinates for that intersection.

**Table D.2** Slope and intercept for TBF data

Line #	Slope	Intercept
1	0.00211	0.02981
2	0.00211	0.05812
3	0.00176	0.09853
4	0.00159	0.12365
5	0.00153	0.17199
6	0.00140	0.21455
7	0.00125	0.29412
8	0.00077	0.29068
9	0.00074	0.37230
10	0.00060	0.34547

Treat the data accordingly if negative values, second or third quadrant, (Cornish-Bowden, 1995). Arrange data in increasing order, independently. The median (row # 23) of columns 3 and 4 represents the best estimates of the corresponding kinetic constant as shown in Table D.4.

**Table D.3** Results by pairs in the direct linear plot for TBF

Line #		Coordinates		Line #		Coordinates	
		x	y			x	Y
1	2	-4095	-8.598	4	10	223.26	0.4792
9	10	-188.8	0.2324	2	9	228.87	0.5419
7	8	-7.155	0.2852	6	9	238.6	0.5491
7	10	78.572	0.3925	1	5	247.18	0.5506
2	3	114.76	0.3007	1	9	250.75	0.5581
6	8	120.7	0.3838	5	9	253.35	0.5601
2	4	125.69	0.3238	1	6	262.16	0.5822
3	4	148.45	0.3601	3	9	268.24	0.5711
7	9	152.88	0.4856	2	7	273.99	0.6373
5	8	156.12	0.4111	4	9	292.04	0.5887
6	10	162.98	0.4431	1	7	309.33	0.6815
2	8	173.25	0.4243	8	10	317.53	0.5357
1	4	182.41	0.4141	3	5	319.43	0.6613
5	10	185.98	0.4569	3	6	322.77	0.6671
2	10	189.68	0.4591	5	6	328.69	0.6754
3	8	194.05	0.4404	3	7	384.11	0.7752
1	8	195.34	0.4414	5	7	437.38	0.8419
2	5	195.62	0.4716	4	6	477.75	0.8845
1	3	199.05	0.4492	4	7	501.36	0.9221
4	8	203.45	0.4476	6	7	531.36	0.9596
1	10	209.33	0.4708	4	5	795.2	1.39
3	10	212.38	0.4727	8	9	2682	2.3598
2	6	219.83	0.5228				

**Table D.4** Sorted values and best estimates of  $k_{max}$  and  $K_s$  for the cometabolism of TBF by *Graphium* sp.

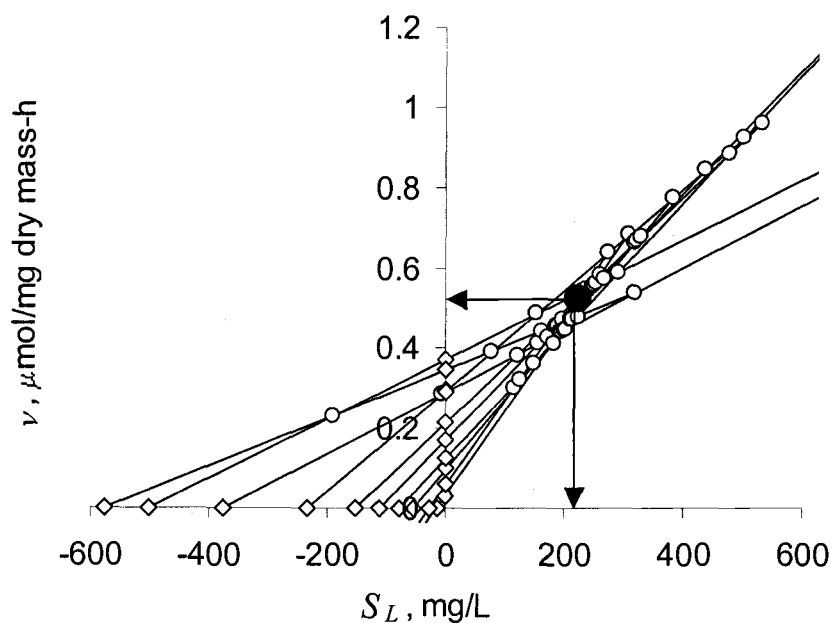
Order	$K_s$ (mg TBF/L)	$k_{max}$ ( $\mu$ mol/mg-h)
1	-188.829	0.232368
2	-7.15451	0.285156
3	78.5721	0.300701
4	114.7598	0.32381
5	120.6954	0.360051
6	125.6924	0.383792
7	148.45	0.392526
8	152.8795	0.411123
9	156.1221	0.414135
10	162.9778	0.424337
11	173.2495	0.440386
12	182.4121	0.441384
13	185.9815	0.443081
14	189.6837	0.447635
15	194.0517	0.449198
16	195.3449	0.456859
17	195.6158	0.459076
18	199.0539	0.470841
19	203.4484	0.471615
20	209.3262	0.472668
21	212.3764	0.479187
22	219.8292	0.485594
<b>23</b>	<b>223.2614</b>	<b>0.522798</b>
24	228.8691	0.53565



Table D.4 Continued.

Order	$K_s$ (mg TBF/L)	$k_{max}$ ( $\mu\text{mol/mg-h}$ )
25	238.5988	0.541907
26	247.1809	0.549117
27	250.7537	0.550597
28	253.353	0.558125
29	262.1574	0.560051
30	268.2426	0.571085
31	273.9863	0.582151
32	292.0447	0.588724
33	309.3347	0.637276
34	317.5318	0.661263
35	319.4319	0.667139
36	322.7672	0.675445
37	328.6911	0.681549
38	384.1083	0.775201
39	437.3773	0.841919
40	477.7512	0.884459
41	501.359	0.922054
42	531.3579	0.959626
43	795.2018	1.389994
44	2681.964	2.359797
45	4094.977	8.597914

Figure D.1 illustrates the results for the direct linear method.



**Figure D.1** Direct linear plot method to determine  $k_{max}$  and  $K_s$  for TBF. Experimental data is plotted by pairs (◇), joined and extrapolated. The small open symbols (○) at the intersection of two lines represents a unique pair of  $k_{max}$  and  $K_s$  that satisfies those two sets of observations. The solid circle (●) represents the median values as the best estimates for  $k_{max}$  and  $K_s$ .

## Appendix E

### Overall studies for propane-grown filter-attached *Graphium sp.* culture

#### E.1 Complete MTBE degradation under aerobic conditions

Degradation of MTBE was followed to completion to see if Drinking Water Advisory Level of 40  $\mu\text{g/L}$  was met. Duplicate bottles, M6 and M7 were set to follow the degradation of 2.5  $\mu\text{mol}$  MTBE by *Graphium sp.* (83 mg dry mass). The corresponding concentration in the liquid phase was estimated to be 25 mg/L. Propane was added to the bottle to enhance the continuous degradation of MTBE and its metabolites, TBF and TBA. Oxygen level was measured to ensure aerobic conditions and pure oxygen was added as needed. An extra bottle, M1 (66 mg dry mass), set at the same conditions was also followed with out the addition of propane to compare the results to the ones enhanced with propane.

Figure E.1 illustrates the results for all three cases. Propane was added in different amounts at different times as shown in table D.1The addition of propane clearly inhibited the degradation of MTBE on bottles M6 and M7. For bottle M1, where propane was not added, liquid concentration of MTBE was taken down to 185  $\mu\text{g/L}$  whereas for bottles M6 and M7 MTBE was degraded to completion. TBF produced from MTBE oxidation was completely degraded in all three bottles with the corresponding

accumulation of TBA. TBA was further oxidized with greater % degradation in bottles M6 and M7 than in M1.

Metabolism of propane and cometabolism of MTBE and metabolites requires oxygen. Oxygen was depleted at 95 hours of initiated the reaction because of metabolism of propane and cometabolism process. It was observed that propane oxidation stopped at hour 95 but it was reinitiated after addition of pure oxygen.

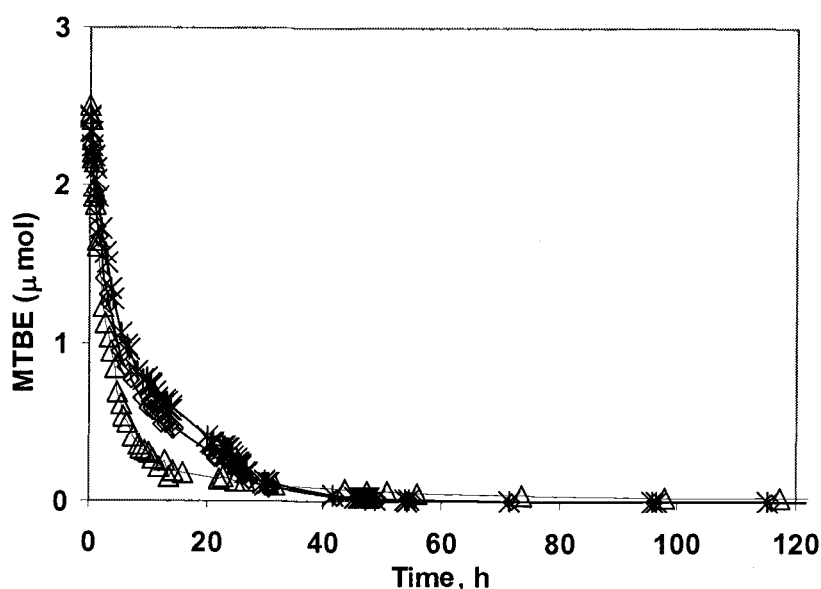


**Figure E.1** Degradation of MTBE in the absence M1 ( $\Delta$ ), and presence of propane M6 (\*) and M7 ( $\diamond$ ) under aerobic conditions by *Graphium sp.*

Figure E.2 illustrates the behavior of all compounds in the killed control bottle. No significant degradation of propane, MTBE, and TBA took place. Again a slight decrease was observed for TBF causing TBA to accumulate in the system as expected, due to abiotic hydrolysis.

**Table E.1** Propane and O<sub>2</sub> added to bottles M6 and M7

Time (h)	Propane ( $\mu$ l)	Pure O <sub>2</sub> (ml)
10	50	-----
13	50	-----
14	1000	-----
21	500	-----
23	50	-----
26	50	-----
30	1000	-----
46	100	-----
50	500	-----
55	1000	-----
72	1000	-----
95	-----	20
96	-----	20

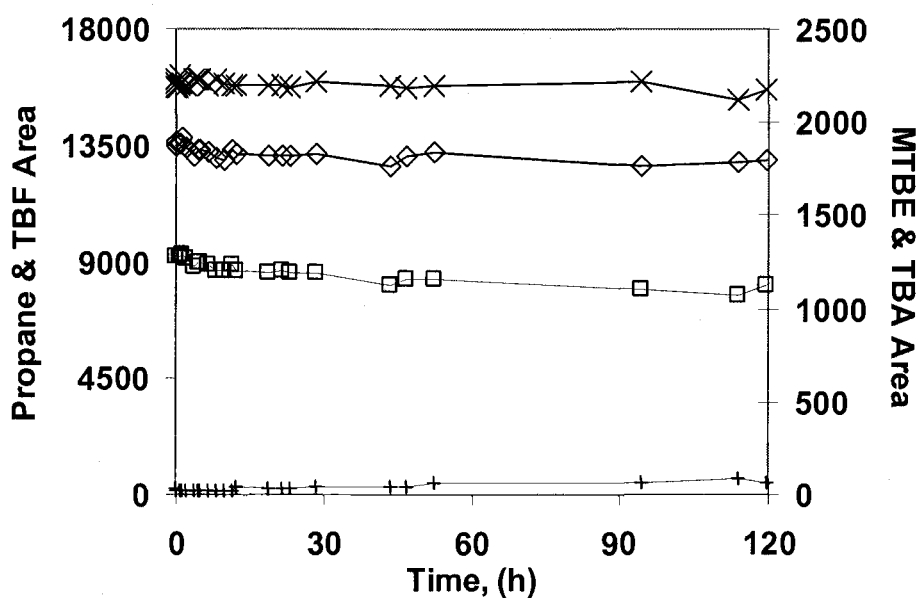


**Figure E.2** *Graphium* sp. killed control bottle. Degradation of propane (x), MTBE (◇), TBF (□), and TBA (+) in killed control bottle by *Graphium* sp. (75 mg dry mass).

## E.2 Acetylene influence on the degradation of propane, MTBE, and TBF

Experiments were performed to evaluate the influence of Acetylene ( $C_2H_2$ ) on the degradation of propane, MTBE and TBF. In all cases harvested propane-grown *Graphium sp* biomass was tested in the absence and presence of  $C_2H_2$  (0.5 % v/v).

### Acetylene influence on propane degradation

Figures E.3, E.4, and E.5 shows reversible inhibition of acetylene on propane degradation. Once  $C_2H_2$  is removed and propane is readded again, *Graphium sp.* recovered propane oxidation activity.

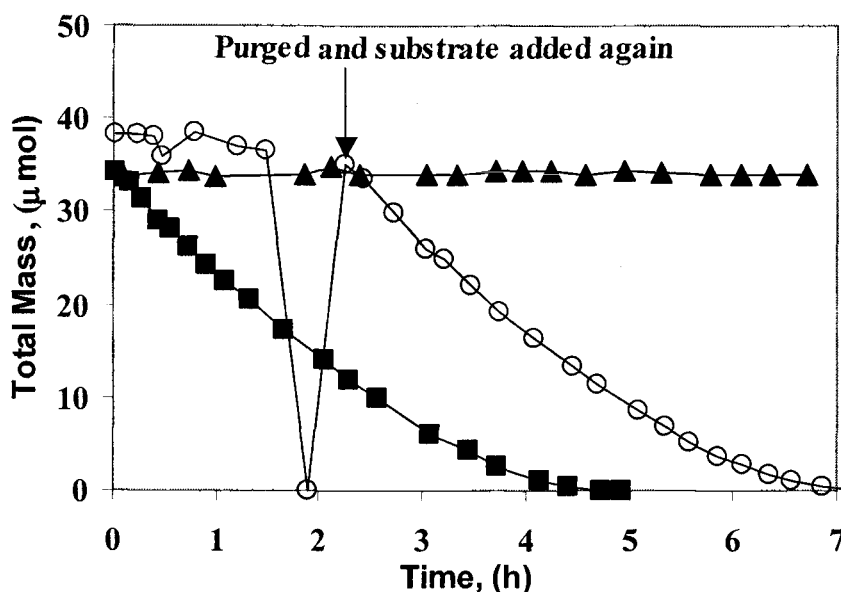


**Figure E.3** Inhibition of propane oxidation by acetylene. *Graphium sp.* (40 mg dry mass) was incubated with propane in the absence (■) and presence of  $C_2H_2$  (○). Culture recovered oxidation activity after  $C_2H_2$  removed. No degradation in killed control (▲)

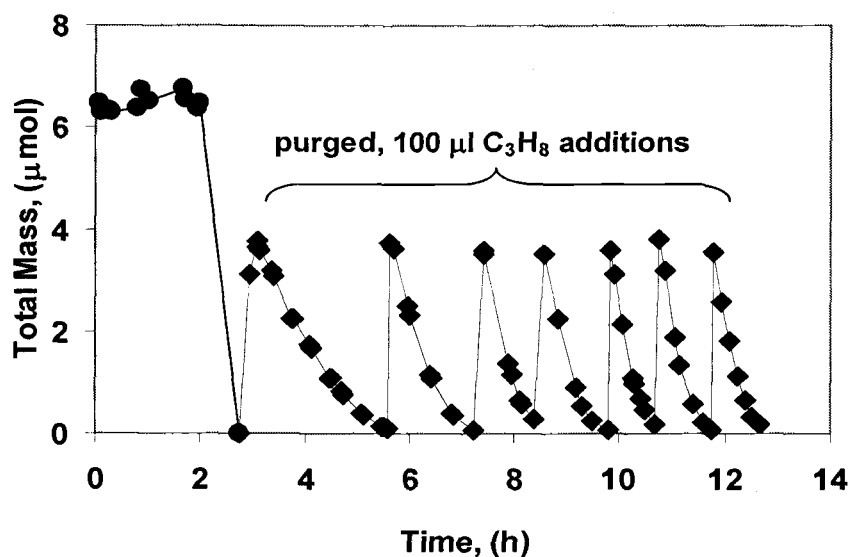


**Figure E.4** Inhibition on propane degradation by acetylene. *Graphium* sp. (34.3 mg dry mass) incubated with propane +  $\text{C}_2\text{H}_2$  (●) and after  $\text{C}_2\text{H}_2$  removed and new propane additions (◆)

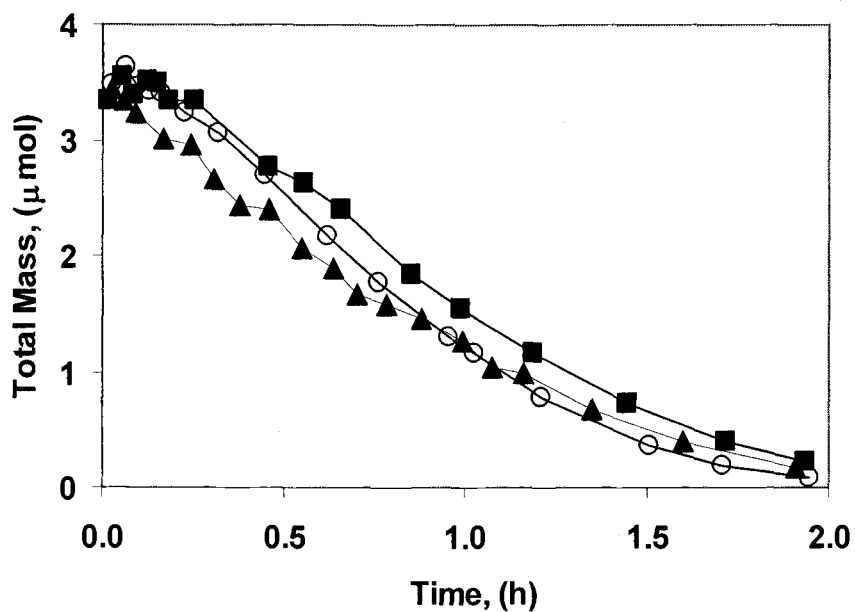


**Figure E.5** Inhibition of propane degradation by acetylene. *Graphium* sp. (30 mg dry mass) incubated with propane in the absence (▲) and presence of  $\text{C}_2\text{H}_2$ . Propane oxidation after  $\text{C}_2\text{H}_2$  removed and propane readdded: Rep 1 (○), and Rep 2 (■)

### Acetylene influence on MTBE transformation

Figure E.6, shows inhibition of acetylene on MTBE degradation

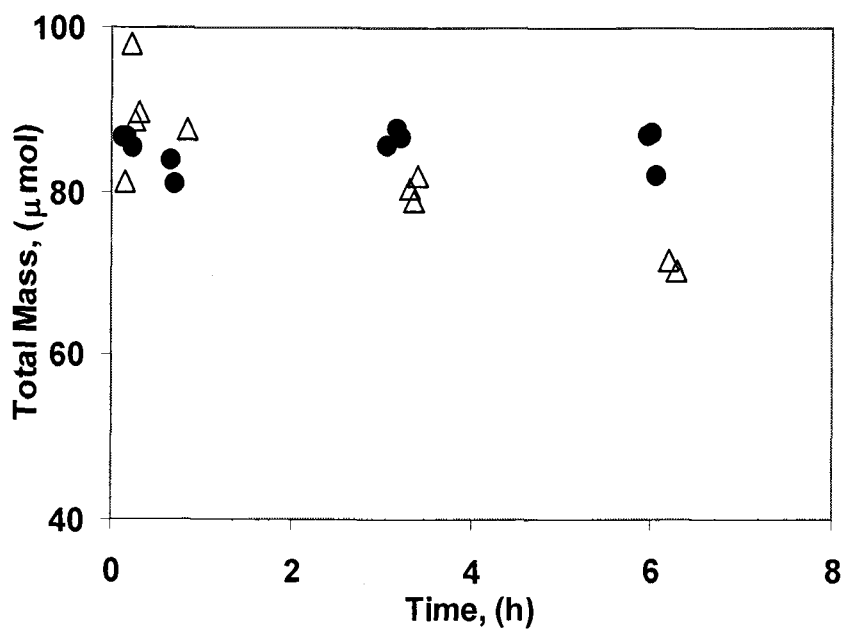


**Figure E.6** Acetylene influence on MTBE degradation. Propane grown filter-attached *Graphium sp.* (50 mg dry mass) were incubated with MTBE in the presence (●) and absence (△) of Acetylene.



### Acetylene influence on TBF transformation

Figure E.7 shows no inhibition of acetylene on TBF transformation

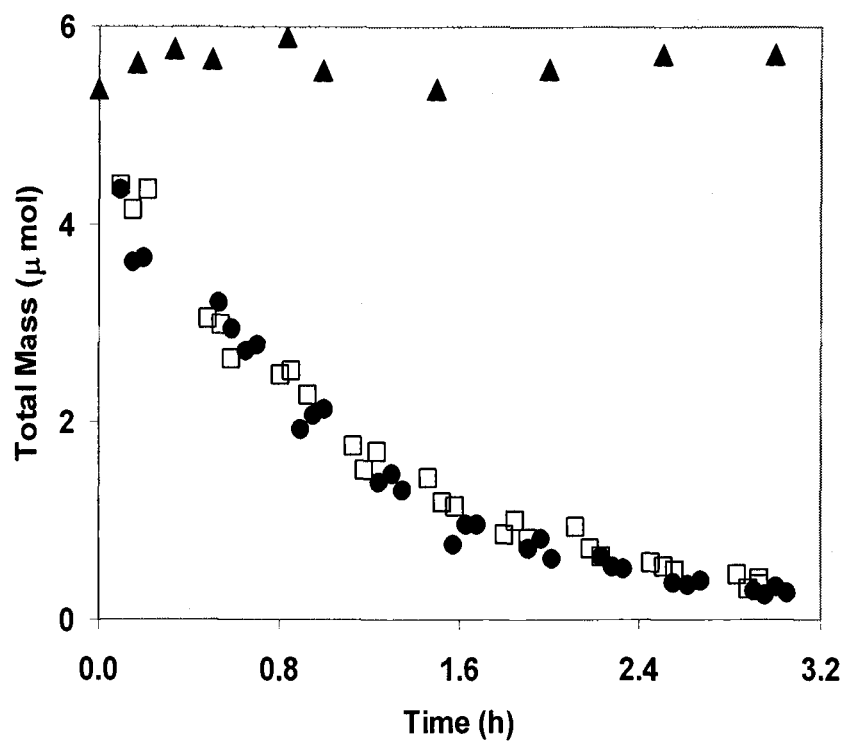


**Figure E.7** Acetylene influence on TBF degradation. *Graphium* sp. (115 mg dry mass) was incubated with TBF in the presence (□) and absence (●) of Acetylene. No degradation in killed control (▲).

### TBF influence on propane degradation

Experiments were performed to evaluate the influence of TBF on the degradation of propane. Figure E.8 shows inhibition of propane oxidation due to the presence of TBF. Once TBF is degraded to a certain level the oxidation of propane takes place to completion.

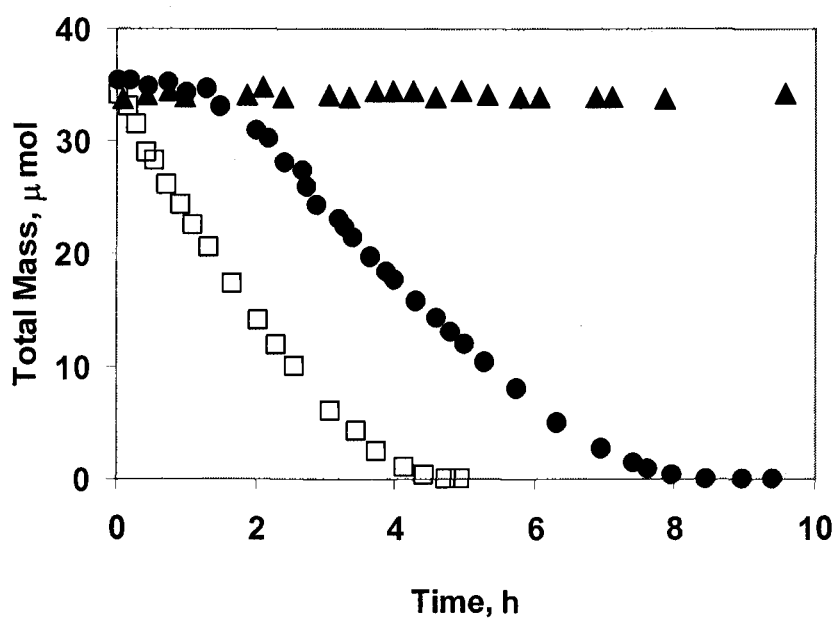


**Figure E.8** TBF influence on propane oxidation. *Graphium* sp. (40 mg dry mass) was incubated with propane in the presence (●) and absence (□) of TBF (25  $\mu\text{mol}$ ) No degradation observed in the killed control bottle (▲).

### E.3 Degradation under anaerobic conditions

To create anaerobic conditions crimp-sealed bottles, containing propane-grown filter attached culture, were purged with nitrogen treated in a tube furnace at 600 °C for 45 minutes. Headspace samples were analyzed by GC-TCD to confirm that anaerobic conditions were established. Chemicals were added to initiate the reaction. Figure E.9 illustrates the influence of the absence of oxygen in the degradation of all five compounds

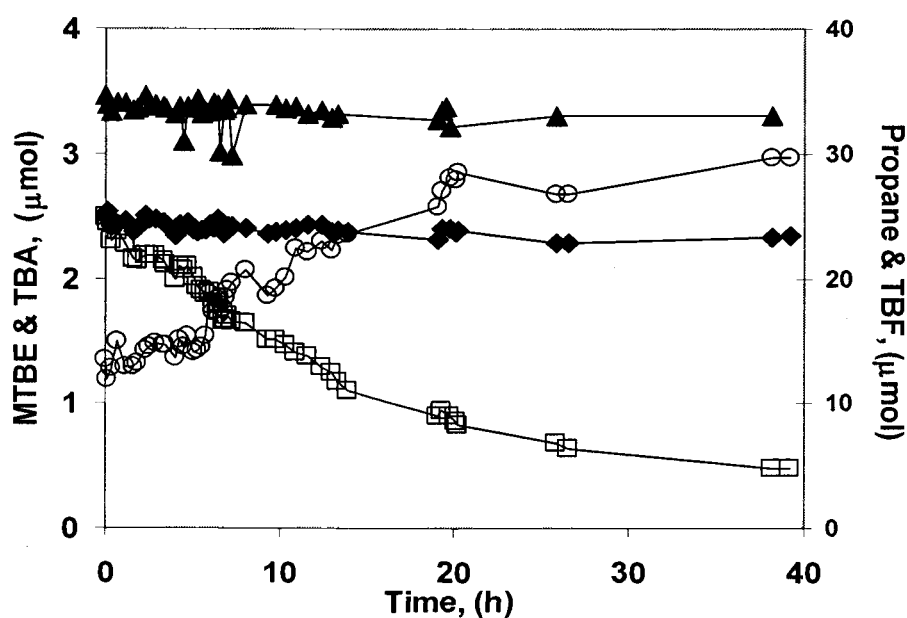


**Figure E.9** Degradation of propane (▲), MTBE (◆), TBF (□), and TBA (○) under anaerobic conditions by *Graphium sp.* (40 mg dry mass)

## E.4 Degradation under anaerobic/aerobic conditions

Anaerobic degradation was followed four hours as described above. After that bottles were opened and equilibrated with the ambient atmosphere under sterile conditions, in order to re-establish aerobic conditions, and recapped again. Headspace samples were analyzed by GC-TCD to confirm aerobic conditions. Substrate and co-substrates were reinjected and their consumption was followed over time to quantitate the recovery of enzyme activity. (see Figure E.10)

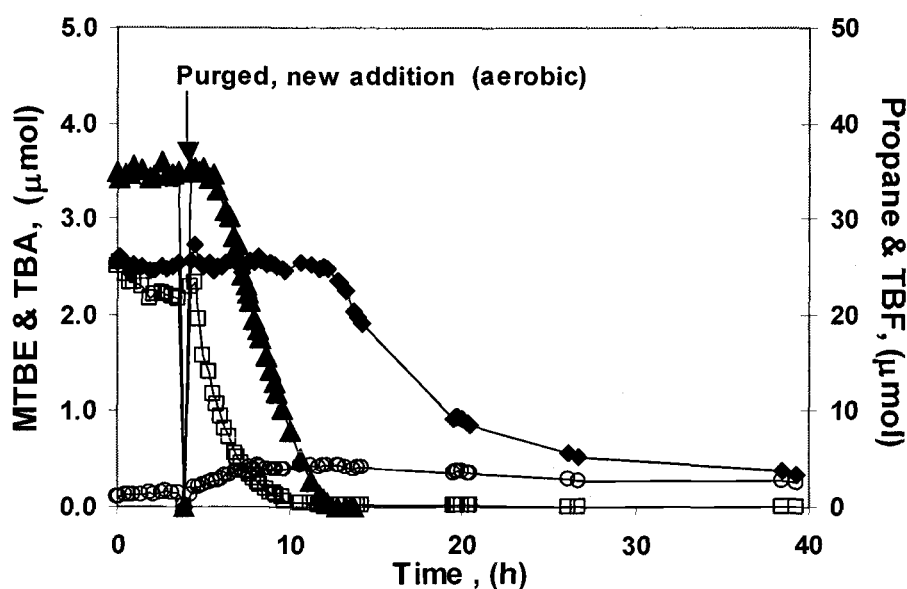


**Figure E.10** Degradation of propane (▲), MTBE (◆), TBF (◊), and TBA (○) under anaerobic/aerobic conditions by *Graphium* sp. (44 mg dry mass).

Figure E.11 illustrates that no significant degradation of propane, MTBE, and TBA took place in the killed control bottle. A slight decrease was

observed on TBF with its corresponding accumulation of TBA, mainly due to abiotic TBF hydrolysis.

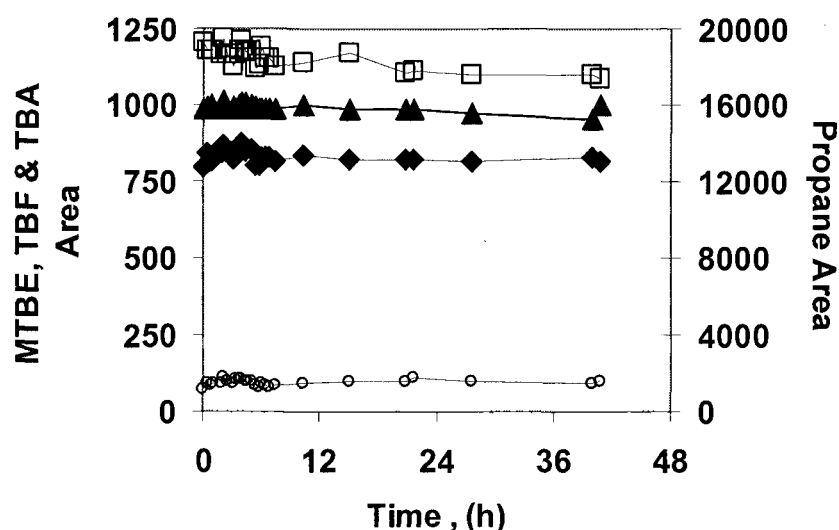


**Figure E.11** Degradation of propane (▲), MTBE (◆), TBF (□), and TBA (○) in killed control bottle by *Graphium* sp. (44 mg dry mass).

## E.5 Estimation of TBA degradation rate

An experimental set-up of eight bottles was designed to follow TBA degradation in the liquid phase for a single initial concentration in all bottles. Three filters with harvested mycelia were incubated in each experimental bottle and 10  $\mu\text{L}$  of 0.116  $\mu\text{mol}/\mu\text{L}$  TBA stock solution were added to crimp-sealed bottles. The resulting initial concentration of TBA was calculated to be 25 mg/L based on an estimation of the liquid contained in the filters.

The bottles were equilibrated for one hour. Filters were removed from the experimental bottle and centrifuged to collect all liquid samples. Liquid samples were filtered to removed biomass present and 2  $\mu$ l were directly injected into the gas chromatogram. The bottles were sacrificed and analyzed over a period of 48 hours. Bottle A8 was incubated in the presence of acetylene (0.5 % v/v) No significant change in concentration was observed. Table E.2 summarizes the experimental data.

**Table E.2** TBA Kinetics experimental data by liquid sample analysis

Bottle ID	Biomass (mg)	Time (h)	FID AREA
A1	47	0	2.85E+06
A2	45	3	2.74E+06
A3	43	6.5	3.14E+06
A4	35	9	2.92E+06
A5	38	12	2.68E+06
A6	37	25	2.63E+06
A7	35	48	2.68E+06
A8	35	48	3.42E+06

TBA oxidation rates were estimated from experiments originally designed for characterization of TBF degradation. Because of the rapid TBF degradation, large amounts of TBA accumulated and were detectable in headspace samples. An approximate degradation rate was estimated from the slope of each of the three lines as shown in Figure E.12 and summarized in Table E.3.

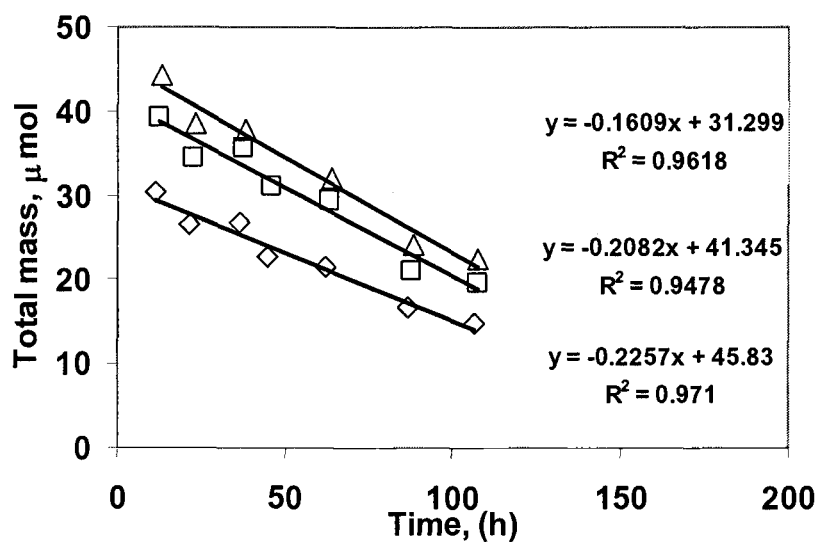


**Figure E.12** TBA degradation from TBF bottles by *Graphium* sp F8( $\diamond$ ), F9( $\square$ ) and F10( $\triangle$ ).

**Table E.3** TBA degradation rate from TBF experimental bottles

Bottle ID	Biomass (mg)	Slope ( $\mu\text{mol/h}$ )	Rate ( $\mu\text{mol/mg-h}$ )
F8	67	0.161	0.0024
F9	64	0.208	0.0033
F10	70	0.226	0.0032

An approximate TBA degradation rate of  $0.003 \pm 0.0005 \mu\text{mol/mg dry mass-h}$  was estimated from these TBF degradation experiments.

## E.6 Estimation of kinetic constants for propane-grown filter-attached *Graphium sp.*

Tables E.4, E.5, and E.6 summarize the experimental data for propane, MTBE, and TBF, respectively.

**Table E.4** Propane experimental data

ID	Biomass (mg)	C <sub>liq</sub> (μg/L)	Rate (μmol/mg-h)
P1	38.0	75.75	0.2666
P2	59.1	168.23	0.3205
P3	11.3	8.153	0.0161
P4	20.9	15.29	0.0598
P5	35.9	33.55	0.1183
P6	39.0	327.1	0.1745
P7	69.4	489.43	0.1902
P8	25.8	7.55	0.0245
P9	34.4	32.57	0.0870
P10	47.5	83.65	0.1621
P11	64.4	178.43	0.2041
P12	78.1	10.98	0.0278
P13	78.1	15.66	0.0326
P14	54.8	93.84	0.0810
P15	73.6	190.6	0.1159
P16	103.5	376.3	0.140
P17	105.0	589.23	0.163
P18	39.9	319.57	0.2617
P19	40.5	330.82	0.2614
P20	51.1	33.80	0.0848
P21	51.1	33.2	0.0891
P22	29.2	31.55	0.0759
P23	32.5	34.82	0.0767
P24	29.1	34.23	0.0713



**Table E.5** MTBE experimental data

ID	Biomass (mg)	C <sub>liq</sub> (mg/L)	Rate ( $\mu$ mol/mg-h)
M1	12.8	30.3	0.0084
M2	33.3	57.2	0.0109
M3	45.5	84.03	0.0166
M4	56.7	158.9	0.0298
M5	66.3	110.4	0.0222
M6	25.1	313.9	0.245
M7	35.1	688.8	0.0435
M8	51	1150.4	0.0549
M9	60.4	1526.1	0.0598
M10	50.8	333.5	0.0221
M11	59.4	669.3	0.0385
M12	49.5	1087.2	0.0614
M13	61.4	1399.3	0.0595
M14	45.8	1718.2	0.0609
M15	90.9	20.63	0.0017
M16	89	38.54	0.0036
M17	100.5	76.17	0.0055
M18	94.2	114.34	0.0096
M19	83.4	157.8	0.0125
M20	89.3	1006	0.0508
M21	91.3	1865.5	0.0409

**Table E.6** TBF experimental data

ID	Biomass (mg)	C <sub>liq</sub> (mg/L)	RATE ( $\mu$ mol/mg-h)
F1	10.3	14.149	0.0298
F2	11.5	27.495	0.0581
F3	23.8	55.932	0.0985
F4	38	77.644	0.1236
F5	41.2	112.29	0.1720
F6	57.8	153.01	0.2146
F7	70.9	234.83	0.2941
F8	67.3	376.77	0.2907
F9	63.8	502.39	0.3723
F10	70	576.79	0.3455

### Non-linear least squares regression (NLSR) analysis

The initial degradation rate ( $dM/dt$ ), was measured experimentally at different substrate concentration, and the two unknowns ( $k_{max}$  and  $K_s$ ) were determined by fitting Equation 3.1 to the experimental data with the statistical software SPLUS (Mathsoft Inc., Cambridge, MA). The initial entry values of the kinetic constants,  $k_{max}$  and  $K_s$ , for the NLSR analysis, were obtained visually from initial rate versus concentration plots.

a) Propane Metabolism. Experimental data was analyzed for all experiments as a whole set and for each single experiment and then averaged. Estimated kinetic constants are summarized in Table E.7.

**Table E.7** Kinetic constants for propane metabolism with their 95% C.I. by NLSR

Data set	$k_{max}$ $\mu\text{mol/mg dry mass-h}$	$K_s$ $\mu\text{g/L}$
1	0.369 ( $\pm$ 0.057)	81.7 ( $\pm$ 29.9)
2	0.215 ( $\pm$ 0.018)	37.7 ( $\pm$ 14.2)
3	0.185 ( $\pm$ 0.13)	106.6 ( $\pm$ 24.7)
Whole set	0.234 ( $\pm$ 0.029)	47.3 ( $\pm$ 19.7)
Average	0.256 ( $\pm$ 0.0294)	75.3 ( $\pm$ 22.9)
STDEV	0.0978 ( $\pm$ 0.0239)	34.9 ( $\pm$ 8.0)

- b) MTBE cometabolism. Experimental data from all experiments was analyzed as a whole set, and for each single experiment and then averaged, as shown in Table E.8.

**Table E.8** Kinetic constants for MTBE cometabolism with their 95% C.I. by NLSR

Data set	$k_{max}$ $\mu\text{mol/mg dry mass-h}$	$K_s$ $\text{mg/L}$
1	0.10 ( $\pm$ 0.012)	963 ( $\pm$ 245)
2	0.074 ( $\pm$ 0.009)	374 ( $\pm$ 133)
3	0.06 ( $\pm$ 0.011)	488 ( $\pm$ 248)
Whole set	0.0725 ( $\pm$ 0.007 )	458 ( $\pm$ 128)
Average	0.0766 ( $\pm$ 0.01)	571 ( $\pm$ 188)
STDEV	0.0168 ( $\pm$ 0.002)	265.8 ( $\pm$ 67)

- c) TBF cometabolism. Experimental data was analyzed as a whole set, as shown in Table E.9.

**Table E.9** Kinetic constants for TBF cometabolism with their 95% C.I. by NLSR

$k_{max}$ $\mu\text{mol/mg dry mass-h}$	$K_s$ $\text{mg/L}$
0.488 ( $\pm$ 0.034)	202 ( $\pm$ 34)

### Lineweaver-Burk reciprocal plot.

Equation 3.2, (where  $v$  is the substrate degradation rate and  $S_L$  is the aqueous substrate concentration) was used to estimate  $K_S / k_{max}$  as slope and  $1/k_{max}$  as the y-intercept of a plot of  $1/v$  versus  $1/S_L$ .

a) Propane Metabolism. Experimental data was analyzed for all experiments as a whole set and for each single experiment and then averaged. Estimated kinetic constants are summarized in Table E.10.

**Table E.10** Kinetic constants for propane metabolism by reciprocal plot

DATA SET	Slope ( $\mu\text{mol/L-h}$ ) <sup>-1</sup>	intercept mg-h/ $\mu\text{mol}$	$k_{max}$ $\mu\text{mol/mg-h}$	$K_s$	
				$\mu\text{g/L}$	$\mu\text{mol/L}$
A	498.91	4.78	0.209	104.37	2.37
B	278.03	3.79	0.264	73.36	1.66
C	336.53	6.98	0.143	48.21	1.09
D	327.4	2.858	0.350	114.56	2.60
Whole set	357.8	2.955	0.338	121.08	2.75
		Average=	0.242	85.126	1.930
		STDEV =	0.087	30.208	0.685

b) MTBE cometabolism. Experimental data from all experiments was analyzed for each single experiment, as a whole set, and then averaged, as shown in Table E.11

**Table E.11** Kinetic constants for MTBE cometabolism by reciprocal plot.

DATA SET	Slope ( $\mu\text{mol/L-h}$ ) <sup>-1</sup>	intercept mg-h/ $\mu\text{mol}$	$k_{max}$ $\mu\text{mol/mg-h}$	$K_s$	
				mg/L	mmol/L
A	3193.9	20.329	0.049	157.11	1.7823
B	9655.3	9.8249	0.102	982.74	11.148
C	12537	7.3286	0.136	1710.70	19.407
D	11671	8.93	0.112	1306.94	14.826
Whole set	9313.2	1.588	0.630	5864.74	66.531
		Average =	0.10	1039.37	11.79
		STDEV =	0.04	659.26	7.4788

c) TBF cometabolism. Experimental data was analyzed as a whole set, as shown in Table E.12.

**Table E.12** Kinetic constants for TBF cometabolism by reciprocal plot.

Slope ( $\mu\text{mol/L-h}$ ) <sup>-1</sup>	intercept mg-h/ $\mu\text{mol}$	$k_{max}$ $\mu\text{mol/mg-h}$	$K_s$	
			mg/L	mmol/L
443	1.93	0.518	225	2.25

### Direct Linear plot.

Experimental data pairs of aqueous concentration (x,0) and initial degradation rate (0,y) are plotted, joined with a straight line and extrapolated as previously described. Values of  $k_{max}$  and  $K_s$  were arranged in increasing order and the median of each represented the best estimates. The medians of each set are the best estimates of the kinetic constants.

The median, unlike the averages, is very robust thus less sensitive to outliers or extreme values that inevitably occur in the direct linear plot

The best estimates were obtained with a visual basic program designed for this purpose. Instructions and program are summarized in Appendix F. Experimental data of all individual experiments was analyzed as a whole set and the constants determined as the median values as shown in Table E.13

**Table E.13** Kinetic constants by direct linear plot.

Compound	$k_{max}$ $\mu\text{mol/mg-h}$	$K_s$	
		mg/L	mmol/L
Propane	0.202	$57.4 \times 10^{-3}$	$1.3 \times 10^{-3}$
MTBE	0.070	400	4.54
TBF	0.522	223	2.19

An example of estimation of the constants is illustrated in Appendix D using TBF experimental data shown in Table E.6.